SYNTHESIS AND PHOTOPHYSICS OF PLATINUM(II) TERDENTATE AND BIDENTATE COMPLEXES

A Thesis
Submitted to the Graduate Faculty
of the
North Dakota State University
of Agriculture and Applied Science

By

Jing Yi

In Partial Fulfillment of the Requirements
for the Degree of
MASTER OF SCIENCE

Major Department:
Chemistry and Biochemistry

May 2010
Fargo, North Dakota

North Dakota State University

Graduate School

Title

SYNTHESIS AND PHOTOPHYSICS OF PLATINUM(II)

TERDENTATE AND BIDENTATE COMPLEXES

By

Jing Yi

The Supervisory Committee certifies that this ***disquisition*** complies with North Dakota State University's regulations and meets the accepted standards for the degree of

MASTER OF SCIENCE

ABSTRACT

Yi, Jing, M.S., Department of Chemistry and Biochemistry, College of Science and Mathematics, North Dakota State University, May 2010. Synthesis and Photophysics of Platinum(II) Terdentate and Bidentate Complexes. Major Professor: Dr. Wenfang Sun.

Platinum(II) terdentate and bidentate complexes possess square-planar d^8 configuration. The moderate metal-to-ligand charge-transfer (^{1}MLCT) absorption, ^{3}MLCT emission, and broadband excited-state absorption are the unique spectroscopic features for these complexes. In my thesis work, two series of terdentate platinum(II) complexes and one bidentate platinum(II) complex were designed and synthesized. The photophysical properties, such as the electronic absorption, photoluminescence, and triplet excited-state absorption, are investigated systematically.

Chapter 1 introduced the representative work on the synthesis and photophysical studies of the terdentate and bidentate platinum(II) complexes reported in the literature. The motivation for my thesis project was briefly discussed.

In Chapter 2, the synthesis and photophysical properties of two platinum 6-phenyl-4-(9,9-dihexylfluoren-2-yl)-2,2'-bipyridine complexes with phenothiazinyl (PTZ) acetylide ligand were discussed. Their UV-vis absorption and emission characteristics in solutions and LB films were systematically investigated. The triplet transient difference absorption and reverse saturable absorption were also studied for these complexes. Both complexes exhibit a broad metal-to-ligand charge-transfer / ligand-to-ligand charge-transfer / intraligand charge-transfer (^{1}MLCT/^{1}LLCT/^{1}ILCT) absorption band between 400 and 500 nm and a ^{3}MLCT/^{3}ILCT/$^3\pi,\pi^*$ emission band at ~594 nm at room temperature, which blue shifts at 77 K. Both UV-vis absorption and emission spectra show negative solvatochromic

effect. Both of the complexes also exhibit broad and moderately strong triplet transient absorption from the near-UV to the near-IR spectral region. In addition, LB films of them were prepared and characterized by AFM technique. The UV-vis absorption and emission spectra of the LB films of them were also investigated and compared with those obtained in solutions.

In Chapter 3, the synthesis and photophysical studies of a series of platinum 6-phenyl-4-(7-benzothiazolyl-9,9-diethylfluoren-2-yl)-2,2`-bipyridine complexes with different acetylides ligands, such as, nitrophenyl acetylide, fluorenyl acetylide, and benzothiazolylfluorenyl acetylide, were discussed. The complex bearing nitrophenyl acetylide ligand exhibited quite distinct photophysical properties compared to the other two complexes.

In Chapter 4, one platinum bis(mesitylimino)acenaphthene complex was synthesized. The lowest-energy absorption band was attributed to ^{1}MLCT transitions, which was much broader and red-shifted (extending from 490 nm to 800 nm) compared to those reported for other diimine Pt(II) complexes.

ACKNOWLEDGEMENTS

I would like to thank my advisor Dr. Wenfang Sun for her instruction and support. I am very grateful to Dr. Gregory Cook, Dr. Pinjing Zhao, Dr. Sivaguru Jayaraman, and Dr. Sanku Mallik for serving as my committee members. Your patience and guidance definitely helped me out from many troubles and helped me in completing my thesis.

I also would like to thank Dr. Bingguang Zhang, Dr. Yunjing Li, Dr. Suyue Li, Dr. Zhiqiang Ji, Dr. Iswarya Mathew, Zhongjing Li, Rui Liu, and Chris Hanson in Dr. Sun's group for their help and collaboration, and my colleagues Jing Zhang, Anoklase Ayitou, Barry Pemberton, Sreehari Seerla, and Nandini Vallavoju for their support.

Last but not least, I would like to express my gratitude to Dr. Angel Ugrinov and Daniel Wanner for tutoring me in operating mass and NMR spectrometers. I would like to thank Wendy Leach, David Tacke and Linda Stoetzer for helping me. I also acknowledge the Department of Chemistry and Biochemistry for providing me the opportunity and partial financial support for me to complete my master's degree here.

TABLE OF CONTENTS

LIST OF TABLES

LIST OF FIGURES

LIST OF SCHEMES

LIST OF CHARTS

LIST OF ABBREVIATIONS

ε	.....	Molar extinction coefficient
σ	.....	Absorption cross-section
Φ	.....	Emission quantum yield
τ	.....	Emission lifetime
Φ_T	.....	The triplet excited-state quantum yield
τ_T	.....	The triplet excited-state lifetime
AFM	.....	Atomic force microscopy
DEC	.....	1,2-Dichloroethane
DMF	.....	*N*,*N*-Dimethylformamide
HOMO	.....	Highest occupied molecular orbital
ILCT	.....	Intraligand charge transfer
IC	.....	Internal conversion
ISC	.....	Intersystem crossing
LB film	.....	Langmuir-Blodgett film
LLCT	.....	Ligand-to-ligand charge transfer
LUMO	.....	Lowest unoccupied molecular orbital
MLCT	.....	Metal-to-ligand charge transfer
NLO	.....	Nonlinear optics
TA	.....	Transient absorption
THF	.....	Tetrahydrofuran

CHAPTER 1. INTRODUCTION

Platinum, the third row transition element, constitutes Group VIII in the periodic table with nickel and palladium.[1] Pt(II) with d^8 electronic configuration always has thermodynamic preference to form square-planar complexes in the presence of other ligands. As Figure 1.1 shows, in the square-planar configuration one unoccupied d orbital (d_{x2-y2}) is pushed into a high energy level, which substantially stabilizes other three occupied d orbitals. The square-planar geometry indicates that Pt(II) complexes are different from other d^6, d^7, and d^9 transition metal complexes, such as, octahedral Ru(II), Rh(III), Ir(III), Os(II) complexes and tetrahedral Cu(I) complexes.[2]

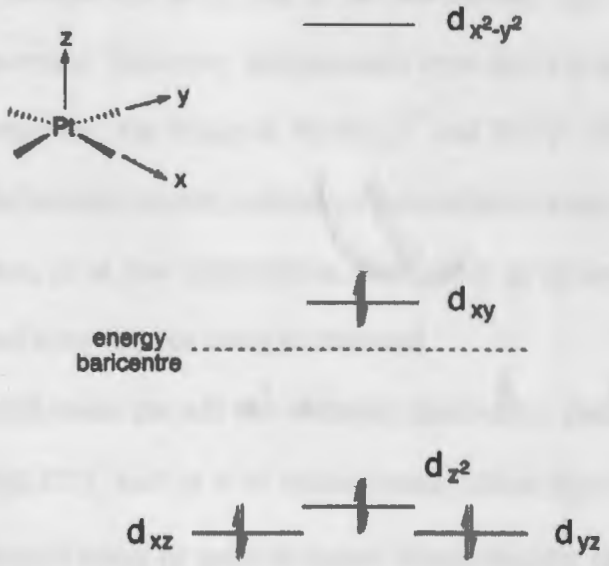

Figure 1.1. Simple ligand field-splitting diagram for Pt *d* orbitals in a square planar complex. By convention, the *z* axis is perpendicular to the plane of the complex and the M – L bonds lie along the *x* and *y* axes. Note that the exact ordering of the lower energy levels depends on the ligand set (*e.g.*, relative importance of σ- and π-effect) but the d_{x2-y2} is always unequivocally the highest. (Reprinted with the permission from Ref 2 Copyright 2007 Springer)

Because of the square-planar nature of the d^8 Pt(II) complexes, they have many implications:

1. The metal-center d-d excited states are inclined to efficient non-radiative decay. As shown in Figure 1.1, the highest antibonding orbital is d_{x2-y2}, which can be populated through absorption of light. In this situation, there is a significant distortion of the Pt-L bond length at the excited states of the Pt(II) complexes. As shown in Figure 1.2 (a), such a distortion would cause a displacement of the potential energy surface of the low-lying *d-d* excited state, resulting in a crossover of the potential energy surface of the *d-d* excited state with that of the ground state. This would increase the decay path of the *d-d* excited state via the non-radiative internal conversion. Therefore, luminescence from the *d-d* excited state generally cannot be observed. For example, $Pt(NH_3)_4^{2+}$ and $PtCl_4^{2-}$ are not luminescent in fluid solution because the rate constant of non-radiative decay is large. In the solid or crystal state, or at low temperatures, the rigidity of environment decreases the distortion, and luminescence could be observed.
2. The *d-d* excited states can add non-radiative deactivation pathway for other lower-lying *d*-π^* (MLCT), π-π^* or *n*-π^* excited states. Either ligand-centered (LC, *n*-π^* or π^*-π^*) excited states or metal-to-ligand charge-transfer (MLCT, *d*-π^*) excited states may lie at lower energies than the d-d states. The radiative decay rate constant k_r for *d*-π^*, π-π^* or *n*-π^* excited states is typically higher than that of the *d-d* excited state. However, the *d-d* excited state still imparts negative influence on luminescence because it is still thermally accessible for the lowest-energy excited

states like Figure 1.2 (b) shows. Thus, the effective method to solve this problem is to increase the ΔE value.

3. The planar configuration of the Pt(II) complexes causes axial intermolecular interactions. The square-planar platinum complexes are flat, which allows close interactions with either other different molecules (*e.g.*, excimer or intermolecular stacking) or other molecules (exciplex). The d_{z2} orbital is perpendicular to the molecular plane, which involves specific metal-metal interactions and forms weakly bonding and antibonding dσ and dσ^* molecular orbitals, shown in Figure 1.3. Thus this type of interactions would raise the energy of the highest occupied metal-based molecular orbital, which causes the red-shift of the lowest-energy electronic transitions. This can lead to a change of the nature of the lowest-energy excited state. For example, in Figure 1.3, π-π^* transition occurs as the lowest-energy transition in monomers without metal-metal interaction, while dσ^*-π^* transition appears as the lowest-energy transition when there is intermolecular/intramolecular interaction between d_{z2} orbitals. Heavy transition metal ion Pt(II) can promote rapid intersystem crossing (ISC) from singlet to triplet excited states, which leads to another important feature for the triplet states of platinum complexes. Because of the larger rate constant of ISC (~ 10^{12} s^{-1}) than radiative rate constant from singlet (~ 10^{8} s^{-1}), the luminescence from platinum complexes is usually from the triplet excited state, which is phosphorescence.

Based on the aforementioned characteristic electronic configuration of the platinum(II) complexes, these complexes generally exhibit interesting spectroscopic properties and great

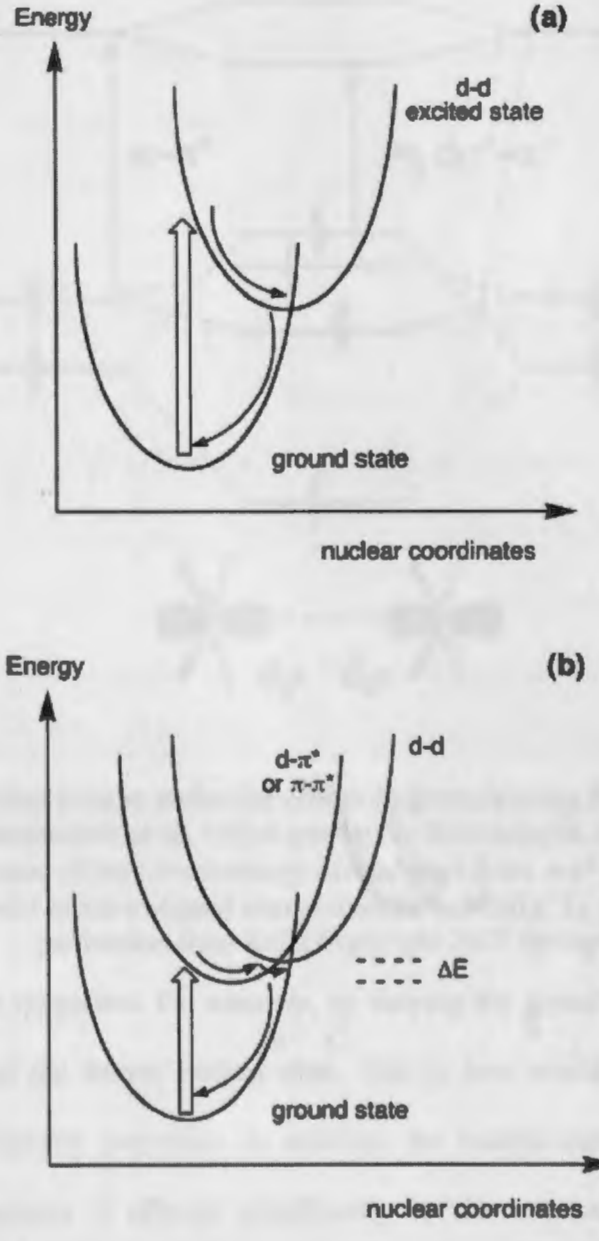

Figure 1.2. (a) Illustration of the displacement of the potential energy surface for the *d-d* excited state in a square-planar d^8 complex, formed by population of the d_{x2-y2} orbital, compared to the ground state. (b) Even though other excited states [*e.g.*, *d-π** (MLCT) or *π-π** (LLCT/ILCT)] may lie at lower energies, the *d-d* excited state can provide a thermally activated non-radiative decay pathway. Thick arrow represent absorption of light; thin ones indicate vibrational relaxation and non-radiative decay. (Reprinted with the permission from Ref 2 Copyright 2007 Springer)

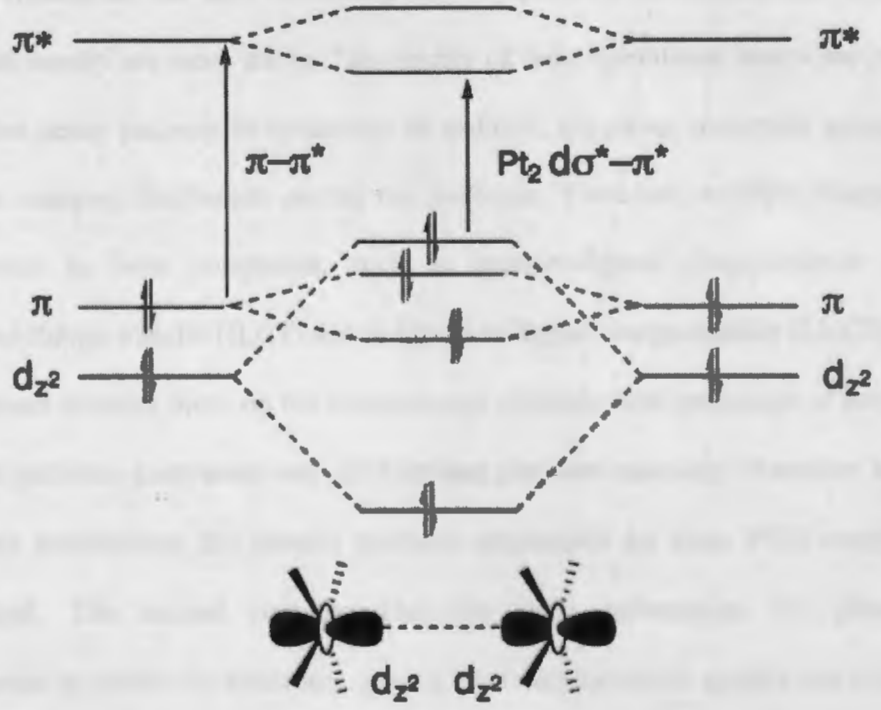

Figure 1.3. Simplified frontier molecular orbital diagram showing the effect of face-to-face interactions and intermolecular d_{z2} orbital overlap. In this example, such interaction leads to a change in the nature of the lowest-energy excited state from π-π^* (ligand-centred or LC) to dσ^*-π^* (metal-metal-to-ligand charge transfer or MMLCT). (Reprinted with the permission from Ref 2 Copyright 2007 Springer)

tunability of these properties. For example, by varying the ligand field strength, one can alter the nature of the lowest excited state. This in turn would change the electronic absorption and emission properties. In addition, the excited-state characteristics of the platinum(II) complexes is affected significantly by the external stimuli, such as pH, temperature, concentration, cation or anion. All these properties lead to a variety of potential applications for the platinum(II) complexes, such as OLED,[10,22,26,41,68] optical sensor,[97,98] DNA intercalator,[81] and protein probe,[99] *etc.* Among the variety platinum(II) complexes reported in the literature, platinum(II) complexes bearing terdentate and

bidentate ligands are the most interesting ones. Because of the multidentate ligand, these complexes usually are more stable. The rigidity of these complexes makes the preference of radiative decay pathway in molecules. In addition, the planar molecular geometry also facilitates electron distribution among the molecule. Therefore, multiple charge-transfer could occur in these complexes, such as metal-to-ligand charge-transfer (MLCT), intraligand charge-transfer (ILCT) and/or ligand-to-ligand charge-transfer (LLCT).

My thesis projects focus on the synthesis and photophysical properties of two series of terdentate platinum complexes and one bidentate platinum complex. Therefore, in the first part of the introduction, the general synthetic approaches for these Pt(II) complexes are summarized. The second part provides the basic information for photophysical measurement to obtain the electronic spectra, photoluminescence spectra and excited-state absorption difference spectra. The third part summarizes the photophysical properties for these two types of Pt(II) complexes reported in the literature. Finally, the objectives of my thesis research are presented.

1.1. Synthetic Approach

1.1.1. Terdentate and Acetylide Ligands

The synthesis of 4,6-diphenyl-2,2'-bipyridine ligand generally uses the condensation between acalkylpyridinium salts and α,β-unsaturated ketones in the presence of ammonium acetate by refluxing in methanol. This method derives from Krohnke condensation (Scheme 1.1).[3] Either changing 2-(α,β-unsaturated-acetyl)pyridine to α,β-unsaturated phenyl ketone, or changing *N*-heteropyridinium salts into 1-(2-oxo-2-phenyl-ethyl)-pyridinium salts is alternative route for the synthesis of terdentate ligand.

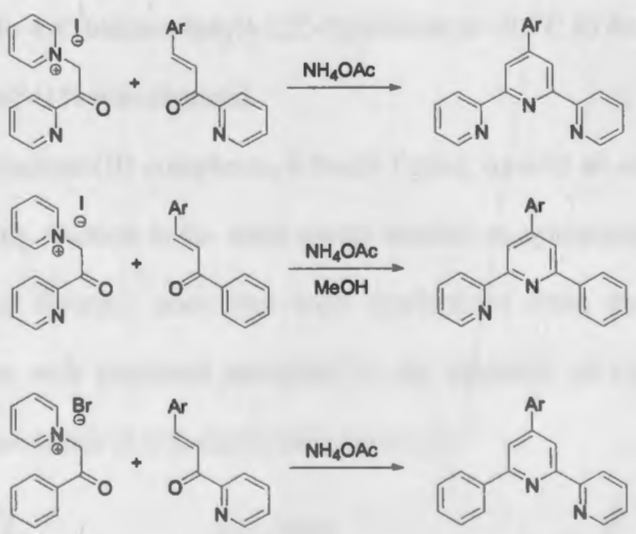

Scheme 1.1. Krohnke condensation.

After ring-closure, chemists have been using Wittig reaction,[4,5] Suzuki coupling,[6-8] or Sonogashira coupling[9] to introduce different functional groups on the C^N^N ligand, which in turn tunes the property of the ligand. In the following section 1.4.3, how the different functional groups significantly influence the photophysical properties of Pt(II) complexes will be discussed.

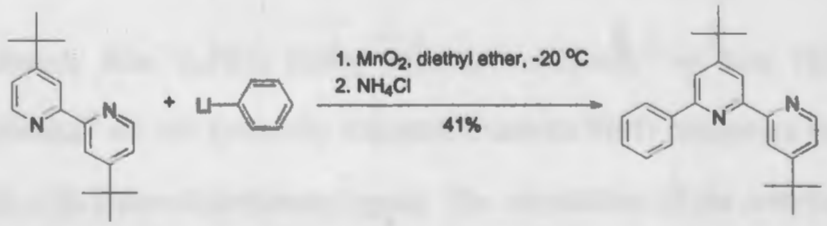

Scheme 1.2. Synthetic route for 6-phenyl-4,4'-bis(*tert*-butyl)-2,2'-bipyridine.

Instead of Krohnke ring-closure reaction, directly attaching phenyl ring to 2,2'-bipyridine ligands was reported by Che and co-workers (Scheme 1.2).[10] The phenyllithium

reagent was added to 4,4'-bis(*tert*-butyl)-2,2'-bipyridine at -20 °C in diethyl ether solution. A reasonable yield of 41% was obtained.

For terdentate platinum(II) complexes, a fourth ligand, usually an acetylide is required. Sonogashira coupling reaction is the most useful method to synthesize acetylide ligands. For example, many fluorene acetylides were synthesized from the iodo- or bromo-substituted fluorene with protected acetylene in the presence of catalytic amounts of $Pd(dba)_2$ and cuprous iodide (CuI), shown in Scheme 1.3.[11]

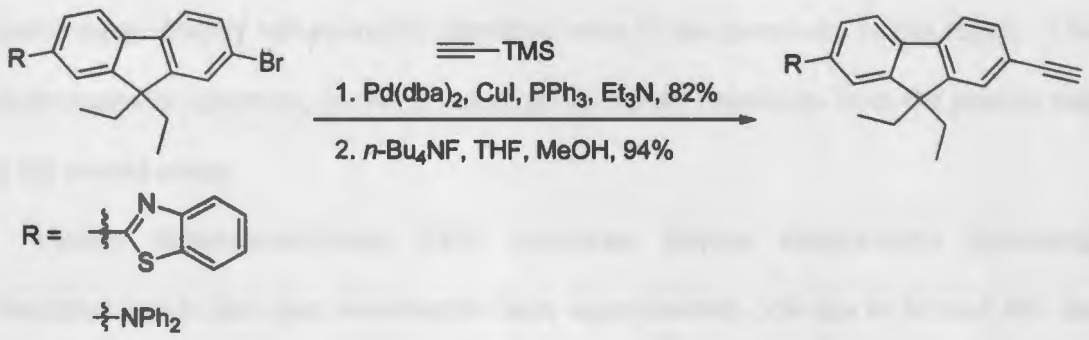

Scheme 1.3. Synthetic route for alkynyl fluorene.

1.1.2. Bidentate/Terdentate Pt(II) Acetylide

Either directly from K_2PtCl_4 (acidic aqueous conditions)[12] or from $Pt(DMSO)_2Cl_2$ (organic solvents)[13] we can synthesize bidentate/tridentate Pt(II) complexes by displacing labile ligands with bidentate/terdentate ligands. The introduction of the acetylide unit(s) to the platinum(II) center is readily accomplished through a chloride-to-acetylide metathesis mediated by a CuI catalyst in an organic solvent/base mixture.[14,15] Although this synthetic method has been extensively utilized, a catalyst-free pathway has also been developed for various triflate precursors.[16] In these situations, the terminal acetylene readily couples to

the metal center at room temperature, producing the metal-acetylide bond in high yield without the need for the CuI catalyst.

1.2. Instruments for Photophysical Measurement

1.2.1. Ultraviolet-visible Spectroscopy (UV-Vis)

UV-Vis spectroscopy refers to the absorption spectroscopy in the UV-Vis spectral region (light in the visible and near-UV or near-infrared ranges). The absorption in the visible range directly influences the perceived color of the chemicals. In this region of the electromagnetic spectrum, molecules undergo electronic transitions from the ground state to the excited states.

Usually bidentate/terdentate Pt(II) complexes display characteristic low-energy absorption bands that span wavelengths from approximately 350 nm to beyond 600 nm, depending on the nature of the bidentate, terdentate ligands and the acetylide ligands. Acetylide-localized π-π^* transitions place at high energies; whereas the low-energy absorption bands were proposed to originate from metal-to-ligand charge transfer (MLCT) transitions.[12, 15, 17, 18] In some circumstances, the inter-/intra-molecular interactions result in a broad and weak metal-metal-to-ligand charge transfer transition in the red region.[97-99]

1.2.2. Photoluminescence Spectroscopy

Photoluminescence (PL) is a process in which a chemical absorbs photons and then re-radiates photons. It also can be described as an excitation to an excited state and then a return to a lower-energy state accompanied by emission of a photon. The simplest PL process is resonant radiation. When a photon is emitted from a singlet excited state it is

called fluorescence; when a photon is emitted from a triplet excited state it is referred as phosphorescence. Since the transition between triplet to singlet ground state is forbidden naturally, phosphorescence is usually much lower in intensity than fluorescence. Transition metals like platinum can increase the intersystem crossing to the triplet excited state, which leads to distinctive photophysical properties of Pt(II) complexes. The emission wavelength provides important information about energy gap between the ground state and the excited state. Emission at different concentrations and in different solvents usually indicates self-quenching effect and polarity of the transition.

1.2.3. Transient Absorption Spectroscopy

In addition to the emission studies, another powerful tool in understanding the excited-state characteristics is the transient absorption measurement of the excited state, which is critical for predicting the nonlinear absorption of the compound. The time-resolved triplet transient difference absorption study not only provides valuable information on the triplet excited-state absorption spectrum but also on the lifetime of the triplet excited state. In general, a positive band in a transient absorption spectrum suggests stronger excited-state absorption than that of the ground state in the respective spectral region, which could cause reverse saturable absorption.

1.3. Photophysical Properties of Bidentate/Terdentate Pt(II) Complexes

It is well known that five- and six-membered chelating rings are generally the most stable ones.[19] Polypyridine ligands were widely used for the synthesis of Pt(II) complexes. In addition to using N as the chelating atom, C, O, and S have been utilized as chelating atoms as well; and some of the C, O and S chelating platinum(II) complexes featured very

interesting photophysical properties. For example, platinum complexes bearing 2-phenylpyridine (N^C ligand),[20-30] biphenyl (C^C ligand),[31] 6-phenyl-2,2'-bipyridine (C^N^N ligand),[10,32-45] 1,3-dipyridylbenzene (N^C^N),[46-59] 2,6-diphenylpyridine (C^N^C)[60-63] have been reported.

1.3.1. Bidentate Pt(II) Complexes

There are many types of bidentate Pt(II) complexes. The simplest of possible complexes is $Pt(bpy)Cl_2$ (bpy = 2,2'-bipyridine). It can exist in either yellow or red polymorphs. After a detailed investigation of the emission properties of these two forms, and of a series of derivatives, Miskowski reported that the emitting state in red $Pt(bpy)Cl_2$ is metal-based, while in yellow $Pt(bpy)Cl_2$ it is metal-metal-to-ligand charge transfer based.[64,65] In other words, the different emission behaviors between the yellow and red forms of $Pt(bpy)Cl_2$ is the result of the different parentage of the HOMO. The shortcoming for this type of $Pt(N^N)Cl_2$ complexes is that the excited states of them are normally short-lived in solution, thus lacking of luminescence in solution.[66]

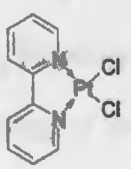

Other than the $Pt(bpy)Cl_2$ complex, $Pt(N^N)(C{\equiv}N)_2$ complexes were reported to be good candidates for studying the self-quenching effect and excimer formation in solution. Using strong-field cyanides instead of weak-field halide ligands can raise the energy of the highest-occupied metal-centered orbitals, which is still below the antibonding π^* orbital of the bpy ligand. Additionally, the introduction of strong-field cyanides raises vacant d_{x2-y2} orbital, which reduces the deactivation pathway via cross-over to the strongly distorted

metal-centered state. Although the increased intermolecular interactions cause self-quenching,[67, 68] researchers can still observe the increased emission intensity and the longer lifetimes of the excited state.

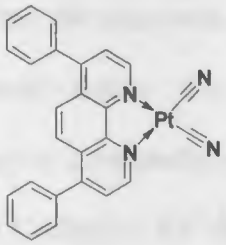

Research on Pt(N^N)(C≡CR)$_2$ complexes is an emerging area in platinum chemistry. Che and co-workers reported the first luminescent bidentate diimine Pt(II) acetylide complexes Pt(phen)(C≡CPh)$_2$ (phen = 1,10-phenanthroline) in 1994, which exhibit intense triplet [5d(Pt) → π^*(phen)] metal-to-ligand charge transfer (MLCT) emission in fluid solution at room temperature.[69] In subsequent research they modified both the diimine ligand and the acetylide auxiliaries to systematically investigate the influence of the ligand alternation on the photophysics of this type of Pt(II) complexes. In addition to Che's work, many groups put efforts to investigate the platinum(II) diimine complexes containing acetylide ligands in the past two decades. Introducing strong-field acetylide ligands to the Pt(II) coordination sphere increases the energy of the deactivating metal-centered d-d state, which results in stronger emission in solution at room temperature.

Regarding the effect of bidentate ligands, Che's group studied a series of bis(arylacetylide) Pt(II) complexes bearing substituted bipyridine and phenanthroline ligands,[70] as shown in Chart 1.1. They synthesized the Pt(II) complexes through reactions that were reported by Sonogashira's and Cross's groups.[71, 72] In accordance with the results of Eisenberg *et al.*,[73] the solution emission maxima for both the **1** and **2** series of

derivatives shift to lower energies as the electron-withdrawing ability of the substituted bipyridine and phenanthroline ligands increases respectively. Assuming all complexes exhibit pure ^{3}MLCT emission and modification of diimine ligands does not affect the Pt-based HOMO level, Che proposed that the electronic donating effect of the α-diimine-based LUMO energy levels should follow this order: 3,4,7,8-tetramethyl-1,10-phenanthroline (tmphen) > 5,5'-dmbpy > 5,6-dimethyl-1,10-phenanthroline (5,6-dmphen) ≈ 4,4'-di-*tert*-butyl-2,2'-bipyridine (4,4'-dtbpy) ≈ 4,4'-dmbpy > 5-mphen > 4-phenyl-1,10-phenanthroline > 4,7-diphenyl-1,10-phenanthroline (dpphen) > 4,4'-diphenyl-2,2'-bipyridine (dpbpy). In other words, the emission energy decreases according to this order: **2a < 1a < 2b ≈ 1b ≈ 1c < 2c < 2e < 2f < 1d**. The ability to fine-tune excited-state energy is very important for applications of Pt(II) complexes.

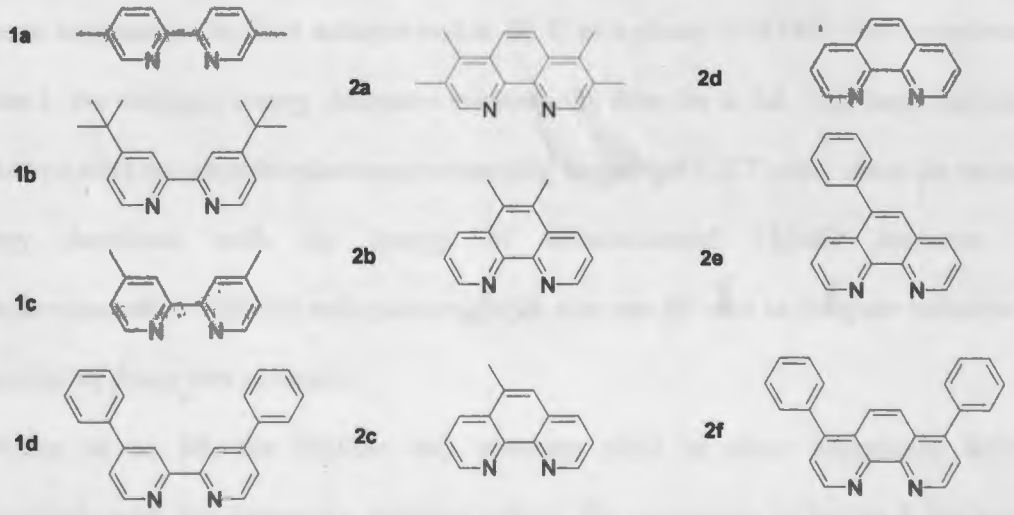

Chart 1.1. Derivatization of substituted bipyridine and phenanthroline ligands. (from Ref 70)

For bidentate Pt(II) diimine complexes, the nature of the acetylide ligands and diimine ligands drastically influence the energy and the width of the charge transfer transitions. Eisenberg and Schanze independently studied two series of Pt(II) diimine acetylides

complexes (**3a** – **3d** and **4a** – **4d**), in which both diimine ligands and the acetylide ligands were varied by introducing different electron-withdrawing or –donating substituents on these ligands.[17,74,75] In the UV-Vis spectra, the ^{1}MLCT band red-shifts by nearly 3000 cm^{-1} from **3a** to **3d**, and the low-energy ^{1}MLCT of **3c**, **3d** consists of two overlapping bands. In other words, all the complexes feature a low-energy absorption band in the 350 – 500 nm region, attributed to a Pt→diimine ^{1}MLCT transition. This assignment is supported by the influence of the substituent on λ_{max}. For **Series 1** complexes, the energy of the band decreases approximately 3000 cm^{-1} along the sequence **3a** < **3b** < **3c** < **3d**, as the substituents become increasingly electron-withdrawing, the diimine π^* (LUMO) energy decreases.

All of the complexes shown in Chart 1.2 feature moderately intense photoluminescence at room temperature in fluid solution and at 80 K in a glassy 2-MTHF. For complexes in **Series 1**, the emission energy decreases substantially from **3a** to **3d**. This large red shift is consistent with the photoluminescence emanating from the MLCT state, since the emission energy decreases with the energy of diimine-based LUMO decrease. The photoluminescence lifetimes and quantum yields also can be used to compute radiative and nonradiative decay rate constants.

From **3a** to **3d**, the lifetime and quantum yield of these complexes decrease systemically with the decreasing emission energy. For complexes in **Series 2**, the trend is not so obvious as that in **Series 1**, although the photoluminescence of most of the complexes also emanates from MLCT state. The complexity partially arises from the different natures of the emitting state for **4b** and **4c**, which has $^3\pi,\pi^*$ character.

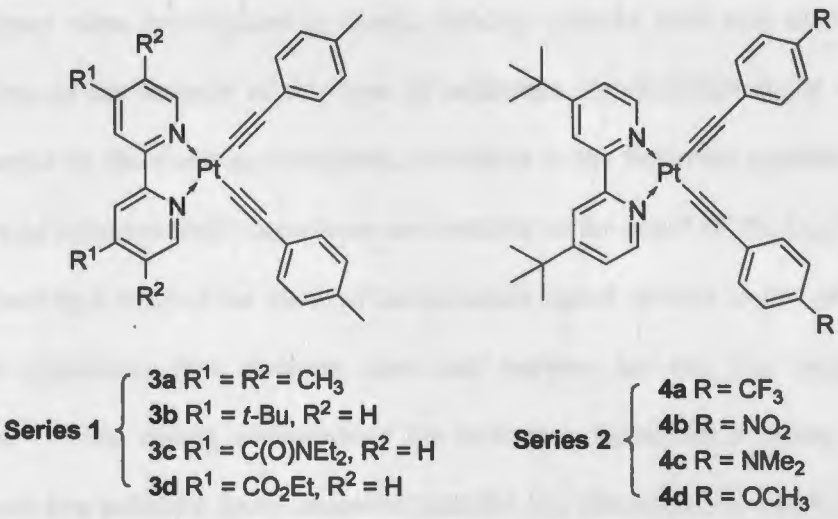

Chart 1.2. Diimine ligands and acetylide ligands of bidentate Pt(II) complexes were varied by introducing different electron-withdrawing or –donating substituents. (from Ref 17)

For most of the bidentate Pt(II) acetylides complexes, the low energy absorption bands show strong hypsochromic shift, indicative of their polar ground states.[77-79] DFT calculations estimate the ground-state dipole moments (μ_{gr}) to be approximately 10.6 D in Pt(bpy)(C≡CPh)$_2$, the vector of which opposes the direction of the charge transfer transition.[79] This makes excited state dipole moments (μ_{ex}) close to or equal to zero. The solvent medium greatly influences their ground-state properties, which to some extent indicates the polarity of the ground state.

1.3.2. Terdentate Pt(II) Complexes

There are many types of terdentate Pt(II) complexes, with different terdentate ligands or different monodentate ligands, analogous to the bidentate systems. Similar to the study on the bidentate Pt(II) complexes, researchers started from the simplest terdentate Pt(II) complex—platinum terpyridyl chloride $[Pt(tpy)Cl]^+$ that has been known since 1934. Howeverer, until the early 1990s the excited state and luminescence properties of terdentate

Pt(II) complexes were investigated in detail, yielding systems with rich photophysical properties. One of the features of this type of terdentate complexation is the additional rigidity imparted on the resulting complexes, compared to the bidentate systems. The *d-d* excited states of bidentate Pt(II) complexes are unstable as the result of the D_{2d} distortion, which is caused by a twist of the plane of the bidentate ligand relative to that of the other two ligands. However, this situation does not happen for the D_{4h} square-planar configuration.[70,71] The strong preference of the terdentate ligand for a planar geometry greatly reduces non-radiative decay observed from the D_{2d} distortion. However, this is not the case for d^6 transition. Crystal structures of Ru(II) complexes reveal that the two central metal-to-ligand bond lengths are similar in bidentate complexes, but not ideal for terdentate complexes due to the constraints imposed by the rigidity of the ligand. Therefore, the strength of the ligand field is reduced, resulting in the decrease of the energy for the *d-d* excited state.[72] For example, $[Ru(tpy)_2]^{2+}$ is almost non-emissive under ambient conditions, incontrast to $[Ru(bpy)_3]^{2+}$.[73] By using a strong-field ancillary ligand in the fourth position, this effect can be counteracted.[72]

Similar to the study on the bidentate platinum(II) complexes, researchers investigated the photophysical properties of the terdentate cyclometalated Pt(II) complexes with different substituents attached on the terdentate ligand. In 2004, Che and co-workers proposed that among the different terdentate Pt(II) lumophores, Pt(C^N^N) exhibit superior emissive properties compared to 2,2':6',2"-terpyridine (tpy) and C^N^C congeners.[10] They modified the substituents on the C^N^N ligand to tune the emission energy for the [(C^N^N)PtC≡C—R] complexes. Over 30 [(C^N^N)PtC≡C—R] complexes have been studied, as shown in Chart 1.2. Attachment of a *para*-substituted aryl ring at the 4-position

of the middle pyridine ring of the C^N^N ligand makes Pt(II) complexes more diverse but less soluble in common organic solvent. **22** that bears an electron-withdrawing nitro group at the *para*-position has a very distinct peak at 446 nm in its absorption spectrum at room temperature in CH_2Cl_2, which is significantly blue-shifted compared to those in **18** – **21**. However, **18** – **22** exhibit similar orange-red emission around 595 nm in CH_2Cl_2 at room temperature, and the emission energies and quantum yields are comparable to those of **5**. This indicates that the impact of 4-aryl ring is very small on the emission properties. The introduction of two *tert*-butyl groups to the bipyridine moiety of the C^N^N ligand affects the emission properties of **23** and **24**. The electron-donating nature of *tert*-butyl group leads to blue-shifted emissions for **23** (571 nm) and **24** (550 nm) compared to the parent complex **5** (582 nm). In addition, the bulky *tert*-butyl groups minimize intermolecular interactions between neighboring Pt(C^N^N) planes. Therefore, bright yellow crystals were obtained for **23** and **24**, which is quite distinct from the dark red/brown colors of many other Pt(C^N^N) complexes. On the other hand, the electron-withdrawing ethoxycarbonyl group at the 4-position of C^N^N ligand causes dramatical red-shift of the emission energy for **26** (620 nm) and **27** (593 nm).

As discussed previously, modification of the terdentate (C^N^N) ligands facilitates fine-tuning of the emission energy of the (C^N^N)Pt(II) acetylide complexes. In the same project, Che and co-workers also modified the arylacetylide by introducing substituents with different steric and electronic properties into the arylacetylide ligand, which drastically tuned their photophysical characteristics as well.[10] Figure 1.4 depicts that the emission maxima of this class of complexes in CH_2Cl_2 at room temperature can be tuned from 630 nm for **7** to 560 nm for **10** upon varying the 4-arylacetylide substituent. Electron-

withdrawing group at the 4-arylacetylide ligand stabilizes the Pt-based HOMO, which leads to blue-shifted emission. Compared to the precursor Pt(II) chloride [(C^N^N)PtCl] complex, the emission energy of the Pt(II) acetylide complexes [(C^N^N)PtC≡CC_6H_4-4-R] are red-shifted. The introduction of strong-field acetylide ligands into the coordination sphere of Pt(II) ensures that the energy of deactivating metal-centered *d-d* states is raised, thus the complexes normally become more emissive in fluid solution at room temperature.

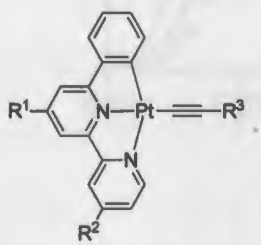

$R^1 = R^2 = H$, R^3 = Ph	5
C_6H_4-4-CH_3	6
C_6H_4-4-OCH_3	7
C_6H_4-4-Cl	8
C_6H_4-4-F	9
C_6H_4-4-NO_2	10
C6F5	11
C≡CPh	12
C(CH3)3	13
$Si(CH_3)_3$	14
C≡C$Si(CH_3)_3$	15
C≡C–C≡C$Si(CH_3)_3$	16
C≡C–C≡C–C≡C$Si(CH_3)_3$	17

R^2 = H, R^3 = Ph, R^1 = Ph	18
4-$CH_3C_6H_4$	19
4-$CH_3OC_6H_4$	20
4-ClC_6H_4	21
4-$NO_2C_6H_4$	22
$R^1 = R^2$ = ^{t}Bu, R^3 = Ph	23
C_6F_5	24
pyrenyl-1	25
R^1 = EtO_2C, R^2 = H, R^3 = Ph	26
C_6F_5	27

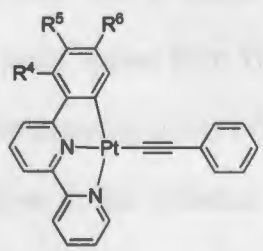

$R^4 = R^6$ = H, $R^5 = CH_3$	28
$R^4 = R^5$ = H, $R^6 = CH_3$	29
$R^4 = R^5$ = H, $R^6 = CF_3$	30
R^5 = H, $R^4 = R^6$ = F	31

Chart 1.3. Derivatization of terdentate 4,6-diphenyl-2,2'-bipyridine cyclometalating ligand. (from Ref 10)

Variation of the arylacetylide ligands also significantly influences the electronic absorption of the Pt(C^N^N) complexes. Compared to the ^{1}MLCT transitions (λ_{max} 380 – 420 nm, $\leq 1.5 \times 10^3$ L·mol^{-1}·cm^{-1}) in the electronic absorption spectra of the complexes **5 – 10** in CH_2Cl_2 solution at 298 K show broader ^{1}MLCT bands in 410 – 470 nm rang ($\varepsilon \approx$

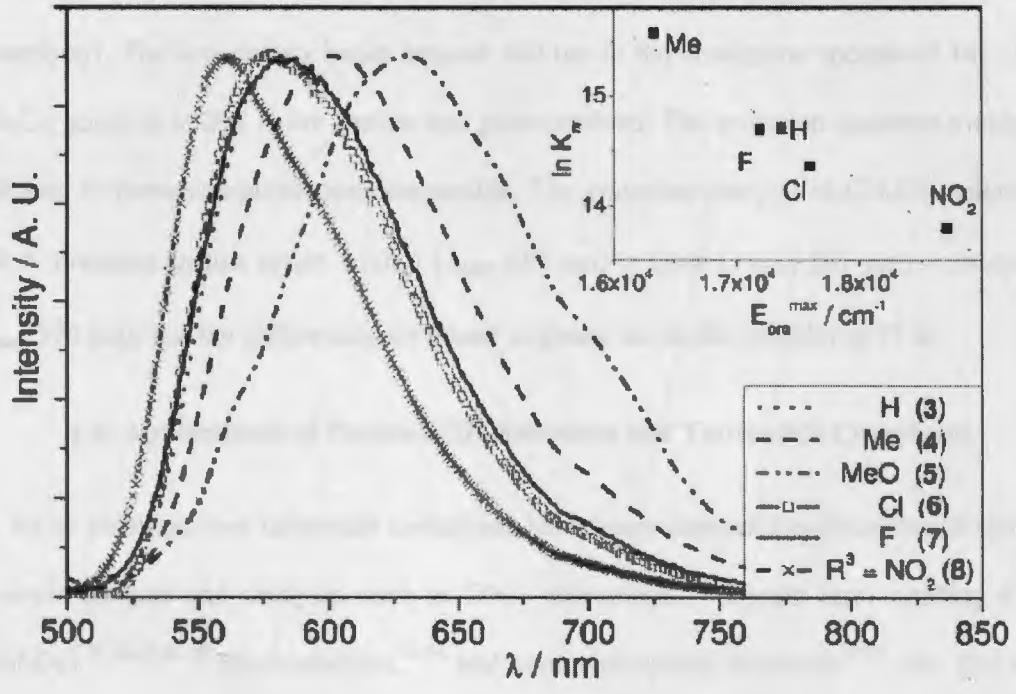

Figure 1.4. Normalized emission spectra of **5** – **10** in CH_2Cl_2 solutions at 298 K (λ_{ex} = 350 nm). Inset: plot of ln k_{nr} versus emission energy (from Ref 10).

5 × 10^3 $L \cdot mol^{-1} \cdot cm^{-1}$), which are red-shifted and more intense.[80] These low-energy absorption peaks appear from 415 to 465 nm, which systematically red-shift in accordance with electron-donating ability of the para-substituent on the phenyl-acetylide ligand.

In addition to the influence of substituent on the C^N^N and acetylide ligands, the effects of the π-conjugation length of the oligoyne ligands on the electronic absorption and emission of [(C^N^N)Pt–$(C{\equiv}C)_n$–R] have been examined. When the alkynyl ligand is extended from phenyl-capped ethynyl (**5**) to butadiynyl (**12**), the lowest-energy absorption band maximum of the MLCT band in CH_2Cl_2 solution blue-shifts from ~460 nm to ~430 nm, while the emission λ_{max} also blue-shifts from 582 nm to 571 nm. In 77 K alcoholic glassy matrix, the emission blue-shifts from 540 nm for **5** to 535 nm for **12**. From **14** to **17**,

the alkynyl ligand is homologously lengthened from trimethylsilyl-capped ethynyl to hexatriynyl. The low-energy bands beyond 400 nm in the absorption spectra of **14** – **17** in CH_2Cl_2 solution at 298 K are similar and poor-resolved. The emission quantum yields and lifetimes of these complexes are comparable. The emission energies in CH_2Cl_2 solution at 298 K decrease in this order: triynyl (λ_{max} 557 nm) > diynyl (λ_{max} 561 nm) > monoynyl (λ_{max} 570 nm), but the differences are minor in glassy alcoholic solution at 77 K.

1.4. Applications of Platinum(II) Bidentate and Terdentate Complexes

Pt(II) bidentate and terdentate complexes have many potential applications in biology, photonic devices and catalysis, such as DNA intercalator,[81] organic light emitting diodes (OLEDs),[10,22,26,41,68] photocatalysis,[82-84] and nonlinear optical materials[85-96] *etc*. The focus of our group has been investigating the nonlinear absorption (reverse saturable absorption and/or two-photon absorption) of the Pt(II) complexes. For example, our group has systematically investigated the photophysics and nonlinear absorption of a series of Pt(II) complexes with alkoxyl substituted 4,6-diphenyl-2,2'-bipyridine ligand (structure shown in Chart 1.4).[96] The triplet transient difference absorption spectra shown in Figure 1.5 revealed that most of these complexes exhibit a broad and strong triplet excited-state absorption in the visible to the near-IR region, which was attributed to ^{3}MLCT state. All complexes show significant transmission decreases with increased incident fluence, which is a characteristic feature of reverse saturable absorption (RSA). Although the RSA of **32** – **35** and **37** is quite similar, the degree of RSA follows this order: **33** ≈ **32** > **34** ≈ **37** ≈ **35** >> **36** because of the influence of alkoxyl group on C^N^N ligand and the effect of different acetylide ligands.

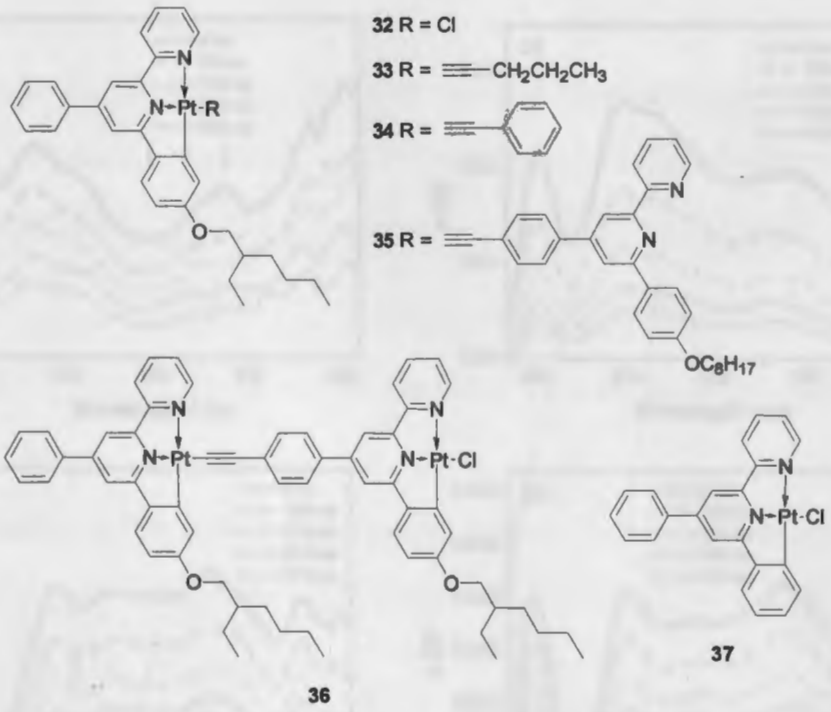

Chart 1.4. Molecular structures of platinum 4,6-diphenyl-2,2'-bipyridine complexes **32** – **37**. (from Ref 96)

1.5. Objective of My Research

Based on the reported work, we know that the platinum (II) terdentate and bidentate complexes possess unique photophysical properties, such as room temperature phosphorescence in fluid solutions, multiple charge transfer states, and broadband excited-state absorption. All these properties make these types of complexes potential candidates for applications in organic light emitting diodes, luminescent sensors, energy conversion materials, and nonlinear optics *etc*. Che, Eisenberg, and Schanze *et al*, have studied a variety of bidentate/terdentate Pt(II) complexes, and provided valuable information on designing these types of complexes. Based on their work, two series of terdentate platinum

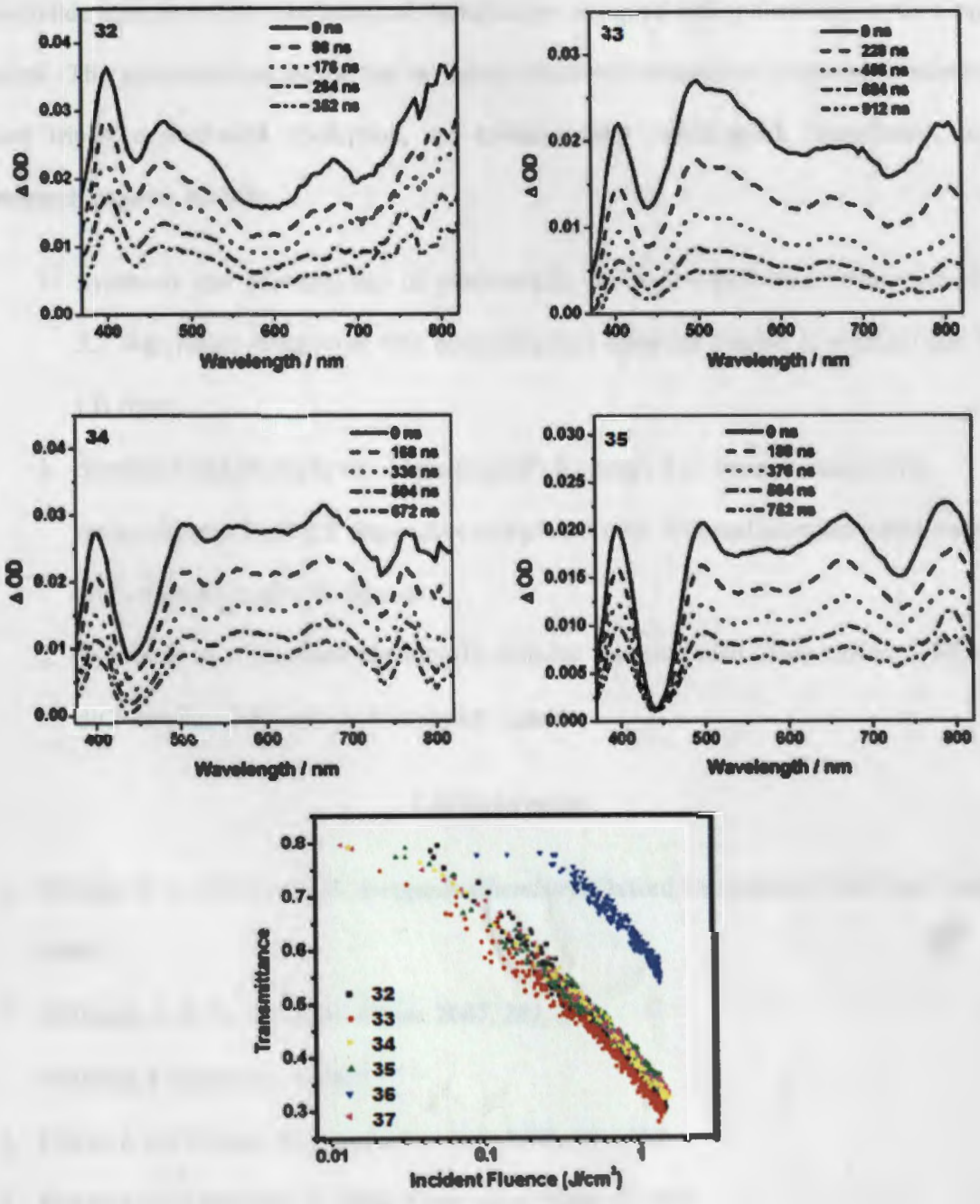

Figure 1.5. Time-resolved triplet transient difference absorption spectra of complexes of **32** – **35** in CH_3CN at room temperature in a 1 cm cuvette, and transmission vs incident fluence curves for **32** – **37** in CH_2Cl_2 solutions for 4.1 ns laser pulses at 532 nm in a 2mm cell. (Reprinted with the permission from Ref 96 Copyright 2009 American Chemical Society)

acetylide complexes and one bidentate complex are designed and synthesized in my thesis work. The photophysical properties including electronic absorption, photoluminescence, and triplet excited-state absorption, are systematically investigated. Specifically, my research projects include:

1. Synthesis and photophysics of platinum(II) 6-phenyl-4-(9,9-dihexylfluoren-2-yl)-2,2'-bipyridine complexes with phenothiazinyl acetylide ligand, in solution and in LB films.
2. Synthesis and photophysics of platinum(II) 6-phenyl-4-(7-benzothiazolyl-9,9-diethylfluoren-2-yl)-2,2'-bipyridine complexes with different electron-withdrawing and –donating acetylide ligands.
3. Synthesis of a bidentate platinum(II) diimine complex with 7-benzothiazolyl-9,9'-di(2-ethylhexylfluoren-2-yl) acetylide ligand.

1.6. References

1. Shriver, D. F.; Atkins, P. W. *Inorganic Chemistry*; Oxford University Press: New York, **2006**.
2. Williams, J. A. G. *Top Curr. Chem.* **2007**, *281*, 205.
3. Krohnke, F. *Synthesis*, **1976**, 1.
4. Pickaert, G.; Ziessel, R. *Tetrahedron Lett.* **1998**, *39*, 3497.
5. Pickaert, G.; Calzaferri, G. *Helv. Chim. Acta*, **1984**, *67*, 450.
6. Aspley, C. J.; Williams, A. G. *New J. Chem.* **2001**, *25*, 1136.
7. El-ghayoury, A.; Ziessel, R. *J. Org. Chem.* **2000**, *65*, 7757.
8. El-ghayoury, A.; Ziessel, R. *Tetrahedron Lett.* **1998**, *39*, 4473.

9. Heller, M.; Schubert, U. S. *Synlett.* **2002**, *5*, 751.

10. Lu, W.; Mi, B. X.; Chan, M. C. W.; Hui, Z.; Che, C. M.; Zhu, N.; Lee, S. T. *J. Am. Chem. Soc.* **2004**, *126*, 4958.

11. Rogers, J. E.; Slagle, J. E.; Krein, D. M.; Burke, A. R.; Hall, B. C.; Fratini, A.; McLean, D. G.; Fleitz, P. A.; Cooper, T. M.; Drobizhev, M.; Makarov, N. S.; Rebane, A.; Kim, K. Y.; Farley, R.; Schanze, K. S. *Inorg. Chem.* **2007**, *46*, 6483.

12. Chan, S. C.; Chan, M. C. W.; Wang, Y.; Che, C. M.; Cheung, K. K.; Zhu, N. *Chem. Eur. J.* **2001**, *7*, 4180.

13. Sonogashira, K.; Fujikura, Y.; Yatake, T.; Toyoshima, N.; Takahashi, S.; Hagihara, N. *J. Organomet. Chem.* **1978**, *145*, 101.

14. Cross, F. J.; Davidson, M. F. *J. Chem. Soc., Dalton Trans.* **1986**, 1987.

15. Hissler, M.; Connick, W. B.; Geiger, D. K.; McGarrah, J. E.; Lipa, D.; Lachicotte, R. J.; Eisenberg, R. *Inorg. Chem.* **2000**, *39*, 447.

16. Hodges, K. D.; Rund, J. V. *Inorg. Chem.* **1975**, *14*, 525.

17. Whittle, C. E.; Weinstein, J. A.; George, M. W.; Schanze, K. S. *Inorg. Chem.* **2001**, *40*, 4053.

18. Yang, Q. Z.; Wu, L. Z.; Wu, Z. X.; Zhang, L. P.; Tung, C. H. *Inorg. Chem.* **2002**, *41*, 5653.

19. Gavrilova, A. L.; Bosnich, B. *Chem. Rev.* **2004**, *104*, 349.

20. Evans, R. C.; Douglas, P.; Winscom, C. J. *Coord. Chem. Rev.* **2006**, *250*, 2093.

21. Chassot, L.; Muller, E.; von Zelewsky, A. *Inorg. Chem.* **1984**, *23*, 4249.

22. Maestri, M.; Sandrini, D.; Balzani, V.; Chassot, L.; Jolliet, P.; von Zelewsky, A. *Chem. Phys. Lett.* **1985**, *122*, 375.

23. Barigelletti, F.; Sandrini, D.; Maestri, M.; Balzani, V.; von Zelewsky, A.; Chassot, L.; Jolliet, P.; Maeder, U. *Inorg. Chem.* **1988**, *27*, 3544.

24. Yersin, H.; Donges, D. *Top Curr. Chem.* **2001**, *214*, 81.

25. Kvam, P. I.; Puzyk, M. V.; Balashev, K. P. Songstad, J. *Acta Chem. Scand.* **1995**, *49*, 335.

26. Brooks, J.; Babayan, Y.; Lamansky, S.; Djurovich, P. I.; Tsyba, I.; Bau, R.; Thompson, M. E. *Inorg. Chem.* **2002**, *41*, 3055.

27. Mdleleni, M. M.; Bridgewater, J. S.; Watts, R. J.; Ford, P. C. *Inorg. Chem.* **1995**, *34*, 2334.

28. Kovelenov, Y. A.; Blake, A. J.; George, M. W. Matousek, P.; Mel'nikov, M. Y.; Parker, A. W., Sun, X. Z.; Towrie, M.; Weinstein, J. A. *Dalton Trans.* **2005**, 2092.

29. Ma, B.; Djurovich, P.; Thompson, M. E. *Coord. Chem. Rev.* **2005**, *249*, 1501.

30. Ma, B.; Li, J.; Djurovich, P. I.; Yousufuddin, M.; Bau, R.; Thompson, M. E. *J. Am. Chem. Soc.* **2005**, *127*, 28.

31. Blanton, C. B.; Murtaza, Z.; Shaver, R. J.; Rillema, D. P. *Inorg. Chem.* **1992**, *31*, 3230.

32. Fernandez, S.; Fornies, J.; Gil, B.; Gomez, L. E. *Dalton Trans.* **2003**, 822.

33. Chan, C. W.; Lai, T. F.; Che, C. M.; Peng, S. M. *J. Am. Chem. Soc.* **1993**, *115*, 11245.

34. Constable, E. C.; Henney, R. P. G.; Leese, T. A.; Tocher, D. A. *J. Chem. Soc. Dalton Trans.* **1990**, 443.

35. Constable, E. C.; Henney, R. P. G.; Leese, T. A.; Tocher, D. A. *J. Chem. Soc. Chem. Commun.* **1990**, 513.

36. Cheung, T. C., Cheung, K. K.; Peng, S. M.; Che, C. M. *J. Chem. Soc. Dalton Trans.* **1996**, 1645.

37. Lai, S. W.; Chan, M. C. W.; Cheung, T. C.; Peng, S. M.; Che, C. M. *Inorg. Chem.* **1999**, *38*, 4046.

38. Neve, F.; Crispini, A.; Campagna, S. *Inorg. Chem.* **1997**, *36*, 6150.

39. Yip, J. H. K.; Suwarno, V. J. J. *Inorg. Chem.* **2000**, *39*, 3537.

40. Lu, W.; Zhu, N.; Che, C. M.; *Chem. Commun.* **2002**, 900

41. Lu, W.; Chan, M. C. W.; Zhu, N.; Che, C. M.; Li, C.; Hui, Z. *J. Am. Chem. Soc.* **2004**, *126*, 7639.

42. Wong, K. H.; Chan, M. C. W.; Che, C. M. *Chem. Eur. J.* **1999**, *5*, 2845.

43. Che, C. M.; Fu, W. F.; Lai, S. W.; Hou, Y. J.; Liu, Y. L. *Chem. Commun.* **2003**, 118.

44. Che, C. M.; Zhang, J. L.; Lin, L. R. *Chem. Commun.* **2002**, 2556.

45. Ma, D. L.; Che, C. M. *Chem. Eur. J.* **2003**, *9*, 6133.

46. Williams, J. A. G.; Beeby, A.; Davies, E. S.; Weinstein, J. A.; Wilson, C. *Inorg. Chem.* **2003**, *42*, 8609.

47. Sotoyama, W.; Satoh, T.; Sato, H.; Matsuura, A.; Sawatari, N. *J. Phys. Chem. A*, **2005**, *109*, 9760.

48. Cocchi, M.; Kalinowski, J.; Virgili, D.; Fattori, V.; Develay, S.; Williams, J. A. G. *Appl. Phys. Lett.* **2007**, *90*, 163508.

49. Farley, S. J.; Rochester, D. L.; Thompson, A. L.; Howard, J. A. K.; Williams, J. A. G. *Inorg. Chem.* **2005**, *44*, 9690.

50. Sotoyama, W.; Satoh, T.; Sawatari, N.; Inoue, H. *Appl. Phys. Lett.* **2005**, *86*, 153505.

51. Cocchi, M.; Virgili, D.; Fattori, V.; Rochester, D. L.; Williams, J. A. G. *Adv. Funct. Mater.* **2007**, *17*, 285.

52. Kalinowski, J.; Cocchi, M.; Virgili, D.; Fattori, V.; Williams, J. A. G. *Chem. Phys. Lett.* **2006**, *432*, 110.

53. Virgili, D.; Cocchi, M.; Fattori, V.; Sabatini, C.; Kalinowski, J.; Williams, J. A. G. *Chem. Phys. Lett.* **2006**, *433*, 145.

54. Cocchi, M.; Virgili, D.; Fattori, V.; Williams, J. A. G.; Kalinowski, J. *Appl. Phys. Lett.* **2007**, *90*, 023506.

55. Evans, R. C.; Douglas, P.; Williams, J. A. G.; Rochester, D. L. *J. Fluorescence*, **2006**, *16*, 201.

56. Okamoto, K.; Kanbara, T.; Yamamoto, T.; Wada, A. *Organometallics*, **2006**, *25*, 4026.

57. Song, D.; Wu, Q.; Hook, A.; Kozin, I.; Wang, S. *Organometallics*, **2001**, *20*, 4683.

58. Jude, H.; Krause Bauer, J. A.; Connick, W. B. *Inorg. Chem.* **2002**, *41*, 2275.

59. Jude, H.; Krause Bauer, J. A.; Connick, W. B. *Inorg. Chem.* **2004**, *43*, 725.

60. Cave, G. W. V.; Fanizzi, F. P.; Deeth, R. J.; Errington, W.; Rourke, J. P. *Organometallics*, **2000**, *19*, 1355.

61. Lu, W.; Chan, M. C. W.; Cheung, K. K.; Che, C. M. *Organometallics*, **2001**, *20*, 2477.

62. Kui, S. C. F.; Chui, S. S. Y.; Che, C. M.; Zhu, N. *J. Am. Chem. Soc.* **2006**, *128*, 8297.

63. Yam, V. W. W.; Tang, R. P. L.; Wong, K. M. C.; Lu, X. X.; Cheung, K. K.; Zhu, N. *Chem. Eur. J.* **2002**, *8*, 4066.

64. Kukushkin, V. Y.; Pombeiro, A. J. L.; Ferreria, C. M. P.; Elding, L. I. *Inorg. Synth.* **2002**, 33.

65. Sonogashira, K.; Fujikura, Y.; Toyoshima, N.; Takahashi, S.; Hagihara, N. *J. Organomet. Chem.* **1978**, *145*, 101.

66. James, S. L.; Younus, M.; Raithby, P. R.; Lewis, J. *J. Organomet. Chem.* **1997**, *543*, 233.

67. Yam, V. W. W.; Tang, R. P. L.; Wong, K. M. C.; Cheung, K. K. *Organometallics*, **2001**, *20*, 4476.

68. Miskowski, V. M.; Houlding, V. H. *Inorg. Chem.* **1989**, *28*, 1529.

69. Chan, C. W.; Cheng, L. K.; Che, C. M. *Coord. Chem. Rev.* **1994**, *132*, 87.

70. Ballhausen, C. J.; Bjerrum, N.; Dingle, R.; Eriks, K.; Hare, C. R. *Inorg. Chem.* **1965**, *4*, 514.

71. Balzani, V.; Carassiti, V. *J. Phys. Chem.* **1968**, *72*, 383.

72. McMillin, D. R.; Moore, J. J. *Coord. Chem. Rev.* **2002**, *229*, 113.

73. Caspar, J. V.; Meyer, T. J. *Inorg. Chem.* **1983**, *22*, 2444.

74. Hissler, M.; Connick, W. B.; Geiger, D. K.; McGarrah, J. E.; Lipa, D.; Lachicotte, R. J.; Eisenberg, R. *Inorg. Chem.* **2000**, *39*, 447.

75. Wadas, T. J.; Lachicotte, R. J.; Eisenberg, R. *Inorg. Chem.* **2003**, *42*, 3772.

76. Whittle, C. E.; Weinstein, J. A.; George, M. W.; Schanze, K. S. *Inorg. Chem.* **2001**, *40*, 4053.

77. McGarrah, J. E.; Eisenberg, R. *Inorg. Chem.* **2003**, *42*, 4355.

78. Pomestchenko, I. E.; Luman, C. R.; Hissler, M.; Ziessel, R.; Castellano, F. N. *Inorg. Chem.* **2003**, *42*, 1394.

79. Pomestchenko, I. E.; Castellano, F. N. *J. Phys. Chem. A*, **2004**, *108*, 3485.

80. Lai, S. W.; Chan, M. C. W.; Cheung, T. C.; Peng, S. M.; Che, C. M. *Inorg. Chem.* **1999**, *38*, 4046.

81. Lippard, S. *J. Acc. Chem. Res.* **1978**, *11*, 211.

82. Du. P.; Schneider, J.; Jarosz, P. Eisenberg, R. *J. Am. Chem. Soc.* **2006**, *128*, 7726.

83. Narayana-Prabhu, R.; Schmehl, R. H. *Inorg. Chem.* **2006**, *45*, 4319.

84. Zhang, D.; Wu, L. Z.; Zhou, L.; Han, X.; Yang, Q. Z.; Zhang, L. P.; Tung, C. H. *J. Am. Chem. Soc.* **2004**, *126*, 3440.

85. Shao, P.; Li, Y.; Azenkeng, A.; Hoffmann R. M.; Sun, W. *Inorg. Chem.* **2009**, *48*, 2407.

86. Ji, Z.; Li, Y.; Sun, W. *Inorg. Chem.* **2008**, *47*, 7599.

87. Shao, P.; Li, Y.; Sun, W. *J. Phys. Chem. A* **2008**, *112*, 1172.

88. Guo, F.; Sun, W. *J. Phys. Chem. B* **2006**, *110*, 15029.

89. Sun, W.; Wu, Z. X.; Yang, Q. Z.; Wu, L. Z.; Tung, C. H. *Appl. Phys. Lett.* **2003**, *82*, 850.

90. Guo, F.; Sun, W.; Liu, Y.; Schanze, K. *Inorg. Chem.* **2005**, *44*, 4055.

91. Pritchett, T. M.; Sun, W.; Guo, F.; Zhang, B.; Ferry, M. J.; Rogers-Haley, J. E.; Shensky, W.; Mott, A. G. *Opt. Lett.* **2008**, *33*, 1053.

92. Shao, P.; Li, Y.; Sun, W. *Organometallics* **2008**, *27*, 2743.

93. Sun, W.; Guo, F. *Chin. Opt. Lett.* **2005**, *S3*, S34.

94. Li, Y.; Pritchett, T. M.; Shao, P.; Haley, J.; Zhu, H.; Sun, W. *J. Organometallic Chem.* **2009**, *694*, 3688.

95. Shao, P.; Sun, W. *Inorg. Chem.* **2007**, *46*, 8603.

96. P. Shao, P.; Li. Y.; Azenkeng, A.; Hoffmann, M. R.; Sun, W. *Inorg. Chem.* **2009**, *48*, 2407.

97. Connick, W. B.; Henling, L. M.; Marsh, R. E. *Acta Crystallogr* **1996**, *52*, 817.

98. Che, C. M.; He, L. Y.; Poon, C. K.; Mak, T. C. W. *Inorg. Chem.* **1989**, *28*, 3081.

99. Kato, M.; Kosuge, C.; Morii, K.; Ahn, J. S.; Kitagawa, H.; Mitani, T.; Matsushita, M.; Kato, T.; Yano, S.; Kimura, M. *Inorg. Chem.* **1999**, *38*, 1638.

CHAPTER 2.

SYNTHESIS AND PHOTOPHYSICS OF PLATINUM(II) 6-PHENYL-4-(9,9-DIHEXYLFLUOREN-2-YL)-2,2'-BIPYRIDINE COMPLEXES WITH PHENOTHIAZINYL ACETYLIDE LIGAND

2.1. Introduction

In recent years, square-planar platinum (II) complexes have attracted great attention because of their unique photophysical properties,[1-2] such as room temperature phosphorescence in solutions, multiple charge transfer states, and broadband excited-state absorption, which lead to a variety of potential applications in areas like organic light emitting diodes (OLEDs),[3-9] chemosensing,[10-11] photocatalysis,[12-14] photovoltaic cells,[15-17] and nonlinear optics *etc.*[18-30] The unique photophysical properties and the variety application of the platinum complexes mainly arise from their square-planar configuration, the intramolecular charge transfer characteristics, and the heavy-atom effect from the platinum that enhances intersystem crossing (ISC) rate to the triplet excited state.

Among these promising applications, our group is particularly interested in the nonlinear absorption of the square-planar platinum terpyridyl and 6-phenyl-2,2'-bipyridyl complexes because of the broadband excited-state absorption in these complexes, the long-lived triplet excited state, the ease of structural modification, and the thermal and photochemical stability of these complexes.[18-30] Among the platinum complexes studied in our group, platinum complexes with 6-phenyl-2,2'-bipyridyl ligand have been demonstrated to exhibit the broadest triplet excited-state absorption in the visible to the near-IR region, and a strong reverse saturable absorption (RSA) for ns laser pulses at 532

nm was observed.[18, 20, 22, 27-30] However, the potential application of these complexes on photonic devices that require broadband spectral response is limited because essentially no ground-state absorption of these complexes above 600 nm, which prevents the population of the triplet excited state via one-photon absorption. To solve this problem, one possible solution is to shift the low-energy absorption band, *i.e.* charge transfer band, to longer wavelength. According to the studies reported in the literature, one of the methods to bathochromically shift the charge-transfer band is to incorporate an electron-donating acetylide ligand into the platinum complex.[23,31] However, if the electron-donating ability of the acetylide ligand is too strong, such as the dimethylaminophenyl acetylide ligand, it would alter the nature of the lowest excited state of the platinum terpyridyl complex from a metal-to-ligand charge transfer state to a ligand-to-ligand charge transfer state, which exhibits no triplet excited-state absorption.[23,32,33] Therefore, it is critical to select an appropriate acetylide ligand that would cause a red-shift of the low-energy absorption band while maintaining the triplet excited-state absorption. For this purpose, phenothiazinyl (PTZ) acetylide ligand was chosen for this work because Eisenberg and co-workers reported that using this ligand as an electron donor in platinum terpyridyl dyad and triad induces intramolecular charge transfer while the complex still show broadband triplet excited-state absorption.[34-36] On the other hand, 6-phenyl-4-(9,9-dihexylfluoren-2-yl)-2,2'-bipyridine is selected as the terdentate ligand because our previous study shows that platinum chloride complex containing this ligand exhibits strong reverse saturable absorption at 532 nm as a result of its long triplet excited-state lifetime and broad excited-state absorption in the visible to the near-IR region.[30] In addition, although it has been reported that platinum (II) 2,6-bis(*N*-alkylbenzimidazol-2'-yl)pyridine complexes can be

fabricated as Langmuir-Blodgett (LB) films,[37-42] few study has been carried out on Pt(C^N^N) complexes.[38] Due to the highly ordered nature of the LB films, the intermolecular interaction of the platinum complexes in LB films may be different from that in solutions. The presence of the alkoxyl substituent on the C^N^N ligand could make the complex amphiphilic, which make it feasible to prepare LB films of the complex.

Taken into account all these factors, we recently synthesized two new platinum 6-phenyl-4-(9,9-dihexylfluoren-2-yl)-2,2'-bipyridine complexes with phenothiazinyl acetylide ligand. The structure of the complexes and the synthetic route are shown in Scheme 2.3. Photophysics of these two complexes are systematically investigated, and the reverse saturable absorption of these two complexes at 532 nm is demonstrated.

2.2. Experimental Section

The details of experiments will be explained in this section. The synthetic route and the experimental details for the complexes will be discussed first. Then the photophysical measurements for the complexes are presented.

2.2.1. Synthesis

All the reagents were purchased from Aldrich and Alfa Aesar and used without further purification. All solvent were purchase from VWR Scientific Company with analytical grade, and used without further purification unless otherwise stated. The silica gel (230×400 mesh) was purchased from Sorbent Technologies Company. All products were characterized by ^{1}H NMR, elemental analysis, and high resolution MS. ^{1}H NMR spectra were obtained using a Varian 300 MHz, 400 MHz or 500 MHz NMR spectrometer.

Elemental analysis were conducted by NuMega Resonance labs, Inc. in San Diego, CA. High resolution MS data was obtained using Bruker Bio Tof III mass spectrometer.

The synthetic route for 6-phenyl-4-(9,9-dihexylfluoren-2-yl)-2,2'-bipyridine Pt(II) chloride is outlined in Scheme 2.1.

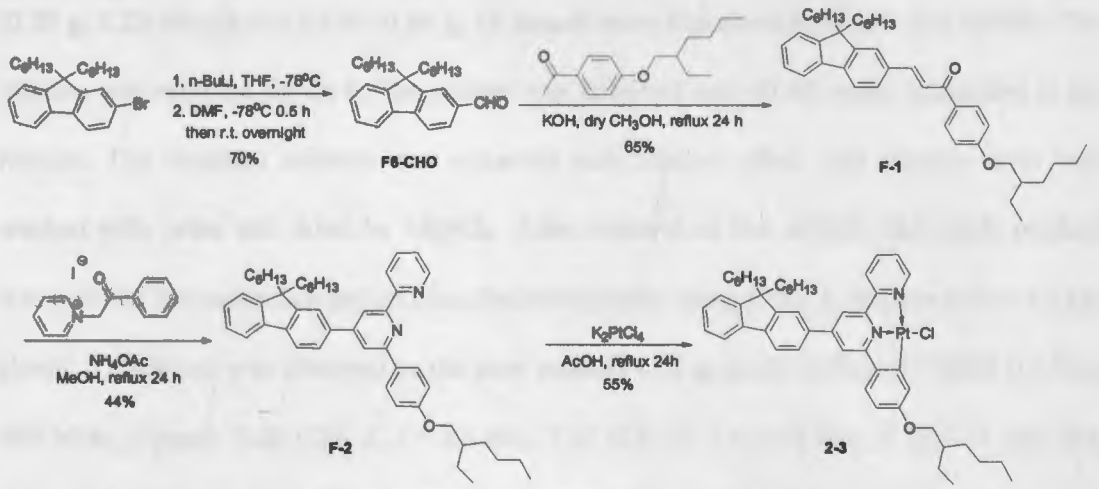

Scheme 2.1. Synthetic route for 6-phenyl-4-(9,9-dihexylfluoren-2-yl)-2,2'-bipyridine Pt(II) chloride (**2-3**).

9,9-Dihexylfluorene-2-carboxaldehyde (F6-CHO)[30]

A mixture of 9,9-dihexylfluorenyl-2-bromide (4.13 g, 0.01 mol) in 50 ml dried THF was cooled to -78 °C under argon, *n*-BuLi (5 ml, 2.5 M in hexane) was added. At -78 °C 1 ml DMF was added into the reaction mixture. 1 hour later, the reaction mixture was warmed up to room temperature and stirred overnight. After removal of the solvent, the residue was dissolved in DCM and washed with brine for 3 times. The crude product was purified through silica gel column chromatography using hexane/CH_2Cl_2 (v/v = 2/1) as eluent. Pale yellow oil was obtained as pure product (2.5 g, yield: 70%). ^{1}H NMR ($CDCl_3$, 400 MHz, δ ppm): 10.05 (1H, s), 7.86 (1H, d, J = 0.8 Hz), 7.84 – 7.83 (2H, m), 7.78 – 7.75

(1H, m), 7.39 – 7. 34 (3H, m), 2.02 – 1.97 (4H, m), 1.10 – 0.97 (12H, m), 0.74 (6H, t, J = 7.2 Hz), 0.60 – 0.52 (4H, m).

Compound F-1[30]

Compound **F6-CHO** (1.17 g, 3.23 mol), 1-[4-(2-ethyl-hexyloxy)-phenyl]-ethanone (0.80 g, 3.23 mmol) and KOH (0.84 g, 15 mmol) were dissolved in 80 mL dry MeOH. The mixture was refluxed for 24 h. The solvent was removed and 40 ml water was added to the residue. The resultant mixture was extracted with diethyl ether. The organic layer was washed with brine and dried by $MgSO_4$. After removal of the solvent, the crude product was purified through silica gel column chromatography using CH_2Cl_2/hexane (v/v = 1/1) as eluent. Yellow oil was obtained as the pure product (1.2 g, yield: 65%). ^{1}H NMR ($CDCl_3$, 400 MHz, δ ppm): 8.09 (2H, d, J = 8.4 Hz), 7.93 (1H, d, J = 15.6 Hz), 7.73-7.71 (2H, m), 7.66 – 7.59 (3H, m), 7.34 (3H, d, J = 2.4 Hz), 7.00 (2H, d, J = 8.4 Hz), 3.93 (2H, d, J = 5.4 Hz), 2.04 – 1.98 (4H, m), 1.77 – 1.75 (1H, m), 1.54 – 1.33 (8H, m), 1.14 – 1.05 (12H, m), 0.86 – 0.97 (6H, m), 0.78 – 0.73 (6H, m), 0.63 (4H, s). ESI-HRMS: m/z calcd for $[C_{42}H_{57}O_2]^+$: 593.4353; found, 593.4363. Anal. Calcd (%) for $C_{42}H_{57}O_2 \cdot C_6H_{14}$: C 84.90, H 10.39, N 0.00; found: C 85.35, H 10.70, N 0.14.

Compound F-2[30]

Compound **F-1** (0.75 g, 1.26 mmol), pyridacylpyridinium iodide (0.41 g, 1.26 mmol) and NH_4OAc (1g, 13 mmol) were dissolved in 20 ml MeOH. The mixture was refluxed for 24 hrs. The solvent was removed and the residue was dissolved in diethyl ether. Then it was washed with brine for 3 times. After removal of the solvent, the crude product was purified through silica column chromatography using CH_2Cl_2/hexane (v/v = 1/1) as eluent. Pale yellow oil was obtained as the pure product (0.50 g, yield: 65%). ^{1}H NMR ($CDCl_3$,

500 MHz, δ ppm): 8.73 (1H, d, J = 4.8 Hz), 8.68 (1H, d, J = 7.8 Hz), 8.61 (1H, d, J = 1.2 Hz), 8.17 (2H, d, J = 8.7 Hz), 7.97 (1H, d, J = 1.2 Hz), 7.90 – 7.84 (1H, m), 7.80 (2H, t, J = 1.2 Hz), 7.76 – 7.73 (2H, m), 7.37 – 7.32 (4H, m), 7.05 (2H, d, J = 9 Hz), 3.93 (2H, d, J = 5.7 Hz), 2.05 – 2.00 (4H, m), 1.80 – 1.73 (1H, m), 1.55 – 1.33 (8H, m), 1.14 – 1.05 (12H, m), 0.97 – 0.91 (6H, m), 0.75 (6H, t, J = 6.3 Hz), 0.66 – 0.64 (4H, m). ESI-HRMS: m/z calcd for $[C_{49}H_{61}N_2O]^+$: 693.4778; found, 693.4809. Anal. Calcd (%) for $C_{49}H_{60}ON_2 \cdot 1/3CCl_2H_2$: C 82.14, H 8.48, N 3.88; found: C 82.23, H 8.27, N 3.56.

Compound 2-3[30]

Compound **F-2** (0.27 g, 0.39 mmol) and K_2PtCl_4 (0.16 g, 0.39 mmol) were dissolved in 60 ml AcOH. The mixture was refluxed for 24 h. After removal of the solvent, the residue was dissolved the in CH_2Cl_2, then washed by $NaHCO_3$ solution and brine. The organic layer was dried by $MgSO_4$. After removal of the solvent, the crude product was purified by silica gel column chromatography using CH_2Cl_2 as eluent. The pure product was obtained via recrystallization from CH_2Cl_2/ethanol as orange crystal (0.18 g, yield: 55%). ^{1}H NMR ($CDCl_3$, 500 MHz, δ ppm): 8.72 (1H, d, J = 5.1 Hz), 7.82 – 7.77 (5H, m), 7.71 (1H, d, J = 8.1 Hz), 7.46 (1H, s), 7.39 – 7.36 (3H, m), 7.23 – 7.18 (2H, m), 7.15 (1H, d, J = 8.4 Hz), 6.98 (1H, d, J = 2.4 Hz), 6.49 (1H, d, J = 8.4 Hz), 3.72 (2H, d, J = 5.7 Hz), 2.12 – 2.06 (4H, m), 1.72 – 1.67 (1H, m), 1.51 – 1.26 (8H, m), 1.15 – 1.05 (12H, m), 0.90 – 0.85 (6H, m), 0.79 – 0.72 (10H, m). ESI-HRMS: m/z calcd for $[C_{49}H_{59}N_2OPt+CH_3CN]^+$: 927.4539; found, 927.4551. Anal. Calcd (%) for $C_{49}H_{59}ClN_2OPt$: C 63.79, H 6.45, N 3.04; found: C 64.03, H 6.80, N 3.04.

The synthetic route for 4-ethynylbenzyl-*N*-phenothiazine (**2-1**) and 10-(prop-2-ynyl)-10H-phenothiazine (**2-2**) is outlined in Scheme 2.2.

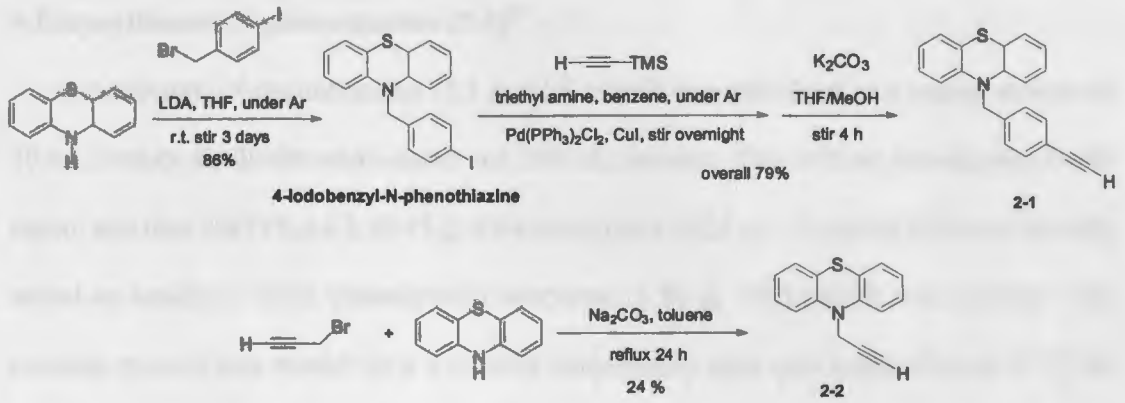

Scheme 2.2. Synthetic route for acetylide ligand 4-ethynylbenzyl-*N*-phenothiazine (**2-1**) and 10-(prop-2-ynyl)-10H-phenothiazine (**2-2**).

4-Iodobenzyl-*N*-phenothiazine[43]

Under argon atmosphere 7.5 mL 2M lithium diisopropylamide (LDA) at ~ 0 °C was added to the 30 mL THF solution of 3.0 g (15 mmol) phenothiazine. The bright yellow solution was allowed to warm up to room temperature. *p*-Iodobenzylbromide (4.5 g, 15 mmol) dissolved in 30 mL of THF was added via cannula to the stirred solution. The solution turned to reddish-brown within a few minutes and was kept stirring for 3 days. The reaction was monitored by TLC. After removal of the solvent, the residue was dissolved in 200 mL CH_2Cl_2 and washed with brine for 3 times. The organic layer was dried over $MgSO_4$. After removal of the solvent, the crude product was purified through silica gel column chromatography using hexane as eluent. Yellow solid was obtained as the pure product (5.4 g, yield: 86 %). ^{1}H NMR ($CDCl_3$, 300 MHz, δ ppm): 7.67 (2H, d, J = 8.1 Hz), 7.17 (2H, dd, J_1 = 7.2 Hz, J_2 = 1.5 Hz), 7.10 (2H, d, J = 8.4 Hz), 7.03 (2H, t, J = 7.2 Hz), 6.93 (2H, t, J =7.2 Hz), 9.65 (2H, d, J = 8.1 Hz), 5.02 (s, 2H).

4-Ethynylbenzyl-*N*-phenothiazine (2-1)[43]

4-Iodobenzyl-*N*-phenothiazine (5.3 g, 12.7 mmol) was dissolved in a mixed solvent of 40 mL freshly distilled triethyl amine and 200 mL benzene. The mixture was degassed with argon, and then $Pd(PPh_3)_2Cl_2$ (0.45 g, 0.64 mmol) and (0.24 g, 1.3 mmol) CuI were quickly added as catalysts. Then trimethylsilyl acetylene (1.91 g, 19.0 mmol) was injected. The reaction mixture was stirred for 4 h at room temperature, then was warmed up to 45 °C for 20 hrs. After removal of the solvent, the crude product was purified through silica gel column chromatography using CH_2Cl_2/hexane (v/v = 1:1) as eluent. The pale yellow oil intermediate was obtained, and was used for the next reaction immediately. It was dissolved in the mixed solvent of THF/MeOH = 100 mL/100 mL. The reaction mixture was degassed and stirred with 1.78 g K_2CO_3 for 4 hours. Then the solution was quenched with icy water. After removal of the solvent, the residue was dissolved in CH_2Cl_2, and washed with brine for 3 times. The organic layer was dried with Na_2SO_4. After removal of the solvent, the crude product was purified through silica gel column chromatograph using hexane as eluent. Pale yellow oil was obtained as the pure product (3.17 g, yield: 79%). ^1H NMR ($CDCl_3$, 300 MHz, δ ppm): 7.52 (2H, d, J = 8.1 Hz), 7.32 (2H, d, J = 8.1 Hz), 7.18 (2H, dd, J_1 = 7.8 Hz, J_2 = 1.5 Hz), 7.03 (2H, td, J_1 = 7.5 Hz, J_2 = 1.2 Hz), 6.94 (2H, td, J_1 = 7.2 Hz, J_2 = 1.2 Hz), 6.65 (2H, d, J = 8.1 Hz), 5.08 (2H, s), 3.13 (1H, s).

10-(prop-2-ynyl)-10H-phenothiazine (2-2)[43]

Phenothiazine (5.0 g, 25.0 mmol) was dissolved in 50 ml anhydrous toluene under nitrogen. Sodium carbonate (3.98 g, 37.5 mmol) was added into the clear solution. After stirring for 1h, propargyl bromide (13.3 g, 125.5 mmol) was added. The mixture was refluxed for 24 h and then mixed with 2 M hydrochloride acid until the solution was acidic.

After removal of the solvent, the residue was dissolved in CH_2Cl_2, and washed by brine for 3 times. The organic layer was dried over Na_2SO_4. After removal of the solvent the crude product was purified through silica gel column chromatography using toluene as eluent. Pale yellow oil was obtained as the pure product (1.4 g, yield: 24%). ^1H NMR ($CDCl_3$, 300 MHz, δ ppm): 7.34 – 7.25 (8H, m), 4.56 (2H, d, J = 2.4 Hz), 2.55 (1H, t, J = 2.4 Hz).

The synthetic routes for 6-phenyl-4-(9,9-dihexylfluoren-2-yl)-2,2'-bipyridine Pt(II) 4-ethynylbenzyl-*N*-phenothiazine (**2-4**) and 6-phenyl-4-(9,9-dihexylfluoren-2-yl)-2,2'-bipyridine Pt(II) 10-(prop-2-ynyl)-10H-phenothiazine (**2-5**) are shown in Scheme 2.3.

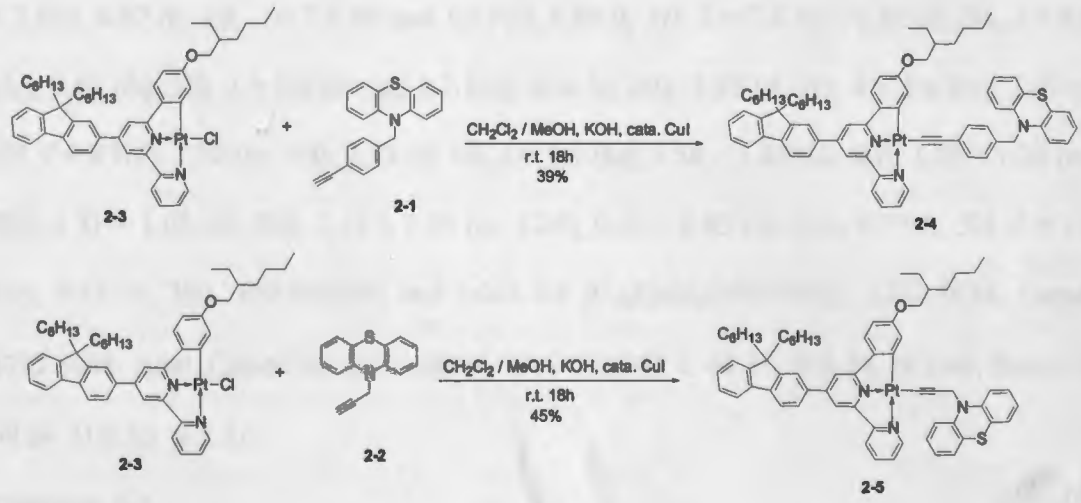

Scheme 2.3. Synthetic route for C^N^N Pt(II) complexes 6-phenyl-4-(9,9-dihexylfluoren-2-yl)-2,2'-bipyridine Pt(II) 4-ethynylbenzyl-N-phenothiazine (**2-4**) and 6-phenyl-4-(9,9-dihexylfluoren-2-yl)-2,2'-bipyridine Pt(II) 10-(prop-2-ynyl)-10H-phenothiazine (**2-5**).

Complex 2-4

Complex **2-3** (0.18 g, 0.20 mmol), compound **2-1** (0.08 g, 0.25 mmol), KOH (0.02 g, 0.36 mmol), and catalytic amount of CuI were dissolved in a mixed solvent of CH_2Cl_2 and CH_3OH (v / v = 50 mL / 30mL). The reaction mixture was stirred at room temperature for 18 hrs. After removal of solvent, the residue was dissolved in CH_2Cl_2, and then washed

with brine three times to remove KOH. The CH_2Cl_2 layer was combined and dried over Na_2SO_4. The solvent was then removed and the crude product was purified by chromatography on a silica gel column using CH_2Cl_2 as the eluent. The pure product was obtained by recrystalization from CH_2Cl_2/ethanol to give 98 mg dark red solid (yield: 39%). ^1H NMR ($CDCl_3$, 400 MHz, δ ppm): 9.26 (d, 1H, J = 4.8 Hz), 8.03 (t, 1H, J = 7.6 Hz), 7.97 (d, 1H, J = 8.4 Hz), 7.80 (d, 1H, J = 8.0 Hz), 7.74 (t, 1H, J = 2.8 Hz), 7.67 (t, 2H, J = 3.8 Hz), 7.60 (d, 2H, J = 6.4 Hz), 7.57 (d, 1H, J = 2.8 Hz), 7.51 (d, 3H, J = 7.2 Hz), 7.40 (d, 1H, J = 7.6 Hz), 7.35 (d, 3H, J = 3.2 Hz), 7.18 (d, 2H, J = 7.6 Hz), 7.06 (dt, 2H, J = 7.6 Hz and 1.2 Hz), 6.97 (tt, 2H, J = 7.2 Hz and 1.2 Hz), 6.84 (t, 2H, J = 7.6 Hz), 6.67 (d, 2H, J = 8.0 Hz), 6.61 (dd, 1H, J = 7.6 Hz and 1.2 Hz), 5.06 (s, 2H), 3.93 (d, 2H, J = 5.6 Hz), 2.02 (t, 4H, J = 8 Hz), 1.72 (m, 1H), 1.51 (d, 1H, J = 1.6 Hz), 1.50 – 1.37 (m, 4H), 1.29 – 1.26 (m, 5H), 1.31 – 1.05 (m, 5H), 1.31 – 1.05 (m, 12H), 0.89 – 0.83 (m, 6H), 0.75 (t, 5H, J = 7.2 Hz), 0.65 (s, 3H). ESI-HRMS: *m/z* calcd for $[C_{70}H_{73}N_3OPtS+Na]^+$: 1222.5034; found, 1222.5048. Anal. Calcd (%) for $C_{70}H_{73}N_3OPtS{\cdot}CH_3OH$: C 69.16, H 6.74, N 3.46; found: C 69.24, H 6.30, N 3.41.

Complex 2-5

Complex **2-3** (0.18 g, 0.20 mmol), compound **2-2** (0.11 g, 0.30 mmol), KOH (0.02 g, 0.36 mmol), and catalytic amount of CuI were dissolved in a mixed solvent of CH_2Cl_2 and CH_3OH (v/v = 50 mL/30 mL). The reaction mixture was stirred at room temperature for 18 hrs. After removal of solvent, the residue was dissolved in CH_2Cl_2, and then washed with brine three times to remove KOH. The CH_2Cl_2 layer was combined and dried over Na_2SO_4. The solvent was then removed and the crude product was purified by chromatography on a silica gel column using CH_2Cl_2 as the eluent. The pure product was obtained by

recrystalization from CH_2Cl_2/ethanol to give 102 mg dark red solid (yield: 46%). ^1H NMR ($CDCl_3$, 400 MHz, δ ppm): 8.58 (d, 1H, J = 4.8 Hz), 7.74 (d, 2H, J = 8.4 Hz), 7.67 (d, 2H, J = 7.6 Hz), 7.58 (t, 2H, J = 3.8 Hz), 7.55 (s, 1H), 7.84 (d, 2H, J = 8.4 Hz), 7.33 – 7.29 (m, 4H), 7.14 – 7.05 (m, 6H), 6.90 (dd, 1H, J = 8.8 Hz and 4.8 Hz), 6.83 (t, 2H, J = 7.6 Hz), 6.36 (dd, 1H, J = 8.4 Hz and 2.4 Hz), 4.84 (s, 2H), 3.43 (d, 2H, J = 5.2 Hz), 1.97 (t, 4H, J = 8.0 Hz), 1.47 – 1.43 (m, 1H), 1.36 – 1.16 (m, 10H), 1.09 - 1.00 (m, 12H), 0.84 – 0.75 (m, 6H), 0.69 (t, 5H, J = 6.8 Hz), 0.62 (s, 3H). ESI-HRMS: *m/z* calcd for $[C_{64}H_{69}N_3OPtS+Na]^+$, 1145.4706; found, 1145.4662. Anal. Calcd (%) for $C_{64}H_{69}N_3OPtS{\cdot}CH_3OH$: C 67.15, H 6.59, N 3.54; found: C 67.57, H 6.37, N 3.64.

2.2.2. Photophysical Measurements

The UV-vis absorption spectra were measured on an Agilent 8453 spectrophotometer in a 1-cm quartz cuvette in different HPLC-grade solvents. The steady state emission spectra were obtained using a SPEX fluorolog-3 fluorometer/phosphorometer. The emission quantum yields were measured by the comparative method[44] in degassed toluene solution. A degassed $[Ru(bpy)_3]Cl_2$ in aqueous solution (Φ_{em} = 0.042, λ_{ex} = 436 nm)[45] was used as the reference. The excited-state lifetime, triplet excited-state quantum yield and the triplet transient difference absorption spectra were gained in toluene solutions on an Edinburgh LP920 laser flash photolysis spectrometer. The third harmonic output (355 nm) of a Nd:YAG laser (Quantel Brilliant, pulse width (fwhm) = 4.1 ns, the repetition rate was set at 1 Hz) was used as the excitation source. Each sample was purged with Ar for 30 min prior to each measurement.

The triplet excited-state absorption coefficient and the triplet excited-state formation quantum yield were measured using partial saturate method.[46]

2.2.3. Nonlinear Transmission Measurement

The experimental setup was similar to that had been described previously.[29] The second harmonic (λ = 532 nm) of a 4.1 ns (fwhm), 10 Hz, Q-switched Quantel Brilliant Nd:YAG laser was used as the light source. The laser beam was focused by a f = 30 cm planoconvex lens to the center of a 2 mm thick quartz cuvette that contained the sample solution. The radius of the beam waist was approximately 75 μm. Two Molectron J4-09 pyroelectric probes and an EPM2000 energy/power meter were used to monitor the incident and output energies.

2.2.4. LB Film Preparation

Surface pressure-mean molecular area isotherm measurement and LB film preparation were carried out by using a KSV minitrough (Teflon coating, 7.5×30×1 cm^3). The trough and the barriers were cleaned using ethanol and ultra pure water with a resistance of 18 MΩ·cm. Both of **2-4** and **2-5** were dissolved in HPLC-grade $CHCl_3$ solvent for the surface pressure – mean molecular area measurement (c = 1.16 mmol/mL for **2-4** and 0.78 mmol/mL for **2-5**). 50 μl of solution was spread on ultra pure water subphase at 25 ± 1 °C and was left for 25 mins. for $CHCl_3$ to evaporate. The compression rate was kept at 5 mm/min. The isotherm measurement for each sample was repeated at least twice.

The LB films of **2-4** and **2-5** were deposited on hydrophilic glass slides using a dipping method with the transfer ratio in a range of 0.6 – 1. The glass slides were cleaned using detergent and water first, followed by soaking in concentrated H_2SO_4 for at least 1 hr. This would make the surfaces hydrophilic before the deposition. The slides were then cleaned by ultra pure water.

The surface morphology of the films prepared was studied by AFM technique using the tapping mode of a Veeco DI-3100 with a silicon nitride probe.

2.3. Results and Discussion

2.3.1. UV-Vis Absorption

The electronic absorption spectra of **2-4** and **2-5** in dichloromethane solution are shown in Figure 2.1. The absorptions for both complexes follow Beer-Lambert's law in the concentration range from 10^{-6} to 10^{-4} mol/L, illustrating that no aggregation occurs in this concentration range. Both complexes exhibit intense high-energy absorption bands at 250-390 nm, which are attributed to the $^1\pi,\pi^*$ transitions within the fluorenyl substituted C^N^N ligand and the BTZ acetylide ligand. The broad low-energy band in the range of 400-500 nm can be tentatively assigned as the ^{1}MLCT/^{1}LLCT transitions with reference to the similar band in other platinum terpyridyl or C^N^N acetylide complexes.[5,19,23,31,47,48] The ^{1}MLCT/^{1}LLCT band in **2-4** is slightly broader than that in **2-5**. This could be due to the presence of the stronger π-donating benzene ring in the acetylide ligand of **2-4**, which could lower the ^{1}LLCT transition slightly. The charge transfer nature of the low-energy absorption band could be supported by the negative solvatochromic effect for these two complexes in different polarity solvents (demonstrated in Figure 2.2). Low-polarity solvents, such as toluene and dichloromethane, cause an pronounced bathochromic shift in the low-energy absorption band in comparison to that in more polar solvents, such as CH_3CN. This indicates that the ground states of both complexes are more polar than that of the excited states, which is a characteristic of a charge-transfer transition.

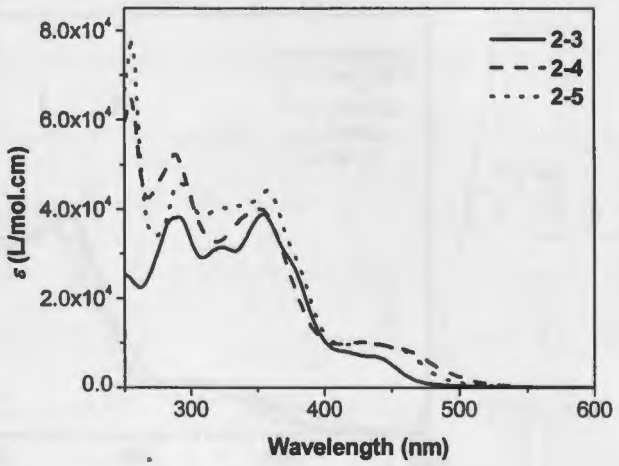

Figure 2.1. UV-vis absorption spectra of 5×10^{-5} mol/L dichloromethane solutions of 6-phenyl-4-(9,9-dihexylfluoren-2-yl)-2,2'-bipyridine Pt(II) chloride (**2-3**), 6-phenyl-4-(9,9-dihexylfluoren-2-yl)-2,2'-bipyridine Pt(II) 4-ethynylbenzyl-*N*-phenothiazine (**2-4**) and 6-phenyl-4-(9,9-dihexylfluoren-2-yl)-2,2'-bipyridine Pt(II) 10-(prop-2-ynyl)-10H-phenothiazine (**2-5**).

In comparison to the UV-vis absorption of the corresponding platinum chloride complex **2-3**, the low-energy absorption band of **2-4** and **2-5** is 23 nm and 12 nm red-shifted, respectively. This is the result of the electron donating PTZ acetylide ligand, which not only causes the red-shift of the ^{1}MLCT band due to the reduced energy gap between the destabilized platinum base HOMO and the N^N based LUMO, but also admixes ^{1}LLCT character into the lowest excited state. In addition, the molar extinction coefficients of **2-4** and **2-5** are somewhat larger than those of **2-3**, reflecting the interactions between the C^N^N ligand and the fluorenyl component as well as the influence of the electron-donating acetylide ligand.

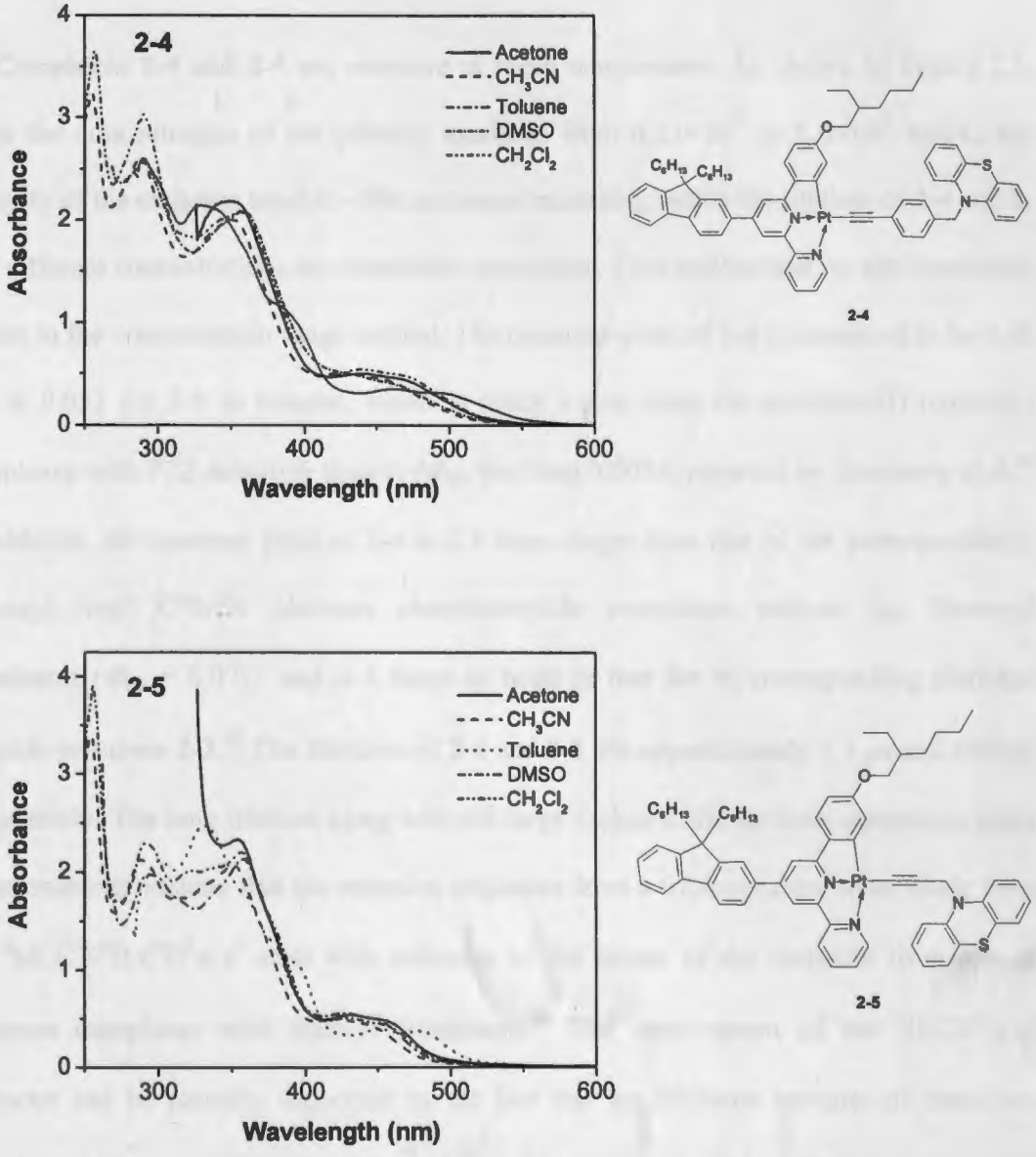

Figure 2.2. UV-vis absorption spectra of 5×10^{-5} mol/L solution of 6-phenyl-4-(9,9-dihexylfluoren-2-yl)-2,2'-bipyridine Pt(II) 4-ethynylbenzyl-*N*-phenothiazine (**2-4**) and 6-phenyl-4-(9,9-dihexylfluoren-2-yl)-2,2'-bipyridine Pt(II) 10-(prop-2-ynyl)-10H-phenothiazine (**2-5**) in different solvents measured in a 1-cm cuvette at room temperature.

2.3.2. Emission

Complexes **2-4** and **2-5** are emissive at room temperature. As shown in Figure 2.3, when the concentration of the solution increases from 6.25×10^{-6} to 5.0×10^{-5} mol/L, the intensity of the emission band at ~590 nm keeps increasing; while the lifetime of **2-4** and **2-5** at different concentrations are essentially unchanged. This implies that no self-quenching occurs in the concentration range studied. The quantum yield of **2-4** is measured to be 0.18 and is 0.053 for **2-5** in toluene, which is much higher than the platinum(II) terpyridyl complexes with PTZ acetylide ligands (Φ_{em} less than 0.0024) reported by Eisenberg et al.[34] In addition, the quantum yield of **2-4** is 2-3 times larger than that of the correspondingly "alkoxyl free" C^N^N platinum phenylacetylide complexes without the fluorenyl substituent (Φ_{em} = 0.07),[5] and is 4 times as large as that for its corresponding platinum chloride precursor **2-3**.[30] The lifetimes of **2-4** and **2-5** are approximately 1.3 μs and 600 ns, respectively. The long lifetime along with the large Stokes shifts for both complexes make it reasonable to assume that the emission originates from a triplet excited state, likely from the ^{3}MLCT/^{3}ILCT/$^3\pi,\pi^*$ state with reference to the nature of the emission from related platinum complexes with alkoxyl substituent.[18] The involvement of the ^{3}ILCT/$^3\pi,\pi^*$ character can be partially supported by the fact that the emission energies of these two complexes are essentially the same, and they are similar to that of their corresponding precursor **2-3**.[30] This similarity indicates that the acetylide ligand has negligible effect on the emission energy, thus the emitting state should primarily be related to the fluorenyl C^N^N platinum component. This phenomenon is similar to that of the platinum C^N^N complexes with alkoxyl substituent.[18]

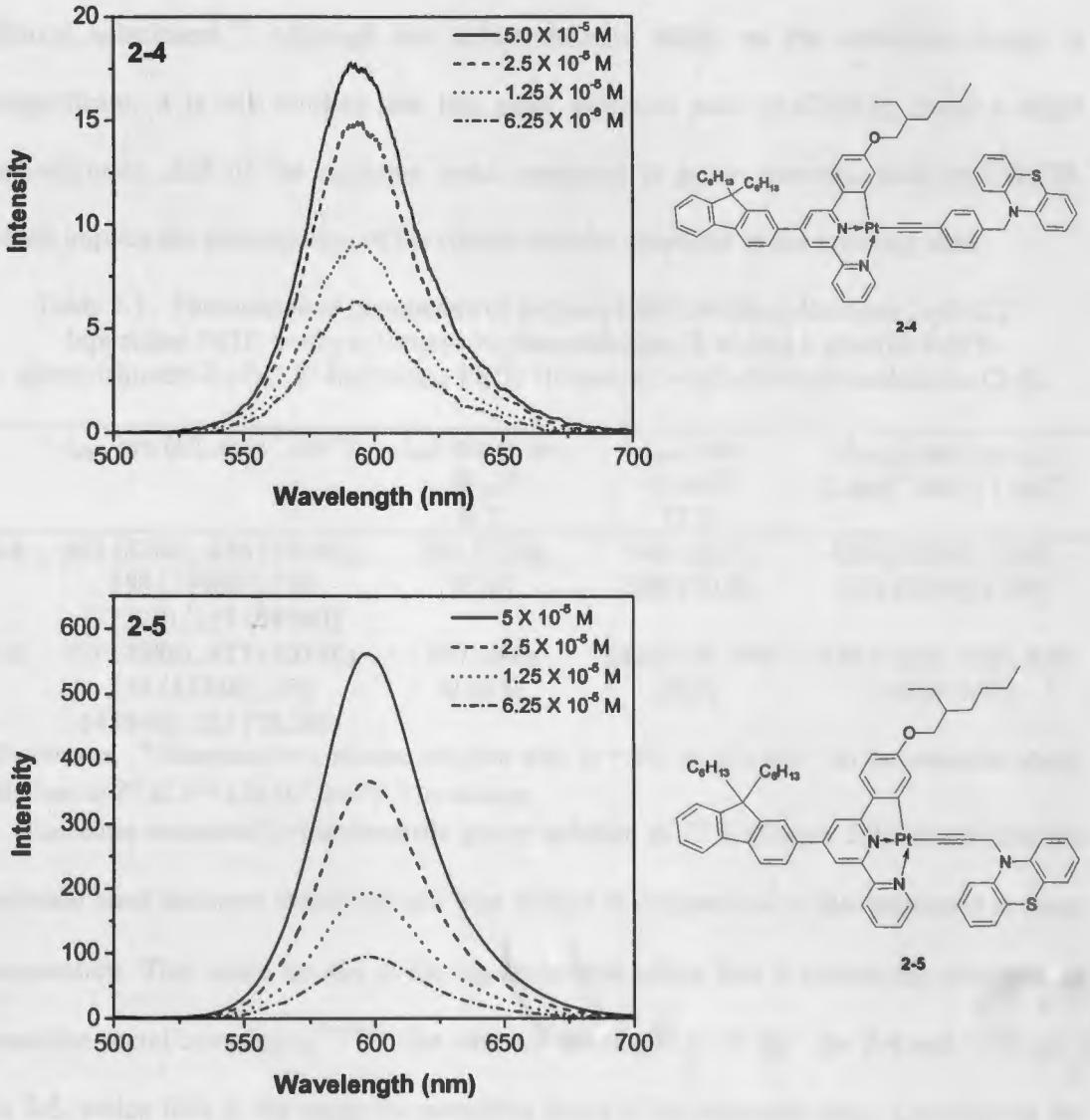

Figure 2.3. Concentration-dependent emission spectra of 6-phenyl-4-(9,9-dihexylfluoren-2-yl)-2,2'-bipyridine Pt(II) 4-ethynylbenzyl-*N*-phenothiazine (**2-4**) (λ_{ex} = 462 nm) and 6-phenyl-4-(9,9-dihexylfluoren-2-yl)-2,2'-bipyridine Pt(II) 10-(prop-2-ynyl)-10H-phenothiazine (**2-5**) (λ_{ex} = 479 nm) in toluene at room temperature.

Another piece of evidence that supports the admixture of the ^{3}ILCT/$^3\pi,\pi^*$ character into the emitting state arises from the minor solvent effect on the emission energy, as listed in Table 2.2 for **2-4** and **2-5** in different solvents. This reflects the delocalization of the

emitting state and is consistent with that observed in the platinum C^N^N complexes with alkoxyl substituent.[18] Although the solvatochromic effect on the emission energy is insignificant, it is still evident that less polar solvents, such as CH_2Cl_2, cause a slight bathochromic shift of the emission band compared to polar solvents, such as CH_3CN, which implies the participation of the charge transfer character in the emitting state.

Table 2.1. Photophysical parameters of 6-phenyl-4-(9,9-dihexylfluoren-2-yl)-2,2'-bipyridine Pt(II) 4-ethynylbenzyl-N-phenothiazine (**2-4**) and 6-phenyl-4-(9,9-dihexylfluoren-2-yl)-2,2'-bipyridine Pt(II) 10-(prop-2-ynyl)-10H-phenothiazine (**2-5**).

	λ_{abs} /nm (ε/L.mol^{-1}.cm^{-1})[a]	λ_{em}/ nm (τ /ns; Φ_{em})[b] R.T.	λ_{em}/ nm (τ /μs)[c] 77 K	λ_{T1-Tn}/ nm (ε_{T1-Tn}/ L.mol^{-1}.cm^{-1}; τ /ns)[d]
2-4	462 (8280), 426 (10160), 350 (39960), 289 (52220), 255 (64540)	594 (1210; 0.18)	546 (10.2), 589 (10.6)	420 (12810; 1260), 636 (8190; 1210)
2-5	451 (8980), 427 (10180), 359 (43840), 292 (45840), 255 (78280)	597 (600; 0.053)	546 (9.7), 590 (9.3)	415 (9560; 560), 505 (4830; 630)

[a] In toluene. [b] Measured at a toluene solution with A = 0.1 at 436 nm. [c] In butyronitrile glassy solutions at 77 K. $c = 3.5\times10^{-5}$ mol/L [d] In toluene.

Emission measured in butyronitrile glassy solution at 77 K (Figure 2.4) reveals that the emission band becomes structured and blue shifted in comparison to that measured at room temperature. This could be due to the rigidochromic effect that is commonly observed in transition-metal complexes.[39,40-52] The vibronic spacing is 1150 cm^{-1} for **2-4** and 1310 cm^{-1} for **2-5**, which falls in the range for stretching mode of the aromatic rings. Considering the similar emission energy and structure of the emission of these two complexes to those reported in the literature for other platinum terpyridyl or C^N^N complexes,[3-11,18-42] the emitting state at 77 K for **2-4** and **2-5** is tentatively assigned as the ^{3}MLCT state, presumably mixed with some ^{3}ILCT and $^3\pi,\pi^*$ character. With an increased concentration from 10^{-6} mol/L to ~7×10^{-5} mol/L, the emission spectra remain the same, suggesting that no

ground-state aggregation occurs in this concentration range. The lifetimes measured at the two vibronic bands are essentially the same, all around 10 μs (Table 2.1).

Table 2.2. Emission lifetimes and quantum yields of 6-phenyl-4-(9,9-dihexylfluoren-2-yl)-2,2'-bipyridine Pt(II) 4-ethynylbenzyl-N-phenothiazine (**2-4**) and 6-phenyl-4-(9,9-dihexylfluoren-2-yl)-2,2'-bipyridine Pt(II) 10-(prop-2-ynyl)-10H-phenothiazine (**2-5**) at room temperature in different solvents at room temperature.

Solvent	λ_{em} / nm (τ / ns; Φ_{em})	
	2-4	**2-5**
CH_2Cl_2	584 (-; 0.036)	584 (-; 0.0012)
Acetonitrile	576 (-; 0.022)	574 (-; 0.0019)
Acetone	579 (30; 0.0048)	-
Toluene	594 (1210; 0.18)	597 (600; 0.053)
DMSO	587 (-; 0.0009)	605 (-; 0.0021)

2.3.3. Triplet Transient Difference Absorption

In addition to the emission studies, another powerful tool in understanding the excited-state characteristics is the transient absorption measurement of the excited state, which is critical for predicting the nonlinear absorption of the compound. The time-resolved triplet transient difference absorption study not only provides valuable information on the triplet excited-state absorption spectrum but also on the lifetime of the triplet excited state. In general, a positive band in a transient absorption spectrum suggests stronger excited-state absorption than that of the ground state in the respective spectral region, which could cause reverse saturable absorption.

The time-resolved triplet transient difference absorption spectra of **2-4** and **2-5** are illustrated in Figure 2.5 and the lifetimes of the triplet exited state deduced from the decay of the transient absorption are listed in Table 2.1. Both complexes exhibit positive absorption bands from 400 to 820 nm, indicating stronger triplet excited-state absorption than that of the ground state in this spectral region, and a bleaching band in the UV region.

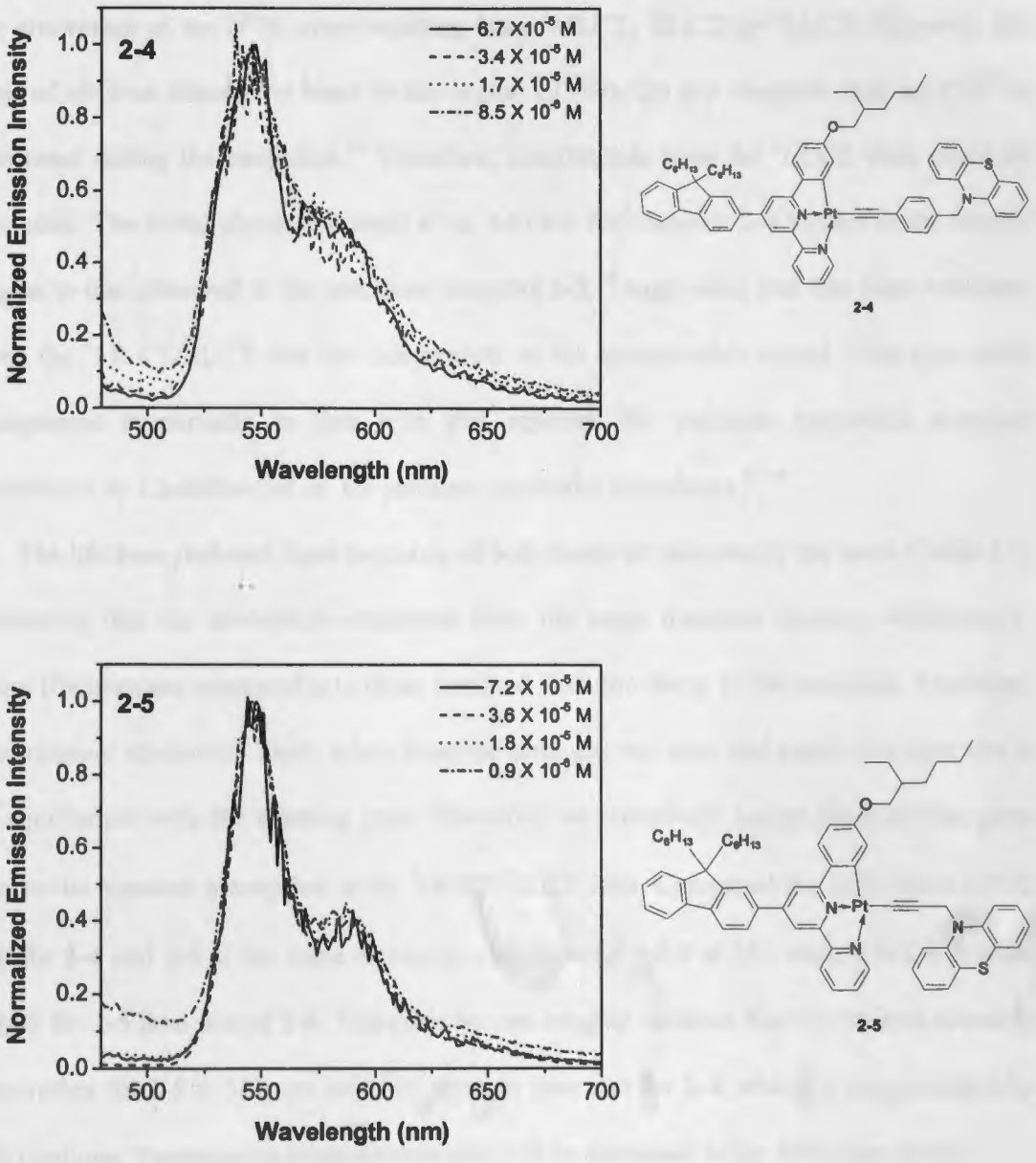

Figure 2.4. Emission spectra of 6-phenyl-4-(9,9-dihexylfluoren-2-yl)-2,2'-bipyridine Pt(II) 4-ethynylbenzyl-*N*-phenothiazine (2-4) and 6-phenyl-4-(9,9-dihexylfluoren-2-yl)-2,2'-bipyridine Pt(II) 10-(prop-2-ynyl)-10H-phenothiazine (2-5) measured in degassed butyronitrile glassy matrix at 77 K.

The relatively narrower band at ca. 420 nm for both complexes could possibly arise from the absorption of the N^N anion resulting from ^{3}MLCT, ^{3}ILCT, or ^{3}LLCT. However, the lack of obvious absorption band in the region of 480-520 nm suggests that no PTZ^+ is generated during the excitation.[34] Therefore, contribution from the ^{3}LLCT state could be excluded. The broad absorption band at ca. 640 nm for complex **2-4** locates at the similar region to that observed in the precursor complex **2-3**,[30] suggesting that this band emanates from the ^{3}MLCT/^{3}ILCT that are independent on the monodentate ligand. This hypothetic assignment is partially in line with that reported for platinum terpyridyl acetylide complexes by Castellano *et. al.* for platinum terpyridyl complexes.[53-54]

The lifetimes deduced from the decay of both bands are essentially the same (Table 2.1), indicating that the absorption originates from the same transient species. Additionally, these lifetimes are comparable to those obtained from the decay of the emission. Therefore, the transient absorption likely arises from the same excited state that emits or a state that is in equilibrium with the emitting state. Therefore, we tentatively assign the state that gives rise to the transient absorption as the ^{3}MLCT/^{3}ILCT state. Compared the ΔOD value at 532 nm for **2-4** and **2-5** at the same excitation condition (A = 0.4 at 355 nm), it is 2 – 3 times larger for **2-5** than that of **2-4**. Therefore we can roughly estimate that the reverse saturable absorption for **2-5** at 532 nm could be stronger than that for **2-4**, which is demonstrated by the nonlinear transmission measurement and will be discussed in the following section.

2.3.4. Reverse Saturable Absorption

As discussed in the previous section, complexes **2-4** and **2-5** exhibit broad positive triplet transient absorption in the visible to the near-IR region, and both complexes possess long-lived triplet excited state. Therefore, reverse saturable absorption (RSA) is expected to

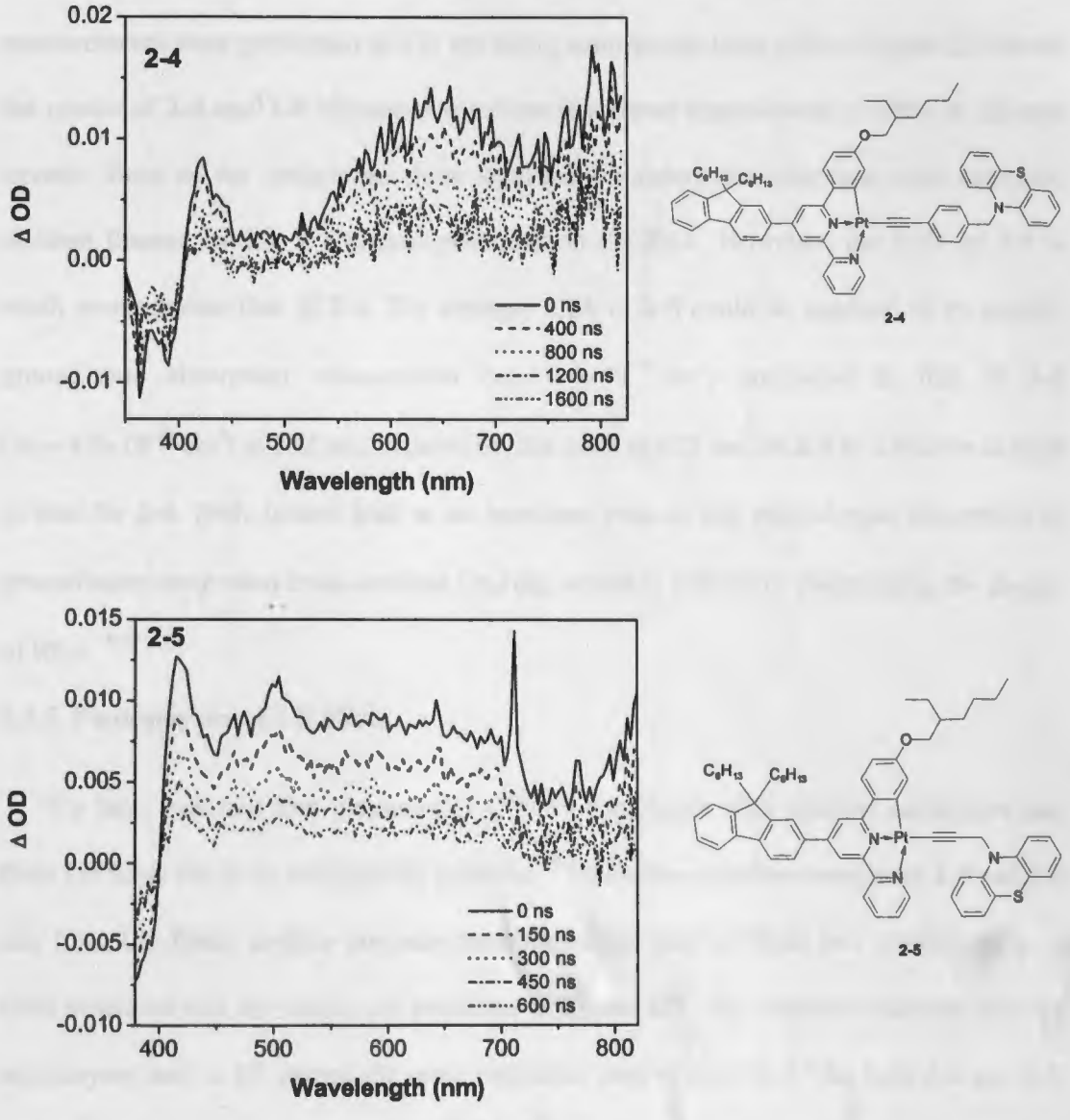

Figure 2.5. Time-resolved triplet transient difference absorption spectra 6-phenyl-4-(9,9-dihexylfluoren-2-yl)-2,2'-bipyridine Pt(II) 4-ethynylbenzyl-*N*-phenothiazine (**2-4**) and 6-phenyl-4-(9,9-dihexylfluoren-2-yl)-2,2'-bipyridine Pt(II) 10-(prop-2-ynyl)-10H-phenothiazine (**2-5**) dissolved in argon degassed toluene at room temperature following 355 nm excitation with A_{abs} = 0.40 at the excitation wavelength. The time listed in the figure is the time delay after the laser pulse.

occur in the visible to the near-IR region. To demonstrate this, nonlinear transmission measurements were performed at 532 nm using nanosecond laser pulses. Figure 2.6 shows the results of **2-4** and **2-5** in toluene solutions at a linear transmission of 80% in a 2-mm cuvette. Both of the complexes show significant transmission decrease with increased incident fluence, which is a typical phenomenon for RSA. However, the RSA of **2-5** is much stronger than that of **2-4**. The stronger RSA of **2-5** could be ascribed to its smaller ground-state absorption cross-section ($\sigma_0 = 2.6\times10^{-19}$ cm^2) compared to that of **2-4** ($\sigma_0 = 4.0\times10^{-19}$ cm^2) at 532 nm; meanwhile, the ΔOD at 532 nm for **2-5** is 2.6 times as high as that for **2-4**. Both factors lead to an increased ratio of the excited-state absorption to ground-state absorption cross-sections (σ_{ex}/σ_0), which is critical in determining the degree of RSA.[18-30]

2.3.5. Photophysics of LB Films

We have reported that platinum(II) C^N^N complexes with alkoxyl substituent can form LB films due to its amphiphilic property.[38] To explore whether complexes **2-4** and **2-5** can form LB films, surface pressure-mean molecular area of these two complexes have been measured and the results are presented in Figure 2.7. The isotherm indicates that the monolayers start to lift around the same molecular area of *ca.* 110 Å^2 for both **2-4** and **2-5**, after which the surface pressure increases sharply. The slopes of the isotherm corresponding to the liquid condensed phase are essentially the same for **2-4** and **2-5**, indicating the similar liquid condensed state for these two complexes. Both complexes collapse at a surface pressure of *ca.* 70 mN/m, but the collapse pressure for **2-5** is slightly higher than that for **2-4**, indicating that **2-5** forms a slightly more stable monolayer than **2-4** does. The limiting molecular areas by extrapolating the plot to zero surface pressure are

app roximately 86 and 103 $Å^2$ for monolayers of **2-4** and **2-5**, respectively, which are much smaller than the estimated molecular areas. This suggests that the molecules take up an "*edge-on*" orientation rather than a "*flat-on*" arrangement.[40] With reference to LB films of the mononuclear C^N^N complex with alkoxyl substituent,[38] the alkyl chain in complexes **2-4** and **2-5** should stick out from the air / water interface.

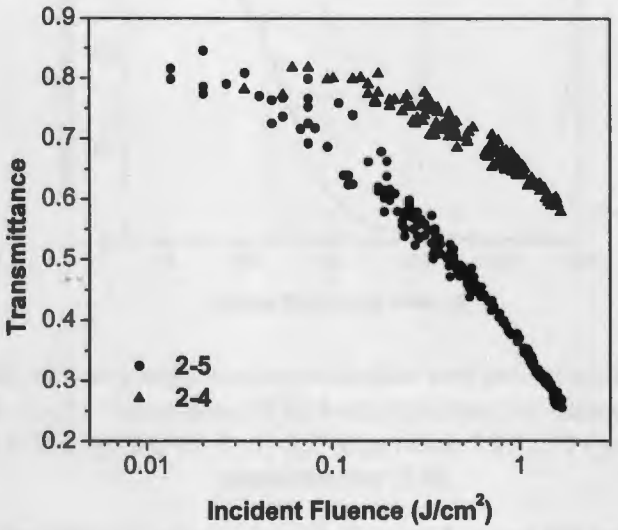

Figure 2.6. Transmission vs incident fluence curves for 6-phenyl-4-(9,9-dihexylfluoren-2-yl)-2,2'-bipyridine Pt(II) 4-ethynylbenzyl-*N*-phenothiazine (**2-4**) and 6-phenyl-4-(9,9-dihexylfluoren-2-yl)-2,2'-bipyridine Pt(II) 10-(prop-2-ynyl)-10H-phenothiazine (**2-5**) in toluene solutions for 4.1 ns laser pulses at 532 nm in a 2-mm cell. The linear transmission was adjusted to 80%.

Figure 2.8 shows the AFM height images of 5-layer and 11-layer LB films of **2-4** and **2-5**, which illustrate the surface morphology of the films. It is obvious that both the 5-layer and 11-layer LB films of **2-5** are smoother than those of **2-4**. Particularly the 5-layer film of **2-5** is uniform and few grain particles observed in its AFM image. The bright grain-like particles should be ascribed to the formation of aggregation in LB films, which is more salient in the LB films of **2-4** in comparison to that in **2-5**. The ease of aggregation in LB

films of **2-4** than in **2-5** could be related to the presence of phenyl ring in the acetylide ligand of **2-4**, which could facilitate π,π stacking in the solid form.

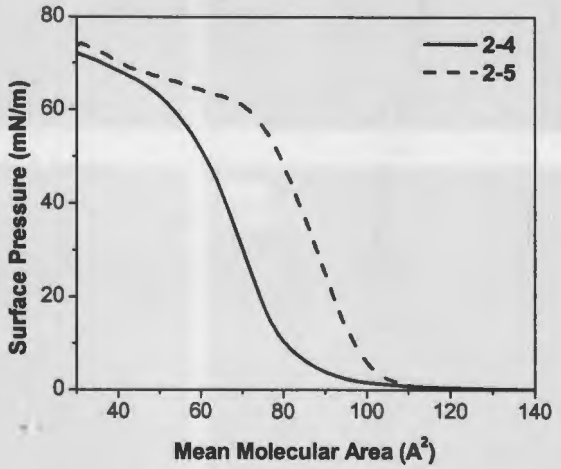

Figure 2.7. The surface pressure-mean molecular area isotherms for 6-phenyl-4-(9,9-dihexylfluoren-2-yl)-2,2'-bipyridine Pt(II) 4-ethynylbenzyl-*N*-phenothiazine (**2-4**) and 6-phenyl-4-(9,9-dihexylfluoren-2-yl)-2,2'-bipyridine Pt(II) 10-(prop-2-ynyl)-10H-phenothiazine (**2-5**).

The UV-vis absorption spectra of the LB films of **2-4** and **2-5** are shown in Figure 2.9. For comparison purpose, the UV-vis absorption spectrum in toluene is also provided in the same figure. The $^1\pi,\pi^*$ transitions in the UV region became a broad and structureless absorption band in the films, and the charge transfer band became a shoulder at ca. 480 nm. The LB films of both complexes are emissive at room temperature. The emission spectra for the 5-layer and 11-layer LB films are shown in Figure 2.10, along with the spectra in toluene at room temperature and the one at 77 K glassy butyronitrile solution. It is apparent that the number of layers shows a negligible effect on the emission energy of the LB films,

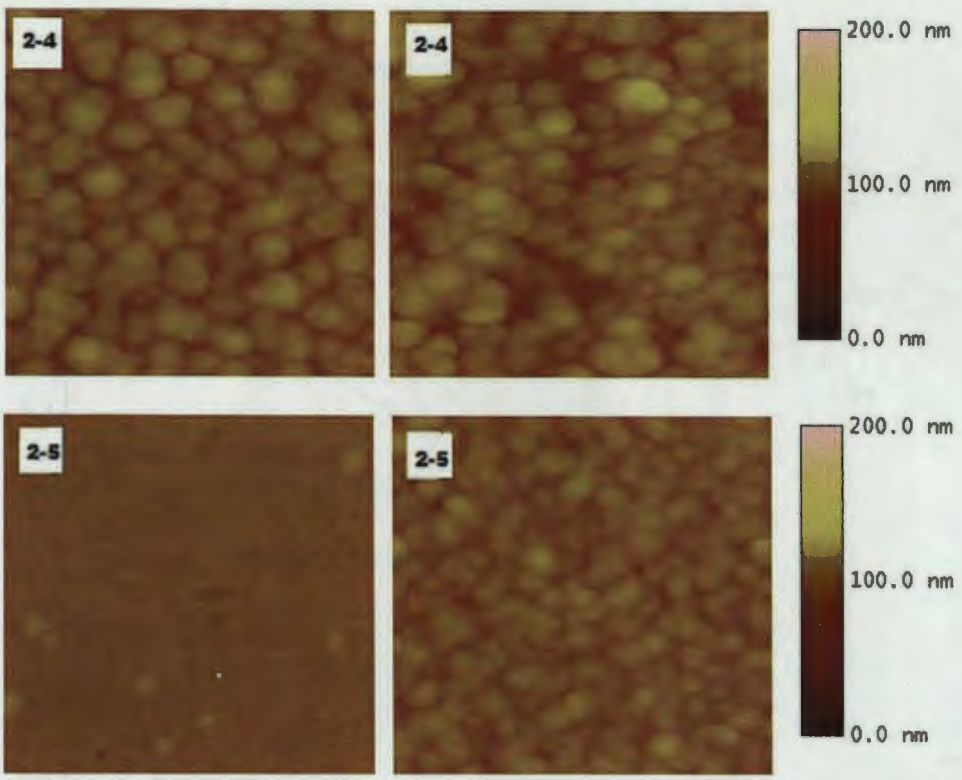

Figure 2.8. AFM height imagines of 5-layer (left) and 11-layer (right) LB films of 6-phenyl-4-(9,9-dihexylfluoren-2-yl)-2,2'-bipyridine Pt(II) 4-ethynylbenzyl-*N*-phenothiazine (**2-4**) and 6-phenyl-4-(9,9-dihexylfluoren-2-yl)-2,2'-bipyridine Pt(II) 10-(prop-2-ynyl)-10H-phenothiazine (**2-5**). The scan area was 1 μm × 1 μm, and the *Z*-range was 200 nm.

and the energy is comparable to that in toluene solution, with a slight blue-shift. This observation suggests that although aggregation was observed via the AFM image in the LB films, the intermolecular distance is probably not close enough in the aggregates to allow for Pt-Pt interactions to occur. Therefore, no red-shifted emission belonging to the metal-metal-to-ligand charge transfer (^{3}MMLCT) is observed, which is in line with that observed in the UV-vis absorption spectra.

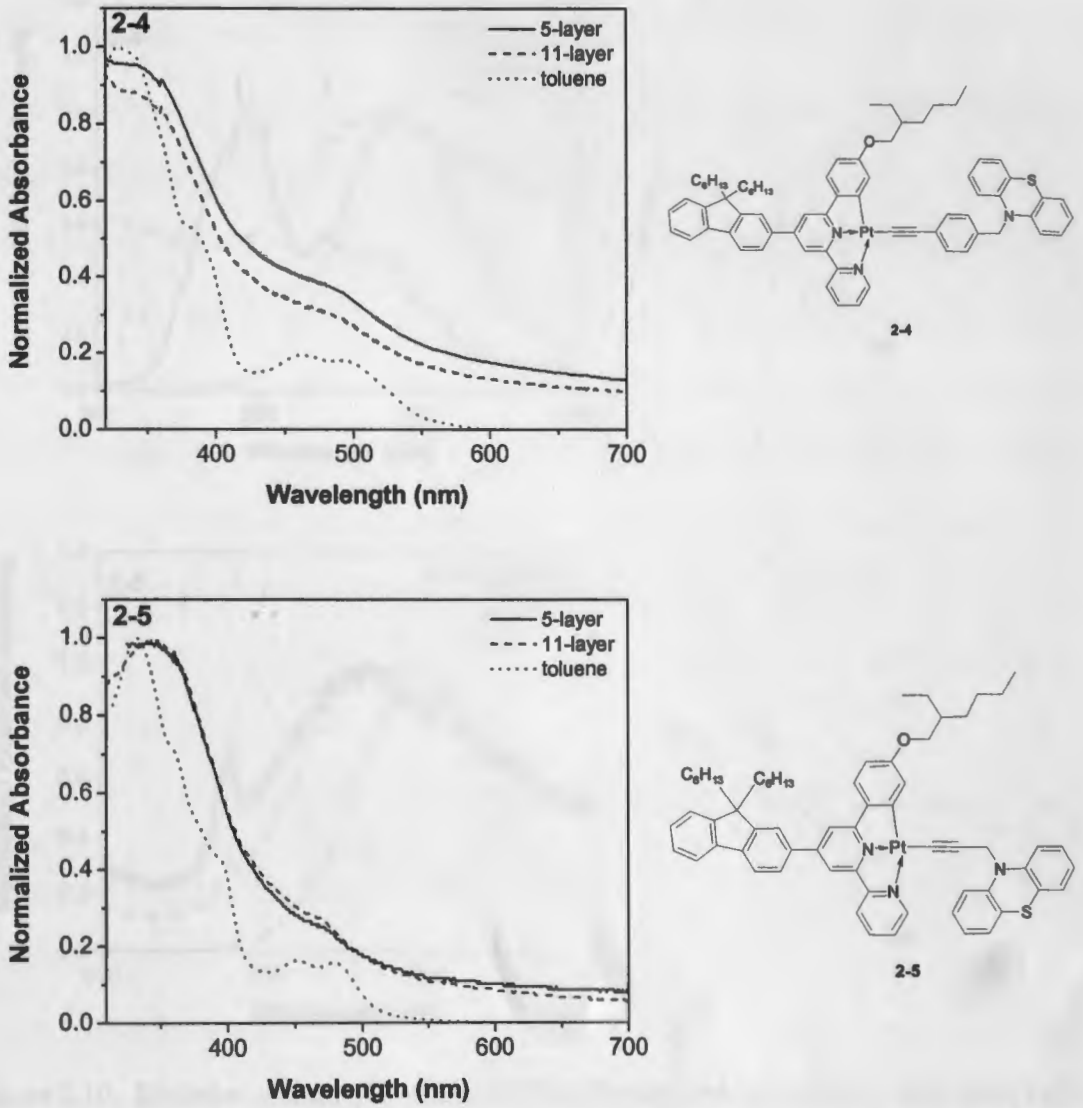

Figure 2.9. UV-vis absorption spectra of 6-phenyl-4-(9,9-dihexylfluoren-2-yl)-2,2'-bipyridine Pt(II) 4-ethynylbenzyl-*N*-phenothiazine (**2-4**) and 6-phenyl-4-(9,9-dihexylfluoren-2-yl)-2,2'-bipyridine Pt(II) 10-(prop-2-ynyl)-10H-phenothiazine (**2-5**) in LB film and in toluene.

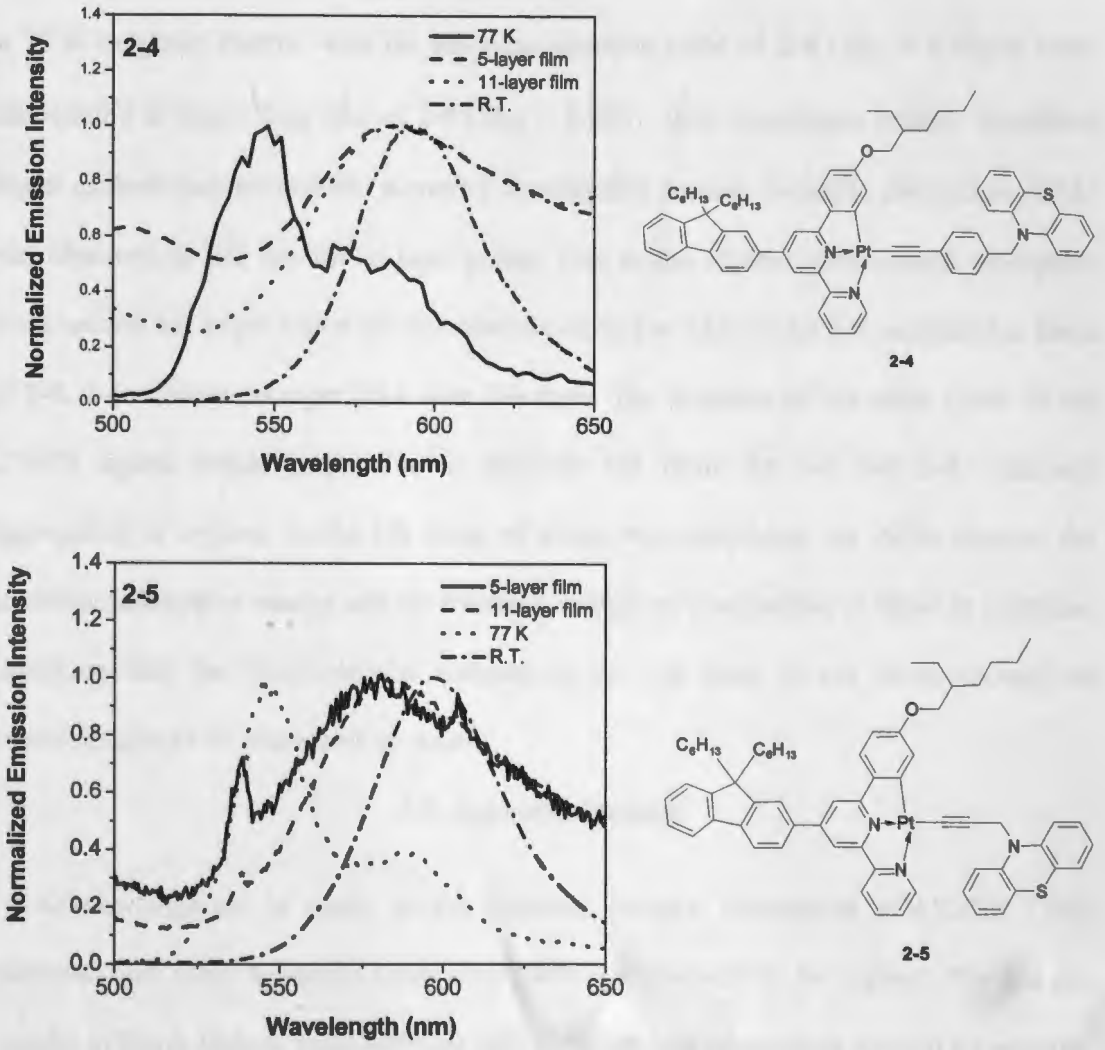

Figure 2.10. Emission spectra of 6-phenyl-4-(9,9-dihexylfluoren-2-yl)-2,2'-bipyridine Pt(II) 4-ethynylbenzyl-*N*-phenothiazine (**2-4**) and 6-phenyl-4-(9,9-dihexylfluoren-2-yl)-2,2'-bipyridine Pt(II) 10-(prop-2-ynyl)-10H-phenothiazine (**2-5**) in butyronitrile glassy matrix at 77 K, in toluene solutions at room temperature and in LB film at room temperature when excited at 355 nm.

2.4. Conclusion

Attaching PTZ acetylide ligands to platinum (II) complexes causes a mixture of LLCT character into the MLCT state due to the electron-donating ability of the PTZ acetylide ligand. The ^{1}MLCT/^{1}LLCT band of **2-4** is slightly broader than that of **2-5** in their UV-vis

absorption spectra. Both complexes are emissive at room temperature in fluid solution and at 77 K in glassy matrix; with the emission quantum yield of **2-4** (Φ_{em} = 0.18) at room temperature is larger than that of **2-5** (Φ_{em} = 0.053). Both complexes exhibit broadband triplet excited-state absorption, therefore considerable reverse saturable absorption (RSA) was observed at 532 nm for ns laser pulses. Due to the smaller ground-state absorption cross-section but larger triplet excited-state absorption at 532 nm for **2-5** compared to those of **2-4**, **2-5** exhibits stronger RSA than **2-4** does. The presence of the alkyl chain on the C^N^N ligand makes it possible to fabricate LB films for **2-4** and **2-5**. Although aggregation is evident in the LB films of these two complexes via AFM images, the electronic absorption energy and the emission energy are comparable to those in solutions, indicating that the intermolecular distance in the LB films is not close enough for intermolecular Pt-Pt interaction to occur.

2.5. Acknowledgement

Acknowledgment is made to the National Science Foundation (CAREER CHE-0449598) and Army Research Laboratory (W911NF-06-2-0032) for support. We are also grateful to North Dakota State EPSCoR (ND EPSCoR Instrumentation Award) for support.

I also would like to thank Dr. Yunjing Li who did the calculation for the triplet excited-state quantum yield and measurement of nonlinear transmission, and Dr. Bingguang Zhang who supervised me on synthetic work patiently.

2.6. References

1. Williams, J. A. G. *Top Curr. Chem.* **2007**, *281*, 205.
2. Eryazici, I.; Moorefield, C. N.; Newkome, G. R. *Chem. Rev.* **2008**, *108*, 1834.

3. Maestri, M.; Sandrini, D.; Balzani, V.; Chassot, L.; Jolliet, P.; von Zelewsky, A. *Chem. Phys. Lett.* **1985**, *122*, 375.

4. Miskowski, V. M.; Houlding, V. H.; *Inorg. Chem.* **1989**, *28*, 1529.

5. Lu, W.; Mi, B. X.; Chan, M. C. W.; Hui, Z.; Che, C. M.; Zhu, N.; Lee, S. T. *J. Am. Chem. Soc.* **2004**, *126*, 4958.

6. Lu, W.; Chan, M. C. W.; Zhu, N.; Che, C. M.; Li, C.; Hui, Z. *J. Am. Chem. Soc.* **2004**, *126*, 7639.

7. Yesin, H.; Donges, D.; Humbs, W.; Strasser, J.; Sitters, R.; Glasbeek, M. *Inorg. Chem.* **2002**, *41*, 4915.

8. Brooks, J.; Babayan, Y.; Lamansky, S.; Djurovich, P. I.; Tsyba, I.; Bau, R.; Thompson, M. E. *Inorg. Chem.* **2002**, *41*, 3055.

9. Wong, W. Y.; He, Z.; So, S. K.; Tong, K. L.; Lin, Z. *Organometallics* **2005**, *24*, 4079.

10. Wong, K. M. C.; Tang, W. S.; Chu, B. W. K.; Zhu, N.; Yam, V. W. W. *Organometallics* **2004**, *23*, 3459.

11. Zhang, H.; Zhang, B.; Li, Y.; Sun, W. *Inorg. Chem.* **2009**, *48*, 3617.

12. Du. P.; Schneider, J.; Jarosz, P. Eisenberg, R. *J. Am. Chem. Soc.* **2006**, *128*, 7726.

13. Narayana-Prabhu, R.; Schmehl, R. H. *Inorg. Chem.* **2006**, *45*, 4319.

14. Zhang, D.; Wu, L. Z.; Zhou, L.; Han, X.; Yang, Q. Z.; Zhang, L. P.; Tung, C. H. *J. Am. Chem. Soc.* **2004**, *126*, 3440.

15. Islam, A.; Sugihara, H.; Hara, K.; Singh, L. P.; Katoh, R.; Yanagida, M.; Takahashi, Y.; Murata, S.; Arakawa, H. *Inorg. Chem.* **2001**, *40*, 5371.

16. Geary, E. A. M.; Yellowlees, L. J.; Jack, L. A.; Oswald, I. D. H.; Parsons, S.; Hirata, N.; Durrant, J. R.; Robertson, N. *Inorg. Chem.* **2005**, *44*, 242.

17. Chakraborty, S.; Wadas, T. J.; Hester, H.; Flaschenreim, C.; Schmehl, R.; Eisenberg, R. *Inorg. Chem.* **2005**, *44*, 6284.

18. Shao, P.; Li, Y.; Azenkeng, A.; Hoffmann R. M.; Sun, W. *Inorg. Chem.* **2009**, *48*, 2407.

19. Ji, Z.; Li, Y.; Sun, W. *Inorg. Chem.* **2008**, *47*, 7599.

20. Shao, P.; Li, Y.; Sun, W. *J. Phys. Chem. A* **2008**, *112*, 1172.

21. Guo, F.; Sun, W. *J. Phys. Chem. B* **2006**, *110*, 15029.

22. Sun, W.; Wu, Z. X.; Yang, Q. Z.; Wu, L. Z.; Tung, C. H. *Appl. Phys. Lett.* **2003**, *82*, 850.

23. Guo, F.; Sun, W.; Liu, Y.; Schanze, K. *Inorg. Chem.* **2005**, *44*, 4055.

24. Pritchett, T. M.; Sun, W.; Guo, F.; Zhang, B.; Ferry, M. J.; Rogers-Haley, J. E.; Shensky, W.; Mott, A. G. *Opt. Lett.* **2008**, *33*, 1053.

25. Shao, P.; Li, Y.; Sun, W. *Organometallics* **2008**, *27*, 2743.

26. Sun, W.; Guo, F. *Chin. Opt. Lett.* **2005**, *S3*, S34.

27. Li, Y.; Pritchett, T. M.; Shao, P.; Haley, J.; Zhu, H.; Sun, W. *J. Organometallic Chem.* **2009**, *694*, 3688.

28. Shao, P.; Sun, W. *Inorg. Chem.* **2007**, *46*, 8603.

29. Sun, W.; Zhu, H.-J.; Barron, P. *Chem. Mater.* **2006**, *18*, 2602.

30. Shao, P.; Li, Y.; Yi, J.; Pritchett, T. M.; Sun, W. *Inorg. Chem.* **2010**, *49*, 4507.

31. Yam, V. W.-W.; Tang, R. P.-L.; Wong, K. M.-C.; Cheung, K.-K. *Organometallics* **2001**, *20*, 4476.

32. Ji, Z.; Azenkeng, A.; Hoffmann, M.; Sun, W. *Dalton Trans.* **2009**, 7725.

33. Wong, K. W.-C.; Tang, W.-S.; Lu, X.-X.; Zhu, N.; Yam, V. W.-W. *Inorg. Chem.* **2005**, *44*, 1492.

34. Chakraborty, S.; Wadas, J. T.; Hester, H.; Schmehl, R.; Eisenberg, R. *Inorg. Chem.* **2005**, *44*, 6865.

35. Jarosz, P.; Lotiio, K.; Schneider, J.; Kumaresan, D.; Schmehl, R.; Eisenberg, R. *Inorg. Chem.* **2009**, *48*, 2420.

36. McGarrah, J. E.; Kim, Y. J.; Hissler, M.; Eisenberg, R. *Inorg. Chem.* **2001**, *40*, 4510.

37. Peterson, I. R. J. *Phys. D: Appl. Phys.* **1990**, *23*, 379.

38. Mathew, I.; Sun, W. *J. Organometallic Chem.* **2009**, *694*, 2750.

39. Kobayashi, K.; Sato, H.; Kishi, S.; Kato, M.; Ishizaka, S.; Kitamura, N.; Yamagishi, A. *J. Phys. Chem. B* **2004**, *108*, 19665.

40. Wang, K.; Haga, M.; Monjushiro, H.; Akiba, M.; Sasaki, Y. *Inorg. Chem.* **2000**, *39*, 4022.

41. Samha, H.; Martinez, T.; De Armond, M. K. *Langmuir* **1992**, *8*, 2001.

42. Samha, H.; De Armond, M. K.; *Coord. Chem. Rev.* **1991**, *111*, 73.

43. Sae-Lim, C.; Sandman, D. J.; Foxman, B. M.; Sukwattanasinitt, A. M. *J. Macromolecular Sci., Part A: Pure Appl. Chem.* **2006**, *43*, 1929.

44. Demas, J. N.; Crosby, G. A. *J. Phys. Chem.* **1971**, *75*, 991.

45. Van Houten, J.; Watts, R. *J. Am. Chem. Soc.* **1976**, *98*, 4853.

46. Carmichael, I.; Hug, G. L. *J. Phys. Chem. Ref. Data* **1986**, *15*, 1.

47. Yang, Q. Z.; Wu, L. Z.; Wu, Z. X.; Zhang, L. P.; Tung, C. H. *Inorg. Chem.* **2002**, *41*, 5653.

48. Liu, X.-J.; Feng, J.-K.; Meng, J.; Pan Q.-J.; Ren, A.-M.; Zhou, X.; Zhang, H.-X. *Eur. J. Inorg. Chem.* **2005**, 1856.

49. Juris, A.; Balzani, V.; Barigelletti, F.; Campagna, S.; Belser, P.; Von Zelewsky, A. *Coord. Chem. Rev.* **1988**, *84*, 85.

50. Cummings, S. D.; Eisenberg, R. *J. Am. Chem. Soc.* **1996**, *118*, 1949.

51. Polo, A. S.; Itokazu, M. K.; Frin, K. M.; Patrocinio, A. O. de T.; Iha, N. Y. M. *Coord. Chem. Rev.* **2006**, *250*, 1669.

52. Lai, S.-W.; Chan, M. C. W.; Cheung, K.-K.; Che, C.-M. *Inorg. Chem.* **1999**, *38*, 4262.

53. Castellano, N. F.; Pomestchenko, E. I.; Shikhova, E.; Hua, F.; Muro, L. M.; Rajapakse, N. *Coord. Chem. Rev.* **2006**, *250*, 1819.

54. Shikhova, E.; Danilov, O. E.; Kinayyigit, S.; Pomestchenko, E. I.; Tregubov, D. A.; Camerel, F.; Retailleau, P.; Ziessel, R.; Castellano, N. F. *Inorg. Chem.* **2007**, *46*, 3038.

CHAPTER 3.

SYNTHESIS AND PHOTOPHYSICS OF PLATINUM(II) 6-PHENYL-4-(7-BENZOTHIAZOLYL-9,9-DIETHYLFLUOREN-2-YL)-2,2'-BIPYRIDINE COMPLEXES WITH ELECTRON-WITHDRAWING AND ELECTRON-DONATING ACETYLIDE LIGANDS

3.1. Introduction

Platinum(II) complexes bearing C^N^N and acetylide ligands, namely [(C^N^N)PtC≡CR] [H(C^N^N) = 6-phenyl-2,2'-bipyridine], was reported to exhibit strong luminescence in fluid solutions both at room temperature and at low temperature glassy matrix.[1-15] Substituents with different steric and electronic properties were introduced to the C^N^N ligands and to the acetylide ligands.[15] However, the platinum complexes containing substituted fluorene group either at the C^N^N ligand or at the acetylide ligand were rarely reported.[16] Fluorene was chosen to serve as a thermally and photochemically stable π-conjugated system because it can be readily functionalized at the 2-, 7-, and 9- positions. Belfield *et al.* in 1999 reported two new fluorene derivatives with phosphonate and nitro electron-withdrawing functionalities, both of them exhibit high nonlinear optical (NLO) absorptivities.[17] After that researchers continued to explore the fluorene-based compounds because of its two-photon absorption and high emission efficiency,[18,19] which have a variety of potential applications, such as in blue light-emitting diode,[20] oxygen photosensitizers,[21] microfabrication,[22] and three-dimensional data-storage.[23] The dialkylfluorene-based donor-acceptor chromophores have been reported to exhibit strong nonlinear absorption via instantaneous two-photon absorption[24-28] and subsequent excited-

state absorption.[29,30] Our group has reported that introducing fluorenyl substituent at the 4-position of the central pyridine ring of the C^N^N ligand can significantly increase the molar extinction coefficients of the charge-transfer band absorption, prolong the triplet excited-state lifetime, promote the emission quantum yield, and increase the ratio of the excited-state absorption cross-section to that of the ground state.[31, 32] We also demonstrated that incorporation of the benzothiazolyl substituent at the 7-position of the fluorenyl acetylide unit can expand the nonlinear absorption of the platinum(II) diimine complex to the near-IR region.[31] To understand the effect of acetylide ligand that contains different electron-donating and –withdrawing substituent at the fluorene unit on the photophysics and nonlinear absorption, three 6-phenyl-4-(7-benzothiazolyl-9,9-diethylfluoren-2-yl)-2,2'-bipyridine platinum(II) complexes with different acetylide ligands are synthesized and investigated. (Chart 3.1)

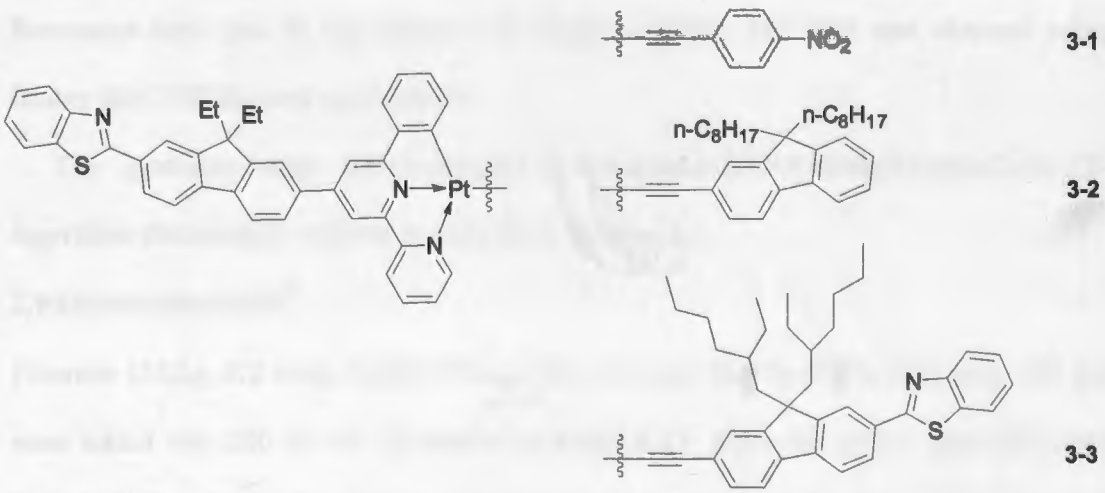

Chart 3.1. Chemical structures of 6-phenyl-4-(7-benzothiazolyl-9,9-diethylfluoren-2-yl)-2,2'-bipyridine Pt(II) complexes **3-1** to **3-3**.

3.2. Experimental Section

The experimental details are described in this section. The first part is the synthetic route and experimental procedure for the complexes. The second part is the photophysical measurement for the complexes.

3.2.1. Synthesis

All the reagents were purchased from Aldrich and Alfa Aesar and used without further purification. All solvent were purchase from VWR with analytical grade, and used without further purification unless otherwise stated. The silica gel (230×400 mesh) was purchased from Sorbent Technologies. All products were characterized by ^{1}H NMR, elemental analysis, and high resolution MS. ^{1}H NMR spectra were obtained using a Varian 300 MHz, 400 MHz or 500 MHz NMR spectrometer. Elemental analysis were conducted by NuMega Resonance labs, Inc. in San Diego, CA. High resolution MS data was obtained using Bruker Bio TOF III mass spectrometer.

The synthetic route for 6-phenyl-4-(7-benzothiazolyl-9,9-diethylfluoren-2-yl)-2,2'-bipyridine platinum(II) chloride is outlined in Scheme 3.1.

2,9-Dibromofluorene[33]

Fluorene (33.2g, 0.2 mol), NaBr (53.4g, 0.52 mol) and H_2SO_4 (10%, 0.36 mol, 360 ml) were added into 200 ml of 1,2-dichloro-ethane(DCE). After the solids were dissolved, H_2O_2 (30%, 0.52 mol, 60 ml) was added to the mixture. The color of the mixture turned into red. After stirring the mixture for 6 hours at room temperature, the mixture was filtered. The solid was washed by a large amount of water and then 100 ml DCE. The white solid was dried in vacuum oven, and 52.1 g (yield: 80%) product was obtained. ^{1}H NMR ($CDCl_3$,

400 MHz, δ ppm):7.65 (2H, s), 7.59 (2H, d, J = 8.0 Hz), 7.49 (2H, d, J = 8.0 Hz), 3.85 (s, 2H).

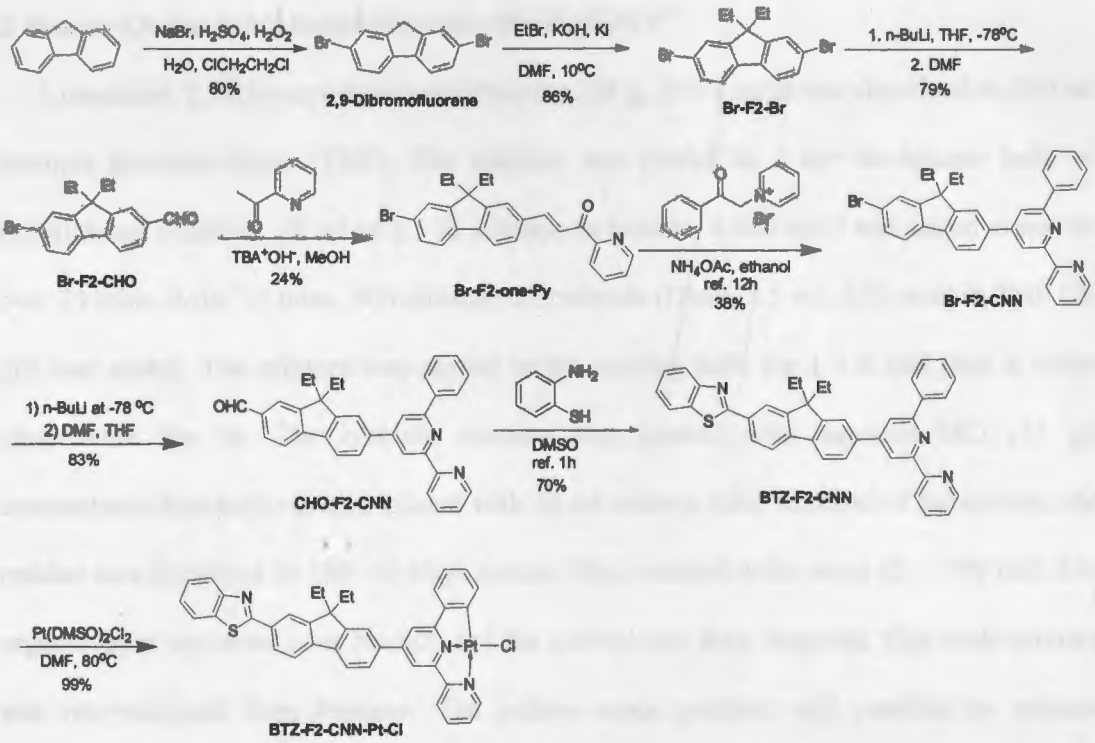

Scheme 3.1. Synthetic route for 6-phenyl-4-(7-benzothiazolyl-9,9-diethylfluoren-2-yl)-2,2'-bipyridine Pt(II) chloride complex (**BTZ-F2-CNN-Pt-Cl**).

2,7-Dibromo-9,9-diethylfluorene (Br-F2-Br)[33]

Compound 2,7-dibromofluorene (39 g, 0.12 mol), powder potassium hydroxide (30 g, 0.54 mol), and potassium iodide (2 g, 0.012 mol) were dissolved in dimethyl sulfoxide (DMSO, 90 ml). The mixture was cooled to 10 °C in an ice bath. Ethyl bromide (19.5 ml, 0.25 mol) was then added dropwise over 45 min. After that the mixture was warmed up to room temperature and stirred overnight. After the reaction, the mixture was poured into water to precipitate the crude product. The crude product was recrystallized from hexane to

yield 39.2 g (yield: 86%) pale yellow crystal. m.p. = 158 °C. ^{1}H NMR ($CDCl_3$, 400 MHz, δ ppm): 7.54-7.44 (6H, m), 1.99 (4H, q, J = 7.2 Hz), 0.314 (6H, t, J = 7.6 Hz).

2-Bromo-9,9-diethyl-7-formylfluorene (Br-F2-CHO)[33]

Compound 2,7-dibromo-9,9-diethylfluorene (28 g, 0.074 mol) was dissolved in 200 ml absolute tetrahydrofuran (THF). The solution was cooled in a dry ice-hexane bath. *n*-Butyllithium (Aldrich, 32 ml of 2.5 M solution in hexane, 0.080 mol) was added dropwise over 25 mins. After 20 mins, *N*,*N*-dimethylformamide (DMF, 8.5 ml, 0.12 mol) in THF (20 ml) was added. The mixture was stirred in the cooling bath for 1.5 h and then at room temperature for 1h. The reaction mixture was treated with aqueous HCl (12 ml concentrated hydrochloric acid diluted with 50 ml water). After removal of the solvent, the residue was dissolved in 100 ml ethyl acetate, then washed with water (3 × 200 ml). The organic layer was dried over Na_2SO_4 and the solvent was then removed. The crude product was recrystallized from heptane. The yellow crude product was purified by column chromatography on silica gel with hexane used as the eluent. A pale yellow solid (19.2 g, yield: 79%) was obtained as the pure product. ^{1}H NMR ($CDCl_3$, 400 MHz, δ ppm): 10.04 (1H, s), 7.80-7.96 (3H, m), 7.63-7.66 (1H, m), 7.50-7.53 (2H, m), 1.99-2.14 (4H, m), 0.28 (6H, t, J = 7.6 Hz).

3-(7-Bromo-9,9-diethyl-9H-fluoren-2-yl)-1-pyridin-2-yl-propenone (Br-F2-one-Py)

Compound **Br-F2-CHO** (16.5 g, 0.05 mol), 2-acetylpyridine (6.1 g, 0.05 mol) and KOH (8.4 g, 0.15 mol) were dissolved in CH_3OH (300 ml). The solution was stirred at 0 °C and slowly warmed up to room temperature overnight. The solvent was removed and the residue was dissolved in ethyl acetate and washed with saturated NaCl solution for 3 times. The organic layer was dried over Na_2SO_4. The crude product was purified through silica

gel column chromatography with CH_2Cl_2 used as the eluent. Recrystallization from heptane yielded pale yellow solid 5.2 g (yield: 24%). ^{1}H NMR ($CDCl_3$, 400 MHz, δ ppm): 8.76 – 8.75 (1H, m), 8.30 (1H, d, J = 16 Hz), 8.19 (1H, dt, J = 8.0 Hz, J = 1.2 Hz), 8.02 (1H, d, J = 16 Hz), 7.86 (1H, dt, J = 8.0 Hz, J = 2.0 Hz), 7.68 (3H, s), 7.56 (1H, d, J = 8.0 Hz), 7.49 – 7.44 (3H, m), 2.10 – 1.98 (4H, m), 0.30 (6H, t, J = 7.2 Hz).

Compound Br-F2-CNN

Compound **Br-F2-one-Py** (6.0 g, 14 mmol), 1-(2-oxo-2-phenyl-ethyl)-pyridinium bromide (3.9 g, 14 mmol) and ammonium acetate (15.4 g, 0.2 mol) were added in 200 ml ethanol. The mixture was refluxed overnight under argon. After removal of the solvent, the residue was dissolved in ethyl acetate, and washed with brine. The organic layer was dried with Na_2SO_4 and the solvent was removed. The residual solid was purified by column chromatography on silica gel with CH_2Cl_2 used as the eluent. A colorless crystal (2.8 g, yield: 38%) was obtained by recrystallization from heptane. m.p. = 193-194°C. ^{1}H NMR ($CDCl_3$, 400 MHz, δ ppm): 8.68-8.77 (3H, m), 8.23 (2H, d, J = 8.1 Hz), 8.03 (1H, d, J = 1.5 Hz), 7.90 (1H, td, J = 7.2 Hz, J = 1.5 Hz), 7.82 (2H, s), 7.75 (1H, d, J = 1.2 Hz), 7.48-7.65 (6H, m), 7.36-7.40 (1H, m), 2.04-2.17 (4H, m), 0.36 (6H, t, J = 7.2 Hz).

Compound CHO-F2-CNN

To an argon-protected dry THF solution (20 mL) of compound **Br-F2-CNN** (5.3 g, 0.01 mol) at -78 °C, a 2.5 M solution of *n*-BuLi in hexane (4.4 mL, 0.011 mol) was added dropwise. After stirred at -78 °C for 20 min, DMF (1 mL, 0.014 mol) was added. The reaction mixture was stirred overnight, first at -78 °C, then warmed up to room temperature gradually. After addition of 10 mL water, the solvent was removed. The residue was dissolved in ethyl acetate, and washed with brine. The organic layer was dried with Na_2SO_4

and the solvent was removed. The crude product was purified by column chromatography on silica gel with CH_2Cl_2 used as eluent. A white solid (4.0 g, yield: 83%) was obtained as the pure product. ^1H NMR ($CDCl_3$, 400 MHz, δ ppm): 10.07 (s, 1H), 8.74 -8.89 (m, 3H), 8.23 (d, 2H, J = 8.0 Hz), 8.03 (d, 1H, J = 1.2 Hz), 7.9 -7.8 (m, 7H), 7.54 (t, 2H, J = 7.2 Hz), 7.47 (t, 1H, J = 6.8 Hz), 7.36 -7.33 (m, 1H), 2.19 - 2.14 (q, 4H, J = 7.2 Hz), 0.34 (t, 6H, J = 7.2 Hz).

Compound BTZ-F2-CNN

A degassed mixture of compound **CHO-F2-CNN** (4.0 g, 8.3 mmol) and 2-aminobenzenethiol (0.9 mL, 8.3 mmol) in DMSO (30 mL) was refluxed for 2 hrs. under argon. After cooled to room temperature, 500 mL water and 100 mL CH_2Cl_2 was added. The organic phase was separated and washed with acetic acid aqueous solution (V/V = 1/4), sodium bicarbonate aqueous solution (5%) and brine. The organic layer was dried with Na_2SO_4 and the solvent was removed. The crude product was purified by column chromatography on silica gel. After removal of the impurity layers by CH_2Cl_2, the pure product was obtained by ethyl acetate. The product was then recrystallized from CH_2Cl_2/heptane to yield 3.4 g yellow crystal as the pure product (yield: 70%). ^1H NMR ($CDCl_3$, 400 MHz, δ ppm): 8.76 – 8.67 (2H, m), 8.69 (1H, s), 8.24 (2H, dd, J = 6.4 Hz, J = 1.2 Hz), 8.17 (1H, s), 8.04 – 8.11 (3H, m), 7.92 – 7.83 (5H, m), 7.80 (1H, d, J = 1.6 Hz), 7.57 – 7.50 (2H, m), 7.50 – 7.45 (2H, m), 7.40 – 7.34 (2H, m), 2.26 – 2.15 (4H, m), 0.40 (6H, t, J = 7.2 Hz).

Compound BTZ-F2-CNN-Pt-Cl

A solution of compound **BTZ-F2-CNN** (1 mmol, 0.6 g) and $Pt(DMSO)_2Cl_2$ (1.25 mmol, 0.53 g) in 10 mL DMF with two drops of water was heated and stirred at 80 °C for

24 h under argon atomsphere. The formed yellow precipitate was collected by filtration, washed with water, CH_2Cl_2, methanol and ether. The crude product was dried in vacuum oven to give 0.81 g crude product (yield: 99%). Due to the poor solubility of this product (insoluble in ethanol, ether, hexane and toluene, and slightly soluble in DMSO, DMF and CH_2Cl_2), it can't be purified by column chromatography or recrystallization. Therefore, this crude product is directly used for the preparation of the target C^N^N Pt(II) acetylide complexes **3-1** to **3-3**.

The synthetic route for 6-phenyl-4-(7-benzothiazolyl-9,9-diethylfluoren-2-yl)-2,2'-bipyridine Pt(II) complex (**3-1**) is shown in Scheme 3.2.

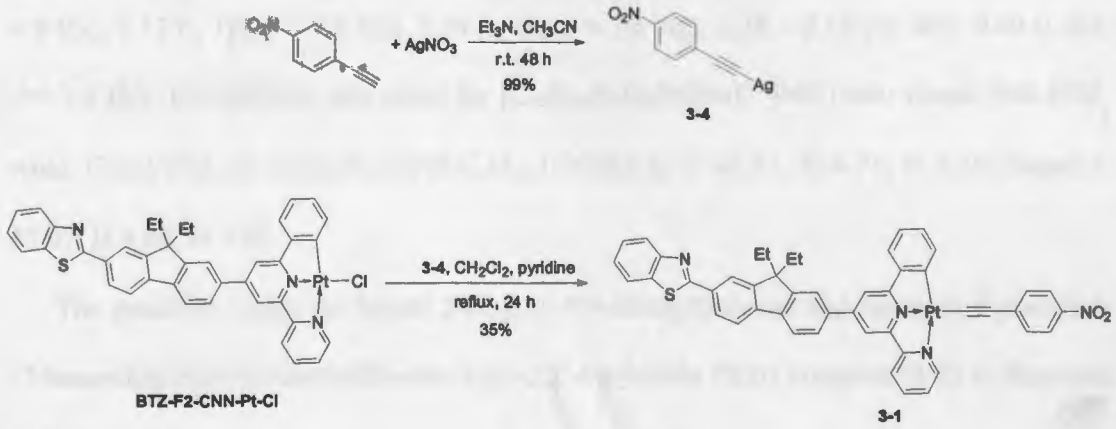

Scheme 3.2. Synthetic route for 6-phenyl-4-(7-benzothiazolyl-9,9-diethylfluoren-2-yl)-2,2'-bipyridine Pt(II) complex (**3-1**).

Compound 3-4

A 10 ml CH_3CN solution of 1-ethynyl-4-nitro-benzene (29 mg, 0.2 mmol) was mixed with a 10 ml Et_3N solution of $AgNO_3$ (34 mg, 0.2 mmol) at room temperature. Pale yellow precipitates were formed immediately after mixing. The solid was filtered out, washed with CH_3CN and MeOH for 3 times, and dried to give 50 mg pale yellow solid (yield: 99%).

Complex 3-1

A mixture of **BTZ-F2-CNN-Pt-Cl** (164 mg, 0.2 mmol), and **3-4** (50 mg, 0.2 mmol) in CH_2Cl_2/pyridine = 15 ml/15 ml solvent was refluxed for 24 hours under Ar atmosphere. After removal of the solvent, the residue was dissolved in CH_2Cl_2. The CH_2Cl_2 solution was washed with brine, and then dried with Na_2SO_4. After the solvent was removed, the crude product was purified by silica gel chromatography with CH_2Cl_2 as the eluent. Yellow solid 62 mg was obtained as the pure product (yield: 35%). ^1H NMR ($CDCl_3$, 400 MHz, δ ppm): 9.16 (1H, d, J = 5.6 Hz), 8.16 (t, 3H, J = 8 Hz), 8.11 – 8.04 (m, 4H), 7.93 – 7.87 (m, 4H), 7.82 (s, 1H), 7.76 – 7.73 (m, 2H), 7.66 (s, 1H), 7.61 – 7.49 (m, 5H), 7.40 (t, 1H, J = 8 Hz), 7.17 (t, 1H, J = 7.6 Hz), 7.10 (t, 1H, J = 7.6 Hz), 2.28 – 2.15 (m, 4H), 0.40 (t, 6H, J = 7.4 Hz). ESI-HRMS: m/z calcd for $[C_{48}H_{34}N_4O_2PtSNa]^+$: 948.1946; found: 948.1935. Anal. Calcd (%) for $C_{48}H_{34}N_4O_2PtS \cdot C_6H_{14} \cdot 1/2CH_2Cl_2$: C 62.72, H 4.71, N 5.38; found: C 63.07, H 4.98, N 5.65.

The synthetic routes for ligand 2-ethynyl-9,9-dioctylfluorene and complex 6-phenyl-4-(7-benzothiazolyl-9,9-diethylfluoren-2-yl)-2,2'-bipyridine Pt(II) complex (**3-2**) is displayed in Scheme 3.3.

2-Iodofluorene[33]

Fluorene (50 g, 0.3 mol) was dissolved in 500 ml of the boiling solvent (CH_3COOH : H_2O : H_2SO_4 = 100 : 20 : 3), followed by cooling to 60 – 65 °C. Periodic acid dehydrate (11.5 g, 0.05 mol) and iodine (25.5 g, 0.1 mol) were then added. After stirring at 60 – 65 °C for 4 h, the elementary iodine almost disappeared and the precipitate was formed. Upon cooling, the pale yellow solid was collected by filtration and washed with 2M aqueous Na_2CO_3 and water. The crude product was recrystallized from hexane to give 70 g white

solid (yield: 77%). ^{1}H NMR ($CDCl_3$, 400 MHz, δ ppm): 7.66 – 7.62 (m, 3H), 7.43 (d, 1H, J =8 Hz), 7.33 – 7.30 (m, 3H), 3.85 (s, 2H).

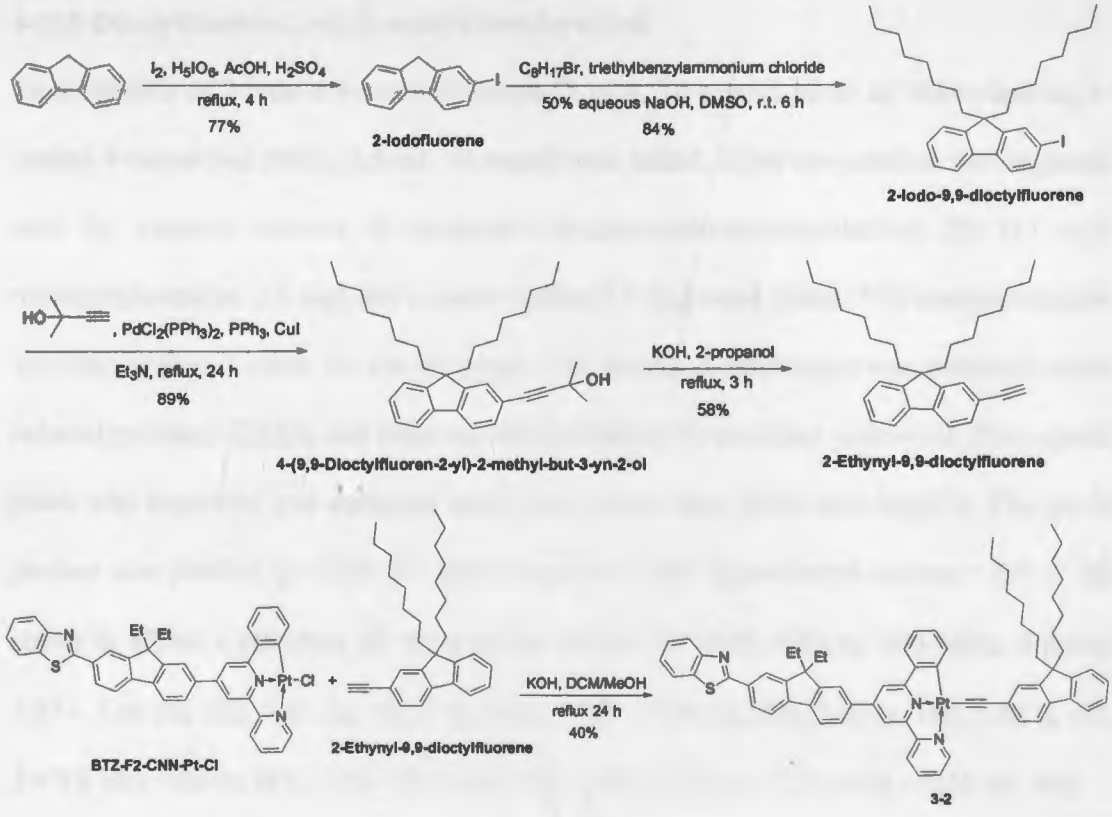

Scheme 3.3. Synthetic route for 2-ethynyl-9,9-dioctylfluorene and complex 6-phenyl-4-(7-benzothiazolyl-9,9-diethylfluoren-2-yl)-2,2'-bipyridine Pt(II) complex (**3-2**).

2-Iodo-9,9-dioctylfluorene[33]

To a mixture of 2-iodofluorene (4.5 g, 15 mmol) and catalytic amounts of triethylbenzylammonium chloride in 15 mL of DMSO and 10 mL of 50% aqueous NaOH, 1-bromooctane (6 ml, 33 mmol) was added. The reaction mixture was stirred at room temperature for 6 h. The organic layer was washed with dilute HCl twice and brine twice, and dried over $MgSO_4$. The resultant oil was purified by silica gel chromatography with

hexane to afford a pale yellow solid 6.6 g (yield: 84%). ^{1}H NMR ($CDCl_3$, 400 MHz, δppm): 7.66 – 7.62 (m, 3H), 7.43 (d, 1H, J =8 Hz), 7.33 – 7.30 (m, 3H), 2.20 – 2.02 (m, 4H), 0.98 – 0.75 (m, 20H), 0.66 – 0.56 (m, 10H).

4-(9,9-Dioctylfluoren-2-yl)-2-methyl-but-3-yn-2-ol

To a solution of 2-iodo-9,9-dioctylfluorene (5.16 g, 10 mmol) in 40 ml triethylamine, 3-methyl-1-butyn-3-ol (98%, 1.5 ml, 14 mmol) was added. After the solution was degassed with Ar, catalytic amount of dichlorobis-(triphenylphosphine)palladium (II) (15 mg), triphenylphosphine (15 mg) and cuprous iodide (15 mg) were added. The reaction mixture was then refluxed under Ar for 24 hours. The excess triethylamine was removed under reduced pressure. CH_2Cl_2 and brine was then added to the resultant yellow oil. The organic phase was separated and extracted with brine twice, then dried over $MgSO_4$. The crude product was purified by silica gel chromatography with hexane/ethyl acetate = 6/1 as the eluent to afford a colorless oil 4.2 g (yield: 89%). ^{1}H NMR ($CDCl_3$, 400 MHz, δ ppm): 7.67 – 7.64 (m, 1H), 7.61 (d, 1H, J =8.4 Hz), 7.40 – 7.29 (m, 5H), 2.03 (s, 1H), 1.93 (t, 4H, J = 7.8 Hz), 1.65 (s, 6H), 1.26 – 0.95 (m, 12H), 0.81 (t, 6H, J = 7.2), 0.58 – 0.55 (m, 4H).

2-Ethynyl-9,9-dioctylfluorene

A mixture of 4-(9,9-dioctylfluoren-2-yl)-2-methyl-but-3-yn-2-ol (4.2 g, 8.9 mmol) and KOH (3.0 g, 0.05 mol) in 100 ml of 2-propanol was heated at reflux under Ar atmosphere for 3 hours. The solvent was removed. The residue was dissolved in CH_2Cl_2 and washed with brine for 3 times. The CH_2Cl_2 layer was dried with Na_2SO_4 and the solvent was then removed. The crude product was purified by silica gel chromatography with hexane as the eluent. Pale yellow solid 2.15 g was obtained as the pure product (yield: 58%). ^{1}H NMR ($CDCl_3$, 400 MHz, δppm): 7.72 – 7.64 (m, 2H), 7.58 – 7.56 (m, 1H), 7.50 – 7.48 (m, 1H),

7.37 – 7.31 (m, 3H), 3.13 (s, 1H), 2.02 – 1.94 (m, 4H), 1.25 – 1.05 (m, 20H), 0.84 (t, 6H, J =7.2 Hz), 0.65 – 0.62 (m, 4H).

Complex 3-2

A mixture of **BTZ-F2-CNN-Pt-Cl** (164 mg, 0.20 mmol), 2-ethynyl-9,9-dioctylfluorene (105 mg, 0.25 mmol) and 1 g KOH in CH_2Cl_2/MeOH = 15 ml/15 ml solvent was refluxed under Ar atmosphere for 24 hours. After removal of the solvent, the residue was dissolved in CH_2Cl_2, and washed with brine. The CH_2Cl_2 layer was dried with Na_2SO_4, and then the solvent was removed. The crude product was purified by silica gel chromatography with CH_2Cl_2 as the eluent. The pure product was obtained through recrystallization from CH_2Cl_2/EtOH, 95 mg dark red solid was obtained (yield: 40%). ^{1}H NMR ($CDCl_3$, 400 MHz, δ ppm): 9.08 (dd, 1H, J_1 = 9.6 Hz, J_2 = 4.8 Hz), 8.18 (s, 1H), 8.14 – 8.05 (m, 5H), 7.99 (s, 2H), 7.93 – 7.77 (m, 7H), 7.73 – 7.69 (m, 2H), 7.65 (d, 2H, J = 6.4 Hz), 7.60 – 7.50 (m, 4H), 7.42 – 7.35 (m, 4H), 7.05 – 7.02 (m, 2H), 2.29 – 2.07 (m, 8H), 0.98 – 0.75 (m, 20H), 0.66 – 0.56 (m, 10H) 0.42 (t, 6H, J = 7.4 Hz). ESI-HRMS: m/z calcd for $[C_{78}H_{74}N_4PtS_2]^+$, 1193.5094; found, 1193.5121. Anal. Calcd (%) for $C_{71}H_{71}N_3PtS$: C 71.45, H 6.00, N 3.52; found: C 71.31, H 6.40, N 3.63.

The synthetic routes for 7-benzothiazoly-2-ethynyl-9,9-di-(2-ethylhexyl)-fluorene (**BTZ-F8-CC**) and 6-phenyl-4-(7-benzothiazolyl-9,9-diethylfluoren-2-yl)-2,2'-bipyridine Pt(II) complex (**3-3**) are displayed in Scheme 3.4.

The synthetic procedure for 2,9-dibromofluorene, 2,7-dibromo-9,9-di(2-ethylhexyl)fluorene (**Br-F8-Br**), and 7-Bromo-9,9-di-(2-ethylhexyl)-fluorene-2-carboxaldehyde (**Br-F8-CHO**) are similar to the procedures described for synthesizing the

precursors for 6-phenyl-4-(7-benzothiazolyl-9,9-diethylfluoren-2-yl)-2,2'-bipyridine Pt(II) chloride complex (Scheme 3.1).

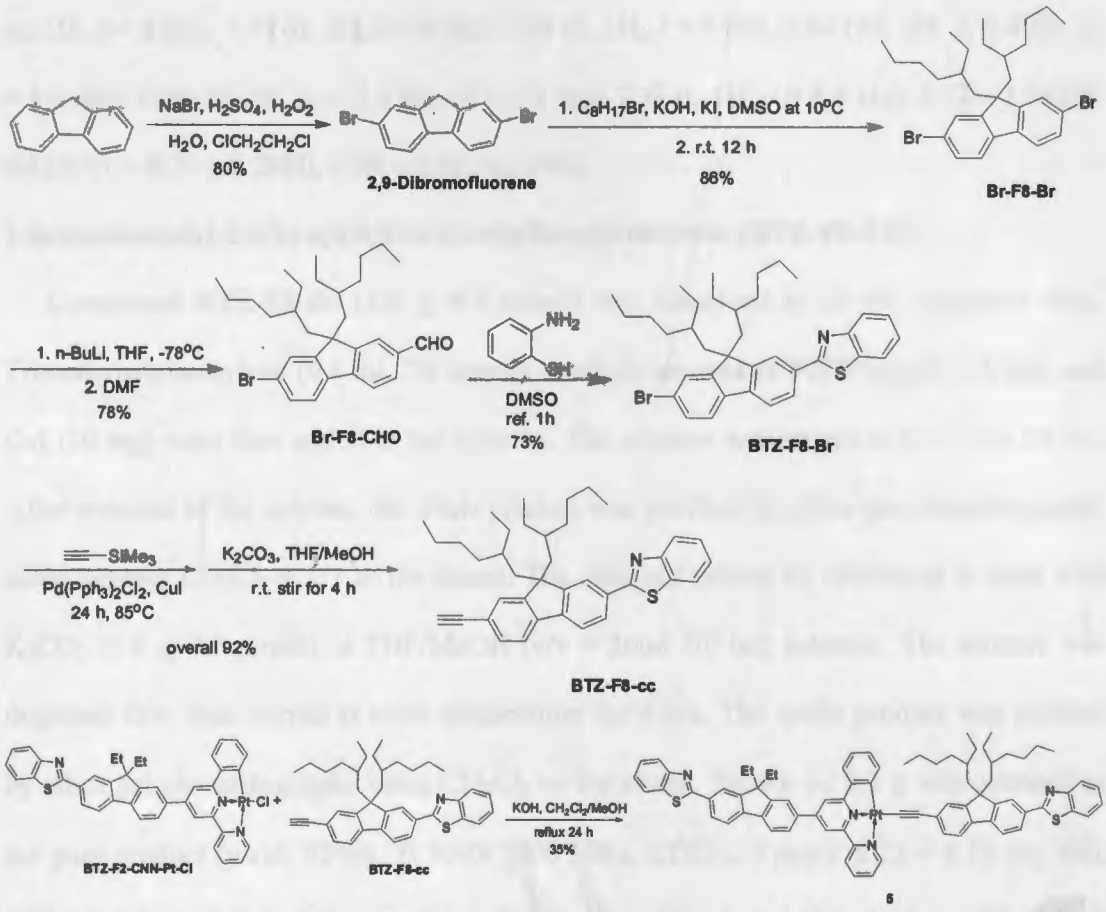

Scheme 3.4. Synthetic route for 7-benzothiazoly-2-ethynyl-9,9-di-(2-ethylhexyl)-fluorene (**BTZ-F8-CC**) and 6-phenyl-4-(7-benzothiazolyl-9,9-diethylfluoren-2-yl)-2,2'-bipyridine Pt(II) complex (**3-3**).

7-Benzothiazol-2-bromide-9,9-di-(2-ethylhexyl)-fluorene (BTZ-F8-Br)

A mixture of **Br-F8-CHO** (2.7 g, 5.4 mmol), 2-amino-benzenethiol (98%, 0.59 ml, 5.4 mmol) and 10 ml DMSO was refluxed for 2 hours under Ar atmosphere. The mixture was poured into 350 ml water and 100 ml CH_2Cl_2 and washed by acetic acid aqueous solution, $NaHCO_3$ aqueous solution and brine subsequently. The crude product was purified by silica

gel chromatography by using CH_2Cl_2 as the eluent. Purple oil 2.4 g was obtained as the pure product (yield: 73%). ^1H NMR (400 MHz, $CDCl_3$, δ ppm): 8.13 – 8.04 (m, 3H), 7.90 (d, 1H, J = 8 Hz), 7.75 (d, 1H, J = 8 Hz), 7.60 (d, 1H, J = 8 Hz), 7.54 (dd, 1H, J_1 = 4 Hz, J_2 = 1.6 Hz), 7.49 (td, 2H, J_1 = 7.2 Hz, J_2 = 1.2 Hz), 7.37 (t, 1H, J = 8.4 Hz), 2.12 – 1.96 (m, 4H), 0.91 – 0.71 (m, 20H), 0.59 – 0.48 (m, 10H).

7-Benzothiazolyl-2-ethynyl-9,9-di-(2-ethylhexyl)-fluorene (BTZ-F8-CC)

Compound **BTZ-F8-Br** (2.6 g, 4.3 mmol) was dissolved in 20 mL degassed NEt_3. Trimethylsilylacetylene (0.8 ml, 7.6 mmol), catalytic amount of $Pd(PPh_3)_2Cl_2$ (15 mg) and CuI (10 mg) were then added to the solution. The mixture was stirred at 85 °C for 24 hrs. After removal of the solvent, the crude product was purified by silica gel chromatography using hexane/ CH_2Cl_2 = 1/1 as the eluent. The obtained yellow oil continued to react with K_2CO_3 (0.6 g, 4.3 mmol) in THF/MeOH (v/v = 30ml /30 ml) solution. The mixture was degassed first, then stirred at room temperature for 4 hrs. The crude product was purified by silica gel chromatography using CH_2Cl_2 as the eluent. Brown oil 2.2 g was obtained as the pure product (yield: 92%). ^1H NMR (400 MHz, $CDCl_3$, δ ppm): 8.25 – 8.10 (m, 3H), 7.88 (d, 1H, J =8 Hz), 7.78 – 7.47 (m, 5H), 7.36 (t, 1H, J =8.4 Hz), 3.19 (s, 1H), 2.20 – 2.02 (m, 4H), 0.98 – 0.75 (m, 20H), 0.66 – 0.56 (m, 10H).

Complex 3-3

A mixture of **BTZ-F2-CNN-Pt-Cl** (164 mg, 0.2 mmol), **BTZ-F8-CC** (51 mg, 0.2 mmol) and 1 g KOH in CH_2Cl_2/MeOH = 15 ml/15 ml solvent was refluxed under Ar atmosphere for 24 hrs. After removal of the solvent, the residue was dissolved in CH_2Cl_2. The CH_2Cl_2 layer was washed with brine, and dried with Na_2SO_4. After removal of solvent, the crude product was purified by silica gel chromatography with CH_2Cl_2 as the eluent.

Recrystallization from DCM/EtOH yielded 58 mg dark red solid as the pure product (yield: 22%). ^{1}H NMR (400 MHz, $CDCl_3$, δ ppm): 9.08 (dd, 1H, J_1 = 9.6 Hz, J_2 = 4.8 Hz), 8.18 (s, 1H), 8.14 – 8.05 (m, 5H), 7.99 (s, 2H), 7.93 – 7.77 (m, 7H), 7.73 – 7.69 (m, 2H), 7.65 (d, 2H, J = 6.4 Hz), 7.60 – 7.50 (m, 4H), 7.42 – 7.35 (m, 4H), 7.05 – 7.02 (m, 2H), 2.29 – 2.07 (m, 8H), 0.98 – 0.75 (m, 20H), 0.66 – 0.56 (m, 10H) 0.42 (t, 6H, J = 7.4 Hz). ESI-HRMS: m/z calcd for $[C_{78}H_{74}N_4PtS_2]^+$, 1326.5016; found, 1326.5051. Anal. Calcd (%) for $C_{78}H_{74}N_4PtS_2 \cdot 2C_6H_{14} \cdot H_2O$: C 71.26, H 6.91, N 3.69; found: C 71.12, H 7.00, N 3.91.

3.2.2. Photophysical Measurement

The UV-vis absorption spectra were measured on SHIMADZU 2501 PC UV-vis spectrophotometer in a 1-cm quartz cuvette in different HPLC-grade solvents. The steady state emission spectra were obtained using a SPEX fluorolog-3 fluorometer/phosphorometer. The emission quantum yields were measured by the comparative method[34] in degassed toluene solution. A degassed $[Ru(bpy)_3]Cl_2$ in aqueous solution (Φ_{em} = 0.042, λ_{ex} = 436 nm)[35] was used as the reference. The excited-state lifetime, triplet excited-state quantum yield and the triplet transient difference absorption spectra were gained in toluene solutions on an Edinburgh LP920 laser flash photolysis spectrometer. The third harmonic output (355 nm) of a Nd:YAG laser (Quantel Brilliant, pulse width (fwhm) = 4.1 ns, the repetition rate was set at 1 Hz) was used as the excitation source. Each sample was purged with Ar for 30 min prior to each measurement.

The emission self-quenching rate constants (k_q) in CH_2Cl_2 can be deduced by the Stern-Volmer equation 3-1 through measuring the excited-state lifetime (τ_{obs}) of the complex at different concentrations:

$$k_{obs} = k_q \cdot [C] + k_0 \qquad (3\text{-}1)$$

In this equation k_{obs} is the observed emission decay rate constants ($k_{obs} = 1/\tau_{em}$) at different concentrations, [C] is the concentration of the complex solution, and k_0 ($k_0 = 1/\tau_0$) is the decay rate constant of the excited state in an infinitely dilute solution. The lifetimes of the complex solutions were measured at different concentrations. The k_{obs} were plotted against the solution concentration. The slope of the straight line is the k_q, and the intercept is the k_0.

The triplet excited-state absorption coefficient (ε_T) was measured using the depletion method and calculated using the following equation 3-2.[36]

$$\varepsilon_T = \frac{\varepsilon_S[\Delta OD_T]}{\Delta OD_S} \qquad (3\text{–}2)$$

In this equation ΔOD_S and ΔOD_T are the ΔOD values at the minimum of the bleaching band and the maximum of the positive band in the triplet transient difference absorption (TA) spectrum, and ε_S is the ground-state molar extinction coefficient at the wavelength of the bleaching band minimum. After obtaining the ε_T value from this equation, the quantum yield of the triplet excited-state (Φ_T) can be obtained using the comparative method,[36] in which SiNc in benzene ($\Phi_T = 0.20 \pm 0.03$, $\varepsilon_{T,\,590\,nm} = 53400\ M^{-1}\cdot cm^{-1}$)[37] as the reference. Equation 3-3 was used to calculate the Φ_T:

$$\Phi_T^S = \Phi_T^{ref} \frac{\Delta OD_T^S}{\Delta OD_T^{ref}} \frac{\varepsilon_T^{ref}}{\varepsilon_T^S} \qquad (3\text{-}3)$$

where ΔOD_T^S and ΔOD_T^{ref} are the ΔOD_T values at the TA spectrum band maximum for the sample and the reference, respectively ε_T^{ref} and ε_T^S are the triplet molar extinction coefficients at the wavelength where the ΔOD_T is observed for the sample and the reference.

3.2.3. Nonlinear Transmission Measurement

The experimental setup was similar to that described previously.[38] The second harmonic (λ = 532 nm) of a 4.1 ns (fwhm), 10 Hz, Q-switched Quantel Brilliant Nd:YAG laser was used as the light source. The laser beam was focused by a f = 30 cm planoconvex lens to the center of a 2 mm thick quartz cuvette that contained the sample solution. The radius of the beam waist was approximately 75 μm. Two Molectron J4-09 pyroelectric probes and an EPM2000 energy/power meter were used to monitor the incident and output energies.

3.3. Results and Discussion

3.3.1. UV-Vis Absorption

The UV-Vis absorption of **3-1** – **3-3** in CH_2Cl_2 obeys Beer-Lambert's law in the concentration range of 10^{-6} – 10^{-4} mol/L, indicating that no ground-state aggregation occurs in this concentration range. As depicted in Figure 3.1, the high-energy absorption bands below 400 nm are assigned as intraligand π,π^* transitions within the C^N^N ligand or the acetylide ligand. For each complex, a charge-transfer band appears between 400 nm and 600 nm. The extinction coefficients (ε) of the charge-transfer bands of **3-2** and **3-3** are quite similar; however, the ε of the charge-transfer band of **3-1** is much stronger and narrower than those of **3-2** and **3-3**. In addition, **3-1** also exhibits an obvious blue-shift of the charge-transfer band in comparison to those of **3-2** and **3-3**. This is due to the strong electron-withdrawing ability of the nitro substituent on the acetylide ligand. As reported by Sun and co-workers on 4,6-diphenyl-2,2'-bipyridine platinum(II) acetylide complexes via a time-dependent density functional theory (TDDFT) calculation, the highest occupied molecular

orbital (HOMO) in these complexes has a significant contribution from the acetylide moiety, and the 6-phenyl and the central pyridine rings (referred to as C^N component in C^N^N ligand), as well as a minor contribution from the Pt d orbital. In contrast, the lowest unoccupied molecular orbital (LUMO) is exclusively dominated by the bipyridine component in the C^N^N ligand (referred to as N^N moiety).[39] Therefore, the lowest-energy electronic transition in these complexes has mixed ^{1}LLCT/^{1}ILCT/^{1}MLCT characters. The strong electron-withdrawing $-NO_2$ group not only stabilizes the acetylide based molecular orbital, resulting in an increased-energy ^{1}LLCT transition, but also stabilizes the Pt(II) d orbitals, which leads to an blue-shifted ^{1}MLCT transition. Both effects cause the significant hyposochromic shift of the charge-transfer band in **3-1**.

The low-energy absorption bands of **3-1** – **3-3** exhibit solvent dependence. As shown in Figure 3.2, Figure 3.3 and Figure 3.4, **3-1** exhibits a much clear negative solvatochromic effect than **3-2** and **3-3** do, which is a characteristic for charge-transfer transition. Therefore, the lowest-energy absorption band in **3-1** has more charge-transfer character, most likely arising from the ^{1}MLCT. In contrast, the negative solvatochromic effect is much less pronounced in **3-2** and **3-3**, suggesting that the electron density is more delocalized in the HOMOs of **3-2** and **3-3**. Alternatively, we can tentatively assume that the lowest-energy absorption bands in **3-2** and **3-3** between 400 nm and 600 nm admix some ligand-to-ligand charge transfer (^{1}LLCT), intraligand charge transfer (^{1}ILCT), $^1\pi,\pi^*$, and possibly ^{1}MLCT transitions.

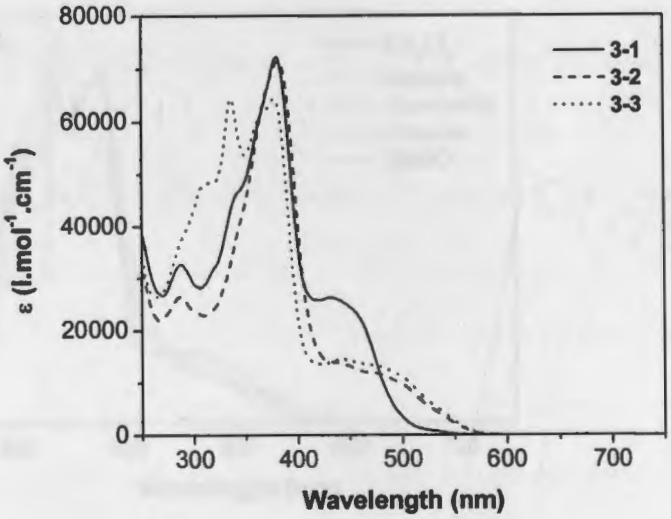

Figure 3.1. Electronic absorption spectra of 6-phenyl-4-(7-benzothiazolyl-9,9-diethylfluoren-2-yl)-2,2'-bipyridine Pt(II) complex **3-1** – **3-3** in CH_2Cl_2.

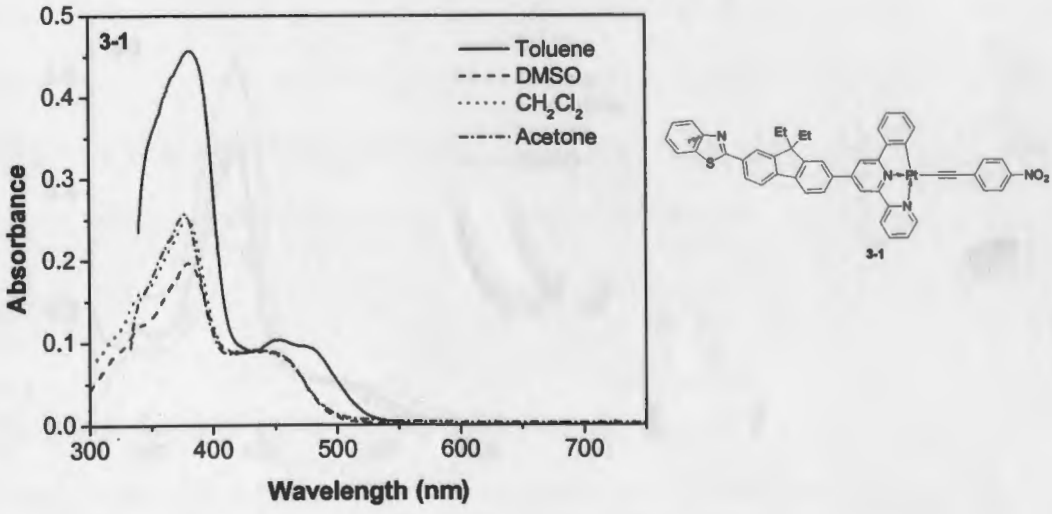

Figure 3.2. UV-vis absorption spectra of 5×10^{-5} mol/L solution of 6-phenyl-4-(7-benzothiazolyl-9,9-diethylfluoren-2-yl)-2,2'-bipyridine Pt(II) complex **3-1** in different solvents measured in a 1-cm cuvette at room temperature.

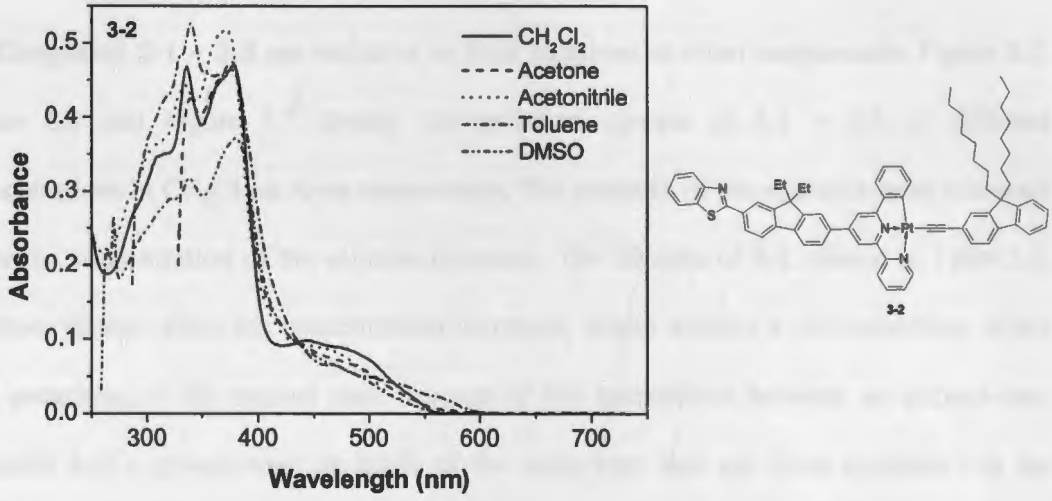

Figure 3.3. UV-vis absorption spectra of 5×10-5 mol/L solution of 6-phenyl-4-(7-benzothiazolyl-9,9-diethylfluoren-2-yl)-2,2'-bipyridine Pt(II) complex **3-2** in different solvents measured in a 1-cm cuvette at room temperature.

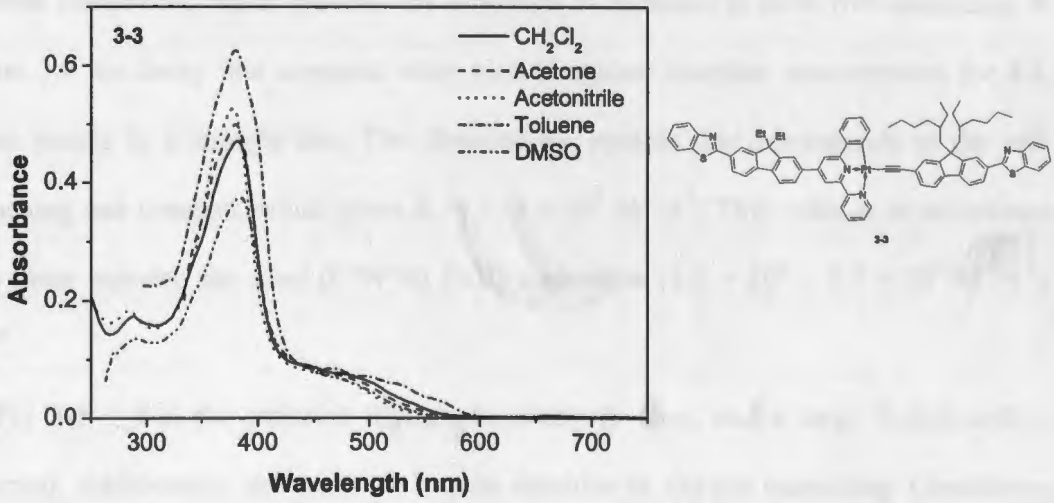

Figure 3.4. UV-vis absorption spectra of 5×10^{-5} mol/L solution of 6-phenyl-4-(7-benzothiazolyl-9,9-diethylfluoren-2-yl)-2,2'-bipyridine Pt(II) complex **3-3** in different solvents measured in a 1-cm cuvette at room temperature.

3.3.2. Emission

Complexes **3-1** – **3-3** are emissive in fluid solutions at room temperature. Figure 3.5, Figure 3.6 and Figure 3.7 display the emission spectra of **3-1** – **3-3** of different concentrations in CH_2Cl_2 at room temperature. The intensity of the emission band increases while the concentration of the solution increases. The lifetime of **3-1**, shown in Table 3.1, becomes shorter when the concentration increases, which implies a self-quenching effect (the quenching of the excited state because of the interactions between an excited-state molecule and a ground-state molecule of the same type that can form excimers.) in the concentration range of from 4.25×10^{-6} to 3.4×10^{-5} mol/L. However, no self-quenching effect was observed for complexes **3-2** and **3-3** in the concentration range studied. This probably can be attributed to the presence of the alkyl chains at the 9-position of the fluorene component, which prevents the formation of excimers in these two complexes. In Figure 3.8 the decay rate constants were plotted against complex concentration for **3-1**, which results in a straight line. The slope of the straight line corresponds to the self-quenching rate constant, which gives $k_q = 3.53 \times 10^9$ $M^{-1} \cdot s^{-1}$. This value is in accordance with those reported for other (C^N^N) Pt(II) complexes ($1.6 \times 10^9 - 5.7 \times 10^9$ $M^{-1} \cdot s^{-1}$). [6,15,39]

For **3-1** – **3-3**, the emission lifetime in relatively long, and a large Stokes shift is observed. Additionally, the emission is quite sensitive to oxygen quenching. Considering these features and with reference to the other Pt(II) C^N^N complexes reported in the literature, we believe that the emission from these three complexes at room temperature originates from a triplet excited state, and we tentatively ascribe the emitting state as

^{3}MLCT excited state. In line with the trend observed in UV-vis spectral measurement, the emission energy of **3-1** also shifts to a higher energy compared to those of **3-2** and **3-3**. The emission of complex **3-1** measured in butyronitrile glassy solution at 77 K (Figure 3.9) shows vibronic structures compared to that at room temperature. The blue-shift of the emission band is attributed to the rigidochromic effect that is a common phenomenon for metal bidentate and terdentate complexes.[6,40] For **3-2** (Figure 3.10) and **3-3** (Figure 3.11), the emission spectra in butyronitrile glassy matrix at 77 K become narrower and simply blue-shifted in comparison to those measured at room temperature. No clear vibronic structures were observed in the spectra of these two complexes. This is probably due to the weak emission from **3-2** and **3-3** (see the emission quantum yield listed in Table 3.1 at room temperature), which would reduce the signal-to-noise ratio of the spectra at 77K. With increased concentrations, the spectral features for all three complexes remain the same, indicating that no ground-state aggregation occurs in the concentration range studied.

3.3.3. Triplet Transient Different Absorption

The time-resolved triplet transient difference absorption spectra of **3-1 – 3-3** in toluene are displayed in Figure 3.12, Figure 3.13 and Figure 3.14 and the lifetimes of the triplet exited state deduced from the decay of the transient absorption are listed in Table 3.1. These measurements could provide valuable information on the triplet excited-state absorption spectrum and the lifetime of the triplet excited state, which would help us predicting the nonlinear absorption of these complexes. A positive band in the triplet transient difference absorption spectrum illustrates stronger excited-state absorption than

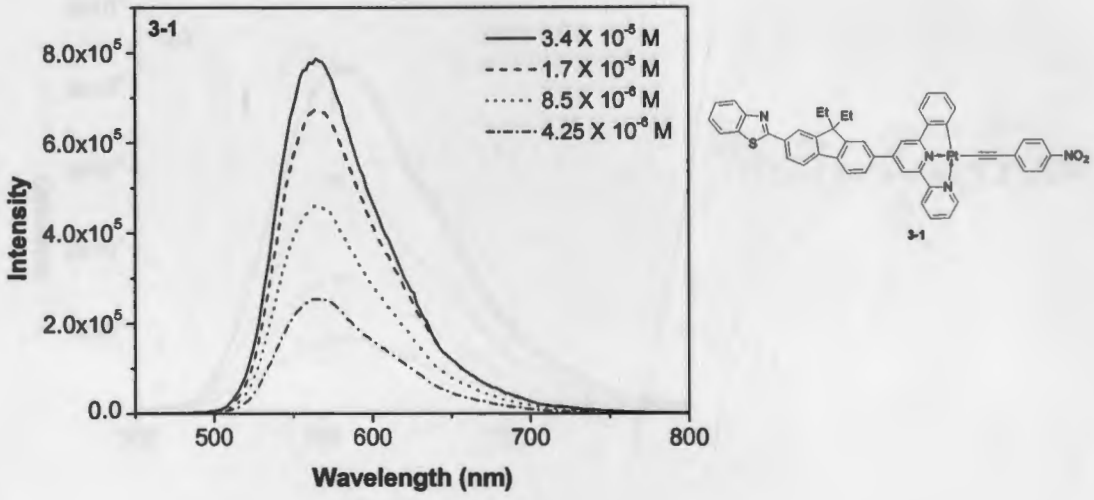

Figure 3.5. Concentration-dependent emission spectra for 6-phenyl-4-(7-benzothiazolyl-9,9-diethylfluoren-2-yl)-2,2'-bipyridine Pt(II) complex **3-1** (λ_{ex} = 433 nm) in CH_2Cl_2 at room temperature.

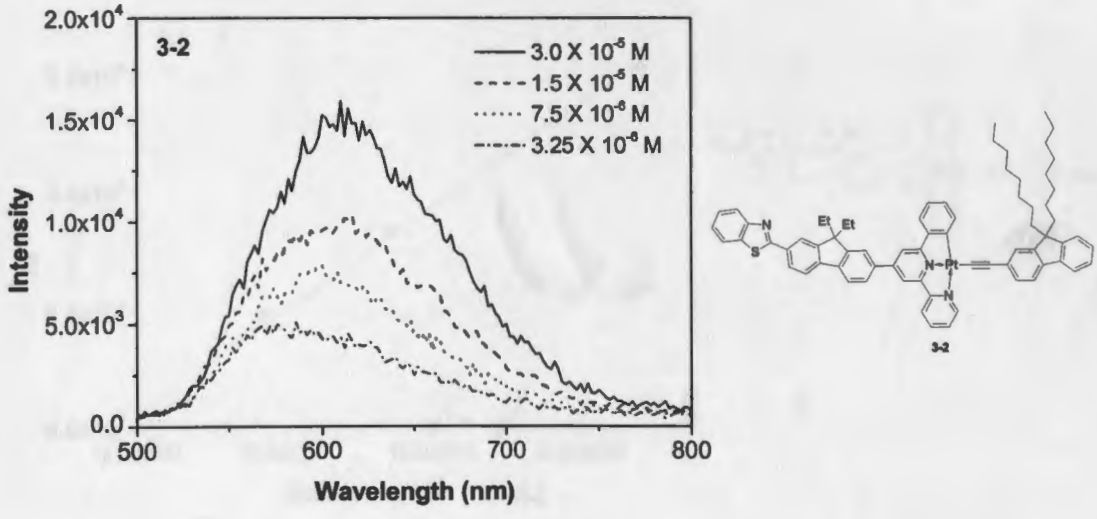

Figure 3.6. Concentration-dependent emission spectra for 6-phenyl-4-(7-benzothiazolyl-9,9-diethylfluoren-2-yl)-2,2'-bipyridine Pt(II) complex **3-2** (λ_{ex} = 444 nm) in CH_2Cl_2 at room temperature.

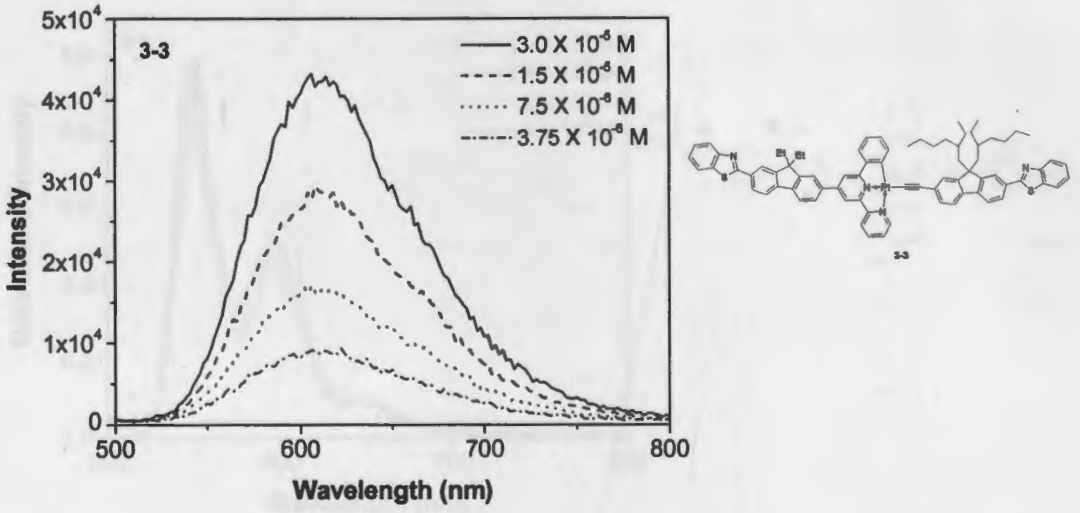

Figure 3.7. Concentration-dependent emission spectra for 6-phenyl-4-(7-benzothiazolyl-9,9-diethylfluoren-2-yl)-2,2'-bipyridine Pt(II) complex **3-3** (λ_{ex} = 440 nm) in CH_2Cl_2 at room temperature.

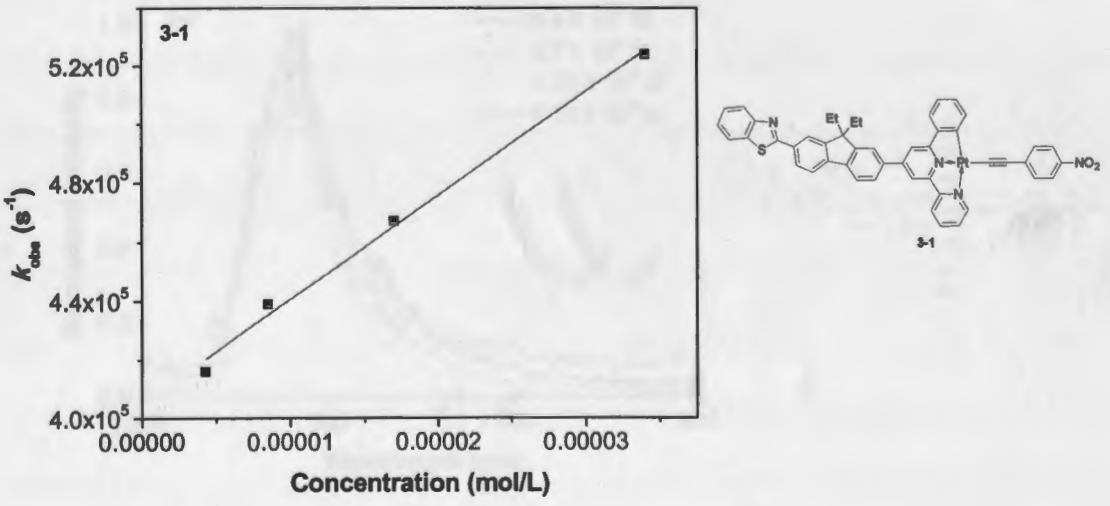

Figure 3.8. Plot of k_{obs} vs. concentration for 6-phenyl-4-(7-benzothiazolyl-9,9-diethylfluoren-2-yl)-2,2'-bipyridine Pt(II) complex **3-1** in CH_2Cl_2.

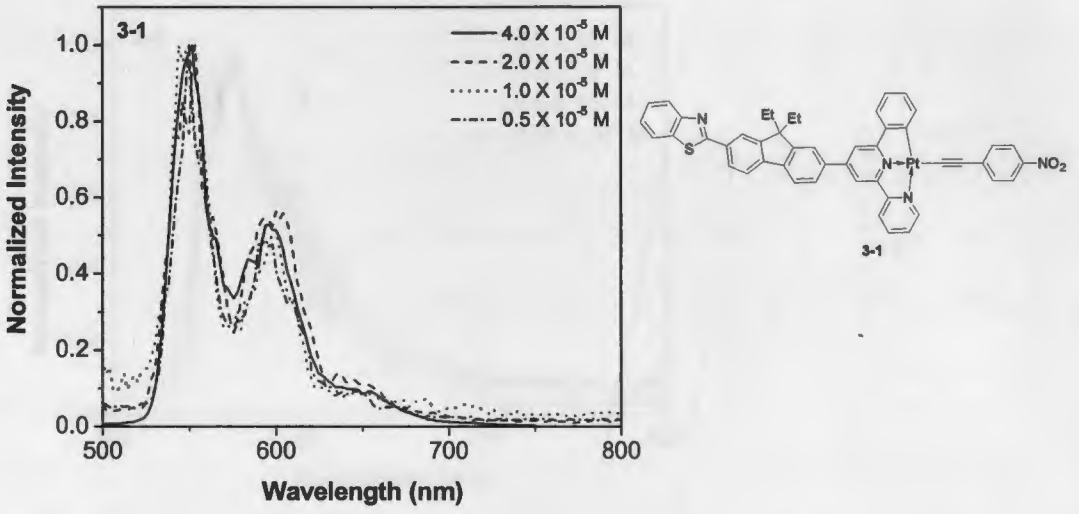

Figure 3.9. Emission spectra of 6-phenyl-4-(7-benzothiazolyl-9,9-diethylfluoren-2-yl)-2,2'-bipyridine Pt(II) complex **3-1** measured in degassed butyronitrile glassy matrix at 77 K.

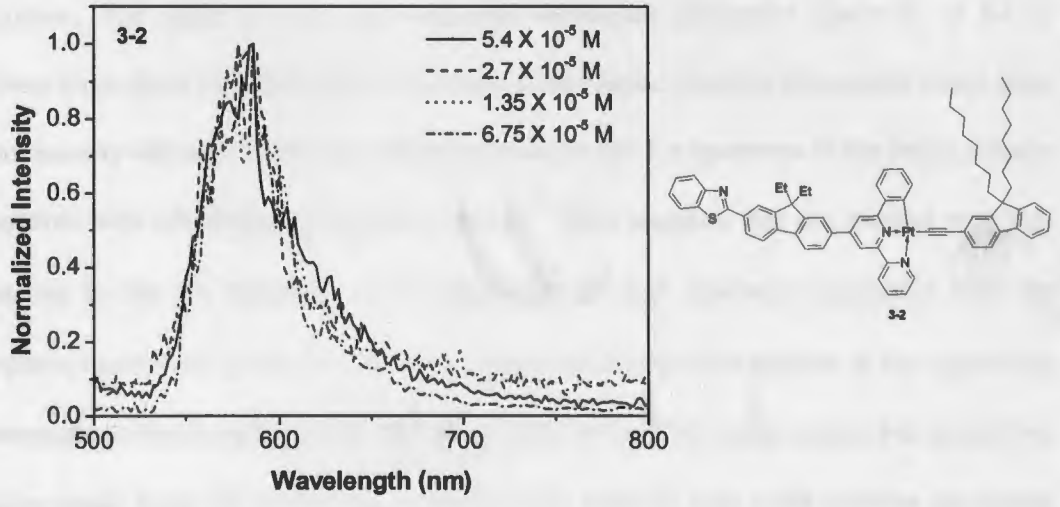

Figure 3.10. Emission spectra of 6-phenyl-4-(7-benzothiazolyl-9,9-diethylfluoren-2-yl)-2,2'-bipyridine Pt(II) complex **3-2** measured in degassed butyronitrile glassy matrix at 77 K.

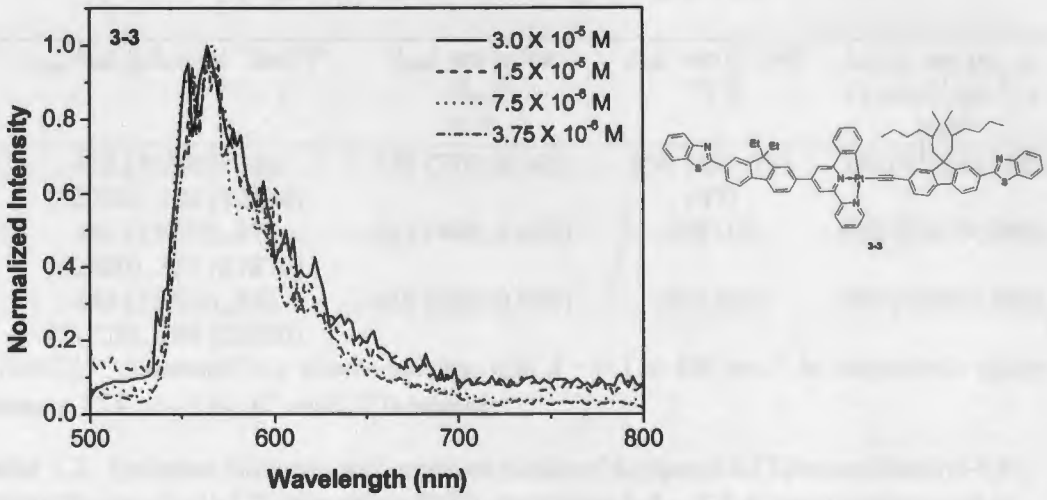

Figure 3.11. Emission spectra of 6-phenyl-4-(7-benzothiazolyl-9,9-diethylfluoren-2-yl)-2,2'-bipyridine Pt(II) complex **3-3** measured in degassed butyronitrile glassy matrix at 77 K.

that of the ground state in the specific region, which could cause reverse saturable absorption. The shape of the triplet transient difference absorption spectrum of **3-1** is different from those of **3-2** and **3-3**. **3-1** shows a very broad positive absorption bands from approximately 480 nm to 800 nm, which is similar to the TA spectrum of the Pt(II) diimine complexes with nitrophenyl acetylide complex.[31] This suggests that the excited state that gives rise to the TA spectrum of **3-1** should have $^3\pi,\pi^*$ character associated with the nitrophenyl acetylide ligand. In addition, a strong bleaching band appears in the region that corresponds to the charge-transfer absorption band in the UV-vis spectrum. **3-2** shows two positive bands from 400 to 800 nm, while **3-3** only exhibits very weak positive absorption in the visible spectral region. The lifetimes deduced from the decay of the TA spectra of **3-1 – 3-3** are quite similar to those obtained from the decay of the emission, implying that the excited state that gives rise to the TA spectra could be the same excited state that emits or is in equilibrium with the emitting state.

Table 3.1. Photophysical parameters of 6-phenyl-4-(7-benzothiazolyl-9,9-diethylfluoren-2-yl)-2,2'-bipyridine Pt(II) complexes **3-1** – **3-3**.

	λ_{abs} /nm (ε/L.mol^{-1}.cm^{-1})[a]	λ_{em}/ nm (τ /ns; Φ_{em})[b] R.T.	λ_{em}/ nm (τ /μs)[c] 77 K	$\lambda_{T1\text{-}Tn}$/ nm ($\varepsilon_{T1\text{-}Tn}$ / L.mol^{-1}.cm^{-1}; τ /ns)[d]
3-1	433 (26350), 380 (72240), 286 (32590)	570 (770; 0.165)	551 (48), 595 (47)	590 (45250; 630)
3-2	441 (13870), 378 (62800), 335 (61870)	612 (400; 0.030)	580 (15)	420 (28070; 390)
3-3	440 (13720), 382 (71220), 286 (26580)	610 (610; 0.066)	564 (34)	495 (12860; 680)

[a] In CH_2Cl_2. [b] Measured in a toluene solution with A = 0.1 at 436 nm. [c] In butyronitrile glassy solutions at 77 K. $c = 3.5\times10^{-5}$ mol/L [d] In toluene.

Table 3.2. Emission lifetimes and quantum yields of 6-phenyl-4-(7-benzothiazolyl-9,9-diethylfluoren-2-yl)-2,2'-bipyridine Pt(II) complexes **3-1** – **3-3** at room temperature in different solvents at room temperature.

Solvent	λ_{em} / nm (τ / ns; Φ_{em})		
	3-1	**3-2**	**3-3**
CH_2Cl_2	564 (1536; 0.188)	614 (160; 0.012)	610 (340; 0.029)
Acetonitrile	-	616 (140; 0.0069)	604 (290; 0.017)
Acetone	579 (1747; 0.169)	625 (150; 0.0072)	609 (280; 0.020)
Toluene	570 (773; 0.165)	612 (400; 0.030)	610 (610; 0.066)
DMSO	-	618 (-; 0.0045)	-

3.3.4. Reverse Saturable Absorption

As previously discussed, complexes 3-1 – 3-3 possess relatively long triplet excited-state lifetimes and 3-1 exhibits moderately strong and broad triplet excited-state absorption in the visible to the near-IR region. Therefore, reverse saturable absorption is expected for these complexes. The concentrations of the solutions were adjusted to obtain the same linear transmission of 80% for all the samples at 532 nm in a 2-mm cell. The nonlinear transmission results for complexes **3-1** – **3-3** are shown in Figure 3.7. Only **3-1** shows significant transmission decrease with increased incident fluence, which is a typical

phenomenon for RSA. The stronger RSA of **3-1** can be ascribed to: (1) the ground-state absorption of **3-1** at 532 nm is much weaker than those of **3-2** and **3-3** (shown in Figure 3.1). (2) the ΔOD at 532 nm for **3-1** is larger than those of **3-2** and **3-3** at the similar excitation condition (Figures 3.12 – 3.14). Both factors lead to an increased ratio of the excited-state absorption to ground-state absorption cross-section (σ_{ex}/σ_0), which is a key parameter in determining the degree of RSA.

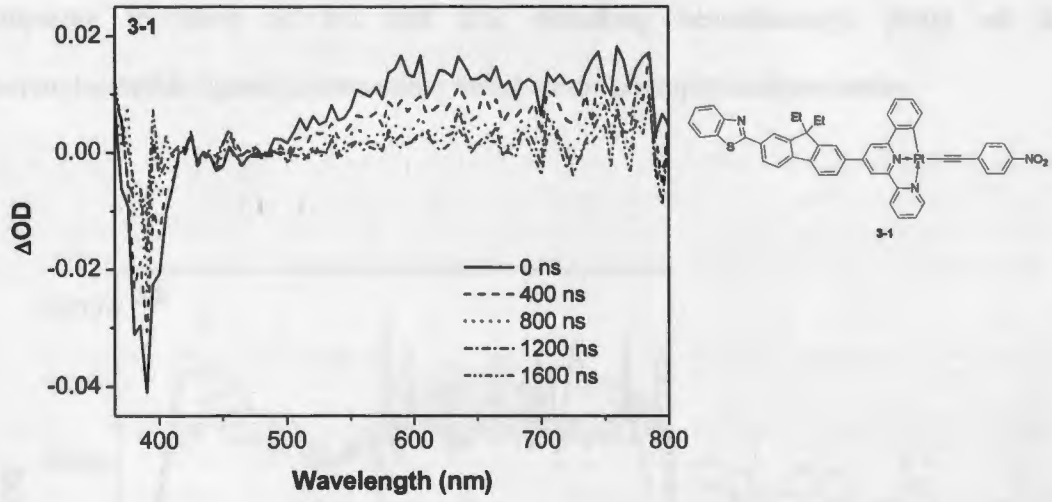

Figure 3.12. Time-resolved triplet transient difference absorption spectra of 6-phenyl-4-(7-benzothiazolyl-9,9-diethylfluoren-2-yl)-2,2'-bipyridine Pt(II) complex **3-1** dissolved in argon degassed toluene solution at room temperature following 355 nm excitation with A_{abs} = 0.40 at the excitation wavelength. The time listed in the figure is the time delay after the laser pulse.

3.4. Summary and Future Directions

In this project, three platinum(II) 6-phenyl-4-(7-benzothiazolyl-9,9-diethylfluoren-2-yl)-2,2'-bipyridine complexes with different acetylide ligands were synthesized and their photophysical properties were systematically investigated. All of the complexes exhibit charge-transfer absorption bands in the visible region and are emissive at room temperature

in fluid solutions and at 77 K in glassy matrix. Although significant self-quenching effect exists in complex **3-1**, the quantum yield and lifetime of **3-1** are higher than those of **3-2** and **3-3**. **3-1** also exhibits stronger and broader positive band in TA spectrum than those of **3-2** and **3-3**, therefore, significant reverse saturable absorption (RSA) was observed at 532 nm for 4.1 ns laser pulses for **3-1**. Introducing the nitrophenylacetylide ligand to the platinum(II) complex increases the contribution of MLCT character into the lowest excited states. The UV-vis spectrum and emission spectrum of **3-1** is narrower and blue-shifted comparing to those of **3-2** and **3-3**. Attaching benzothiazolyl group on the fluorenylacetylide ligand imparts minor effect on the photophysical properties.

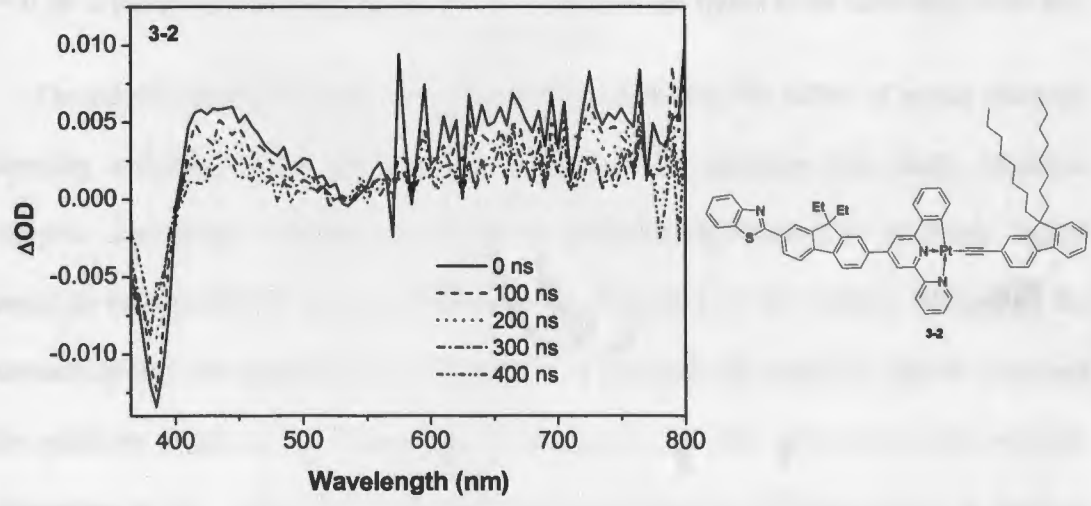

Figure 3.13. Time-resolved triplet transient difference absorption spectra of 6-phenyl-4-(7-benzothiazolyl-9,9-diethylfluoren-2-yl)-2,2'-bipyridine Pt(II) complex **3-2** dissolved in argon degassed toluene solution at room temperature following 355 nm excitation with A_{abs} = 0.40 at the excitation wavelength. The time listed in the figure is the time delay after the laser pulse.

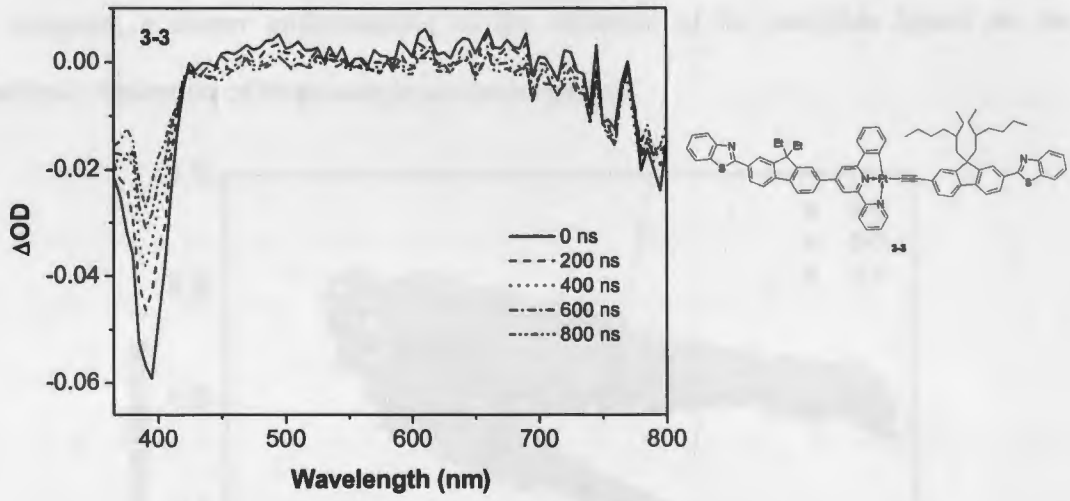

Figure 3.14. Time-resolved triplet transient difference absorption spectra of 6-phenyl-4-(7-benzothiazolyl-9,9-diethylfluoren-2-yl)-2,2'-bipyridine Pt(II) complex **3-3** dissolved in argon degassed toluene solution at room temperature following 355 nm excitation with A_{abs} = 0.40 at the excitation wavelength. The time listed in the figure is the time delay after the laser pulse.

The results obtained to date is very interesting, however, the effect of strong electron-donating acetylide ligand has not been evaluated. To complete this study, platinum complex containing 7-diphenylamino-9,9-di(2-ethylhexyl)fluoren-2-yl acetylide ligand needs to be synthesized and its photophysical properties to be studied. Moreover, the ultimate goal of this project is to investigate how the different acetylide ligands influence the nonlinear absorption of these platinum complexes. To date, only the reverse saturable absorption of **3-1** – **3-3** at 532 nm was demonstrated using ns laser pulses. In order to evaluate the nonlinear absorption characteristics, including the excited-state absorption and two-photon absorption, of these complexes over a broad visible to the near-IR region, wavelength-dispersion Z-scan measurements should be carried out and the Z-scan data should be fitted by a five-band model to abstract the excited-state absorption cross-sections

and two-photon absorption cross-sections at a variety of wavelengths. Only after this work is complete, a deeper understanding of the influence of the acetylide ligand on the nonlinear absorption of these complexes can be gained.

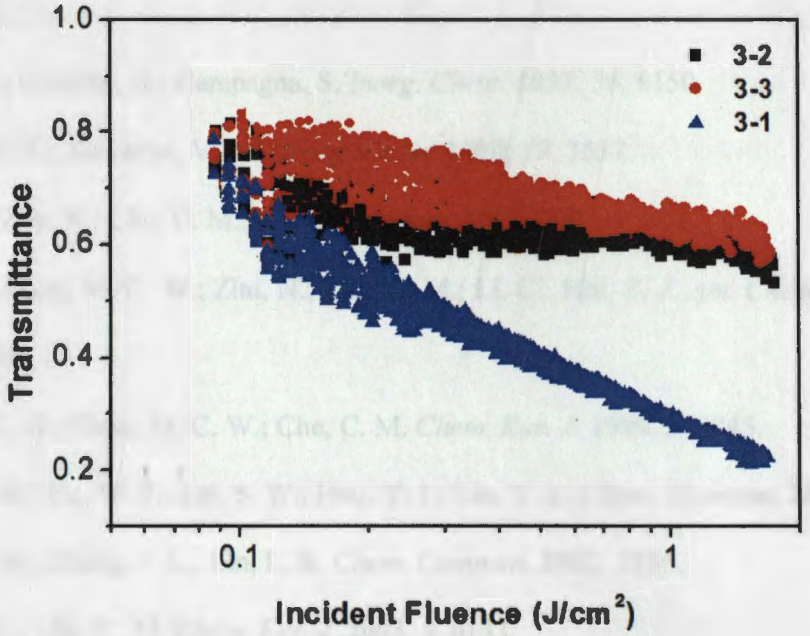

Figure 3.15. Transmission vs incident fluence curves for **3-1** – **3-3** in toluene solutions for 4.1 ns laser pulses at 532 nm in a 2-mm cell. The linear transmission was adjusted to 80%.

3.5. References

1. Fernandez, S.; Fornies, J.; Gil, B.; Gomez, L. E. *Dalton Trans.* **2003**, 822.
2. Chan, C. W.; Lai, T. F.; Che, C. M.; Peng, S. M. *J. Am. Chem. Soc.* **1993**, *115*, 11245.
3. Constable, E. C.; Henney, R. P. G.; Leese, T. A.; Tocher, D. A. *J. Chem. Soc. Dalton Trans.* **1990**, 443.
4. Constable, E. C.; Henney, R. P. G.; Leese, T. A.; Tocher, D. A. *J. Chem. Soc. Chem. Commun.* **1990**, 513.

5. Cheung, T. C., Cheung, K. K.; Peng, S. M.; Che, C. M. *J. Chem. Soc. Dalton Trans.* **1996**, 1645.

6. Lai, S. W.; Chan, M. C. W.; Cheung, T. C.; Peng, S. M.; Che, C. M. *Inorg. Chem.* **1999**, *38*, 4046.

7. Neve, F.; Crispini, A.; Campagna, S. *Inorg. Chem.* **1997**, *36*, 6150.

8. Yip, J. H. K.; Suwarno, V. J. J. *Inorg. Chem.* **2000**, *39*, 3537.

9. Lu, W.; Zhu, N.; Che, C. M.; *Chem. Commun.* **2002**, 900

10. Lu, W.; Chan, M. C. W.; Zhu, N.; Che, C. M.; Li, C.; Hui, Z. *J. Am. Chem. Soc.* **2004**, *126*, 7639.

11. Wong, K. H.; Chan, M. C. W.; Che, C. M. *Chem. Eur. J.* **1999**, *5*, 2845.

12. Che, C. M.; Fu, W. F.; Lai, S. W.; Hou, Y. J.; Liu, Y. L. *Chem. Commun.* **2003**, 118.

13. Che, C. M.; Zhang, J. L.; Lin, L. R. *Chem. Commun.* **2002**, 2556.

14. Ma, D. L.; Che, C. M. *Chem. Eur. J.* **2003**, *9*, 6133.

15. Lu, W.; Mi, B. X.; Chan, M. C. W.; Hui, Z.; Che, C. M.; Zhu, N.; Lee, S. T. *J. Am. Chem. Soc.* **2004**, *126*, 4958.

16. Rogers, J. E.; Slagle, J. E.; Krein, D. M.; Burke, A. R.; Hall, B. C.; Fratini, A.; McLean, D. G.; Fleitz, P. A.; Cooper, T. M.; Drobizhev, M.; Makarov, N. S.; Rebane, A.; Kim, K. Y.; Farley, R.; Schanze, K. S. *Inorg. Chem.* **2007**, *46*, 6483.

17. Belfield, K. D.; Hagan, D. J.; Van Stryland, E. W.; Schafer, K. J.; Negres, R. A. *Org. Lett.* **1999**, *1*, 1575.

18. Sutherland, R. L.; Brant, M. C.; Heinrichs, J.; Rogers, J. E.; Slagle, J. E.; McLean, D. G.; Fleitz, P. A. *J. Opt. Soc. Am. B*, **2005**, *22*, 1939.

19. Sutherland, R. L.; McLean, D. G.; Brant, M. C.; Rogers, J. E.; Fleitz, P. A.; Urbas, A. M. *SPIE Proc.* **2006**, *6330,* 633006.

20. Lee, S. H.; Nakamura, T.; Tsutsui, T. *Org. Lett.* **2001**, *3*, 2005.

21. Belfield, K. D.; Bondar, M. V.; Hernandez, F. E.; Masunov, A. E.; Mikhailov, I. A.; Morales, A. R.; Przhonska, O. V.; Yao, S. *J. Phys. Chem. C*, **2009**, *113*, 4706.

22. Belfield, K. D.; Ren, X.; Van Stryland, E. W.; Hagan, D. J.; Dubikovski, V.; Meisak, E. J. *J. Am. Chem. Soc.* **2000**, *122*, 1217.

23. Parthenopoulos, D. A.; Rentzepis, P. M. *Science* **1989**, *245*, 843.

24. Kannan, R.; He, G. S.; Lin, T. C.; Prasad, P. N.; Vaia, R. A.; Tan, L. S. *Chem. Mater.* **2004**, *16*, 185.

25. He, G. S.; Lin, T. C.; Prasad, P. N.; Kannan, R.; Vaia, R. A.; Tan, L. S. *J. Phys. Chem. B*, **2002**, *106*, 11081.

26. He, G. S.; Lin, T. C.; Dai, J.; Prasad, P. N.; Kannan, R.; Dombroskie, A. G.; Vaia, R. A.; Tan, L. S. *J. Chem. Phys.* **2004**, *120*, 5275.

27. He, G. S.; Swiatkiewicz, J.; Jiang, Y.; Prasad, P. N.; Reinhardt, B. A.; Tan, L. S.; Kannan, R. *J. Phys. Chem. A*, **2000**, *104*, 4810.

28. Schafer, K. J.; Hales, J. M.; Balu, M.; Belfield, K. D.; Van Stryland, E. W.; Hagan, D. J. *J. Photochem. Photobiol. A*, **2004**, *162*, 497.

29. Swiatkiewicz, J.; Prasad, P. N.; Reinhardt, B. A. *Opt. Commun.* **1998**, *157*, 135.

30. Rogers, J. E.; Slagle, J. E.; McLean, D. G.; Sutherland, R. L.; Sankaran, B.; Kannan, R.; Tan, L. S. Fleitz, P. A. *J. Phys. Chem. A*, **2004**, *108*, 5514.

31. Pritchett, T. M.; Sun, W.; Zhang, B.; Ferry, M. J.; Li, Y.; Haley, J. E.; Mackie, D. M.; Shensky III, W.; Mott, A. G. *Opt. Lett.* **2010**, *35*, 1305.

32. Zhang, B.; Li, Y.; Pritchett, T. M.; Sun, W. "Broad-band nonlinear absorbing platinum diimine complex: synthesis, photophysics and nonlinear absorption" (submitted to *J. Am. Chem. Soc.*)

33. Kanna, R.; He, G. S.; Yuan, L.; Xu, F.; Prasad, P. N.; Dombroskie, A. G.; Reinhardt, B. A.; Baur, J. W.; Vaia, R. A.; Tan, L. S. *Chem. Mater.* **2001**, *13*, 1896.

34. Demas, J. N.; Crosby, G. A. *J. Phys. Chem.* **1971**, *75*, 991.

35. Van Houten, J.; Watts, R. *J. Am. Chem. Soc.* **1976**, *98*, 4853.

36. Carmichael, I.; Hug, G. L. *J. Phys. Chem. Ref. Data* **1986**, *15*, 1.

37. Firey, P. A.; Ford, W. E.; Sounik, J. R.; Kenney, M. E.; Rodgers, M. A. J. *J. Am. Chem. Soc.* **1988**, *110*, 7626.

38. Sun, W.; Zhu, H.-J.; Barron, P. *Chem. Mater.* **2006**, *18*, 2602.

39. Shao, P.; Li, Y.; Azenkeng, A.; Hoffmann, M. R.; Sun, W. *Inorg. Chem.* **2009**, *48*, 2407.

40. Cummings, S. D.; Eisenberg, R. *J. Am. Chem. Soc.* **1996**, *118*, 1949.

CHAPTER 4.

SYNTHESIS OF PLATINUM DIIMINE COMPLEX WITH 7-BENZOTHIAZOLYL-9,9-DI(2-ETHYLHEXYLFLUOREN-2-YL) ACETYLIDE LIGAND

4.1. Introduction

In the past, the study on the metal-to-ligand charge transfer (MLCT) has been mainly focused on the d^6 transition metal complexes, such as Ru(II), Os(II) and Re(I).[1-4] The interest in studying the d^8 Pt(II) diimine complexes (diimine)PtL_2 (L = halide, nitrile, thiolate, isonitrile, and acetylide) has been growing emergingly in recent years.[5-17] These (diimine)PtL_2 complexes have long-lived excited states, which is attributed to the ^{3}MLCT from *d*(Pt) to π^* of diimine transition. This unique property potentially can be applied to many fields, such as electroluminescent devices[18,19] dye-sensitized solar cells[20,21] and non-linear optical materials[22,23] *etc.* Most importantly, the excited-state properties of these Pt(II) diimine complexes can be tuned by modification of either the diimine ligands or the L ligands.

In this work, a new bis(mesitylimino)acenaphthene platinum(II) complex containing alkynyl-benzothiazolylfluorene ligands (**4-1**) was synthesized and its photophysical properties were investigated. The alkynyl-benzothiazolylfluorene moiety was chosen because platinum complexes bearing this ligand were reported recently by our group to exhibit relatively large two-photon absorption in the near-infrared region.[22,24] Diimine ligand bis(mesitylimino)acenaphthene was chosen because the lower-lying π^* orbitals can

shift the charge-transfer transition to much lower energy so that the absorption and emission spectra could extend into the near-IR region.[25]

4.2. Experimental Section

The experimental details are presented in the following paragraphs. The synthetic procedures for the complex are presented first, then the photophysical measurements for the complexes are discussed.

4.2.1. Synthesis

All the reagents were purchased from Aldrich and Alfa Aesar and used without further purification. All solvent were purchased from VWR Scientific Company with analytical grade, and used without further purification unless otherwise stated. The silica gel (230×400 mesh) was purchased from Sorbent Technologies Company. All products were characterized by ^{1}H NMR, elemental analysis, and high resolution MS. ^{1}H NMR spectra were obtained using a Varian 300 MHz, 400 MHz or 500 MHz VNMR spectrometer. Elemental analysis were conducted by NuMega Resonance labs, Inc. in San Diego, CA. High resolution MS data was obtained using a Bruker Bio Tof III mass spectrometer.

The synthetic route for the bis(mesitylimino)acenaphthene Pt(II) acetylide complex (**4-1**) is displayed in Scheme 4.1.

Bis(mesitylimino)acenaphthene (mesBIAN)

Acenaphthenequinone (2.00 g, 0.011 mol) and 2,4,6-trimethylaniline (3.65 ml, 0.026 mol) were stirred in a solution of MeOH/formic acid (100 ml/2 ml) for 60 hours at room temperature. The orange suspension was stored at -5 °C overnight to precipitate the product,

which was isolated by filtration, washed by MeOH, and dried. 4.1 g dark red solid was obtained (yield: 90%). ^{1}H NMR ($CDCl_3$, 500 MHz, δ ppm): 7.91 (2H, d, J = 8.5 Hz), 7.42 (2H, t, J = 7.5 Hz), 7.00 (4H, s), 6.79 (2H, d, J = 7 Hz), 2.40 (6H, s), 2.12 (12H, s).

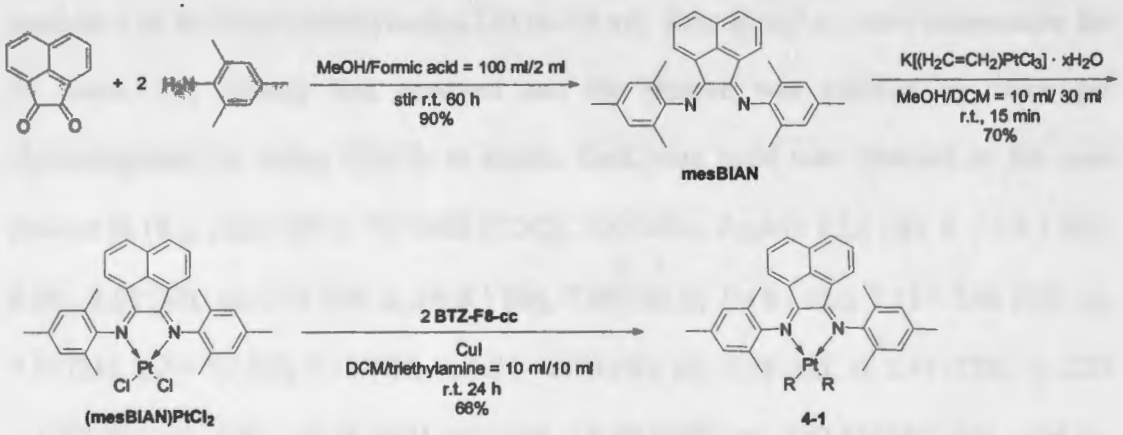

Scheme 4.1. Synthetic route for bis(mesitylimino)acenaphthene Pt(II) acetylide complex **(4-1)**.

Complex (mesBIAN)$PtCl_2$

To a stirred solution of Zeise's salt (0.5 g, 1.35 mmol) in 10 ml MeOH, 30 mL CH_2Cl_2 solution of compound **mesBIAN** (0.6 g, 1.44 mmol) was added. After 15 min stirring at room temperature, the dark solution was treated with charcoal, filtered, and then the solvent was removed. The residue was washed by ether to get crude product as brown microcrystals. The crude product was purified by recrystallization from CH_2Cl_2/hexane to yield brown crystal 0.65 g (yield: 71%). ^{1}H NMR ($CDCl_3$, 500 MHz, δ ppm): 8.31 (2H, d, J = 8.5 Hz), 7.49 (2H, t, J = 8 Hz), 7.13 (4H, s), 6.86 (2H, d, J = 7.5 Hz), 2.44 (6H, s), 2.38 (12H, s).

Complex 4-1

Complex **(mesBIAN)$PtCl_2$** (0.11 g, 0.16 mmol), ligand **BTZ-F8-CC** (the detailed synthetic procedure for this ligand was described in Chapter 3) (0.22 g, 0.40 mmol) and catalytic CuI in CH_2Cl_2/triethylamine (10 ml/10 ml) were stirred at room temperature for 24 hours. The solvent was removed and the residue was purified by silica gel chromatography by using CH_2Cl_2 as eluent. Dark blue solid was obtained as the pure product (0.18 g, yield: 66%). ^{1}H NMR ($CDCl_3$, 500 MHz, δ ppm): 8.22 (2H, d, J = 8.1 Hz), 8.09 – 8.02 (6H, m), 7.91 (2H, d, J = 8.1 Hz), 7.69 (2H, d, J = 8.1 Hz), 7.53 – 7.46 (6H, m), 7.37 (2H, t, J = 7.6 Hz), 7.18 (4H, s), 6.94 – 6.90 (6H, m), 2.58 (6H, s), 2.41 (12H, s), 2.23 – 1.97 (8H, m), 0.92 – 0.70 (40H, m), 0.61 – 0.50 (20H, m). ESI-HRMS: m/z calcd for $[C_{106}H_{116}N_4PtS_2Na]^+$: 1727.8205; found, 1727.8246. Anal. Calcd (%) for $C_{106}H_{116}N_4PtS_2$: C 74.66, H 6.86, N 3.29; found: C 74.53, H 7.13, N 3.35.

4.2.2. Photophysical Measurement

The UV-vis absorption spectra were measured on a SHIMADZU 2501 PC UV-vis spectrophotometer in a 1-cm quartz cuvette in different HPLC-grade solvents. The steady state emission spectra were obtained using a SPEX fluorolog-3 fluorometer/phosphorometer. Each sample was purged with Ar for 30 min prior to each measurement. The triplet transient difference absorption spectra were gained in toluene solutions on an Edinburgh LP920 laser flash photolysis spectrometer. The third harmonic output (355 nm) of a Nd:YAG laser (Quantel Brilliant, pulse width (fwhm) = 4.1 ns, the repetition rate was set at 1 Hz) was used as the excitation source. Each sample was purged with Ar for 30 min prior to each measurement.

4.3. Results and Discussion

4.3.1. UV-vis Absorption

The electronic absorption spectrum of **4-1** in CH_2Cl_2 solution is shown in Figure 4.1. The absorption follows Beer-Lambert's law in the concentration range from 4.5×10^{-6} to 3.6×10^{-5} mol/L. The high-energy band ($\lambda < 420$ nm) is attributed to $^1\pi,\pi^*$ transitions within the bis(mesitylimino)acenaphthene ligand and the alkynyl-benzothiazolylfluorene ligands. This band exhibits much stronger absorption ($\varepsilon \sim 9 \times 10^4$ $M^{-1}\cdot cm^{-1}$) than other diimine Pt(II) complexes ($\varepsilon \sim 5 \times 10^4$ $M^{-1}\cdot cm^{-1}$).[19] A metal-to-ligand charge-transfer band appears between 490 nm and 800 nm, which is weaker and much red-shifted into the near-IR region compared to that of the other diimine Pt(II) complexes,[19] but is comparable to that of the **(mesBIAN)Pt(C≡CPhCF$_3$)$_2$** complex.[30]

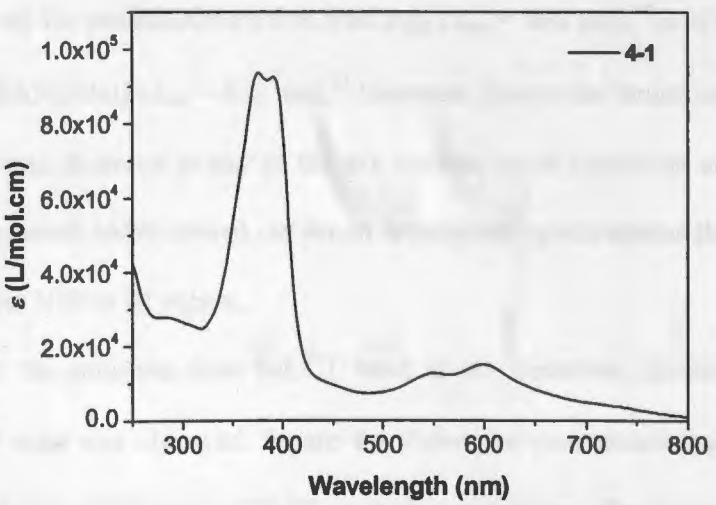

Figure 4.1. UV-vis absorption spectra of 5×10^{-5} mol/L dichloromethane solution of bis(mesitylimino)acenaphthene Pt(II) acetylide (**4-1**).

The low-energy absorption bands of **4-1** exhibit a solvent dependence. As shown in Figure 4.2, **4-1** exhibits a clear negative solvatochromic effect. The low-energy band features at 570 nm in DMSO, but shifts to a lower energy at 585 nm in acetone, and further red-shifts to 599 nm in CH_2Cl_2, finally appears at 645 nm in toluene. These shifts in energy can be easily observed by naked eyes as the colors of solutions changed from purple, to purplish blue, to blue, and finally to green, as shown in Figure 4.3. The apparent hyposochromic effect in low-polarity solvents is a characteristic for charge-transfer transition, and is commonly observed in other transition metal complexes possessing charge-transfer transitions.[18,26-29]

4.3.2. Emission

As a result of the red-shifted charge-transfer band, **4-1** is expected to display emission at the near-IR region when excited at the charge-transfer band, which has been reported by Weinstein *et al.* for **(mesBIAN)Pt(C≡CPhCF$_3$)$_2$** (λ_{em} = 800 nm),[30] and by Castellano *et al.* for [Pt(mesBIAN)(tda)] (λ_{em} = 832 nm).[25] However, due to the limitation of our instrument, no emission was observed in any of the **4-1** solution upon excitation at the ^{1}MLCT band. Further study needs to be carried out on an appropriate spectrometer that can measure the emission in the NIR to IR region.

Although the emission from MLCT band is not observed, emission from the high-energy $^1\pi,\pi^*$ state was observed. Figure 4.4 shows the concentration-dependent emission spectra of **4-1** (λ_{ex} = 374 nm) in CH_2Cl_2 at room temperature. The intensity of the emission decreases while the concentration of solutions increases because of the re-absorption of the

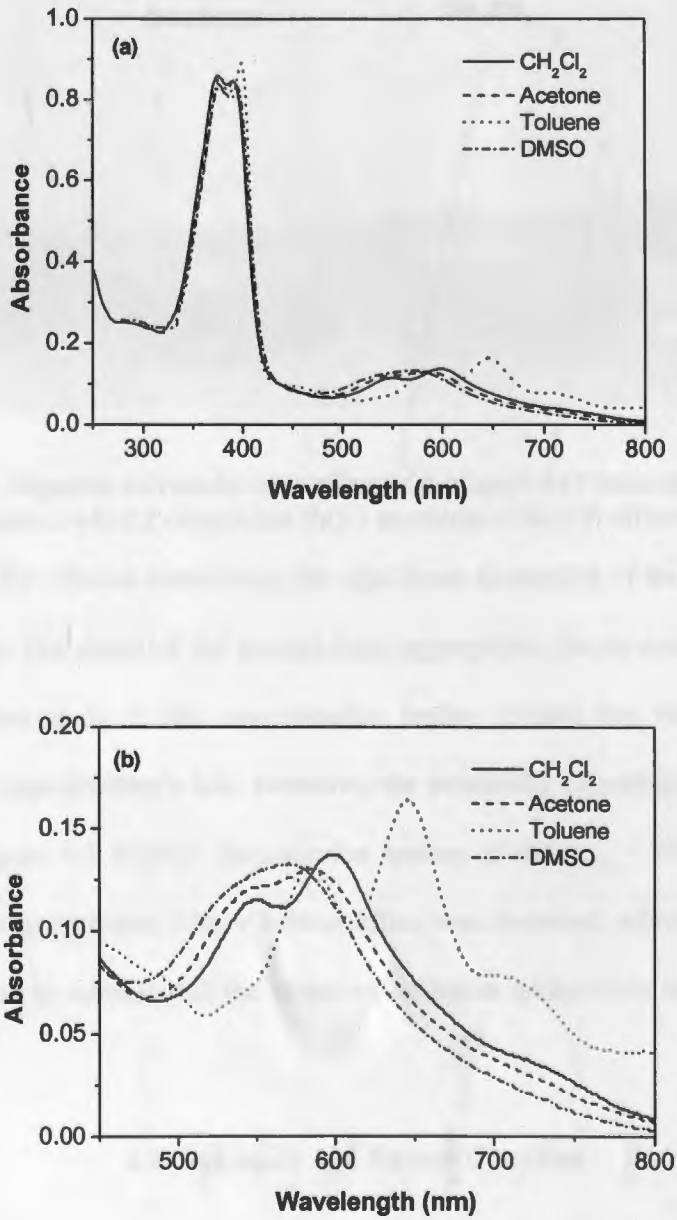

Figure 4.2. UV-vis absorption spectra of bis(mesitylimino)acenaphthene Pt(II) acetylide (**4-1**) in different solvents (A = 0.1 at 436 nm) measured in a 1-cm cuvette at room temperature. (a) Full spectra from 250 to 800 nm; (b) expansion from 450 to 800 nm.

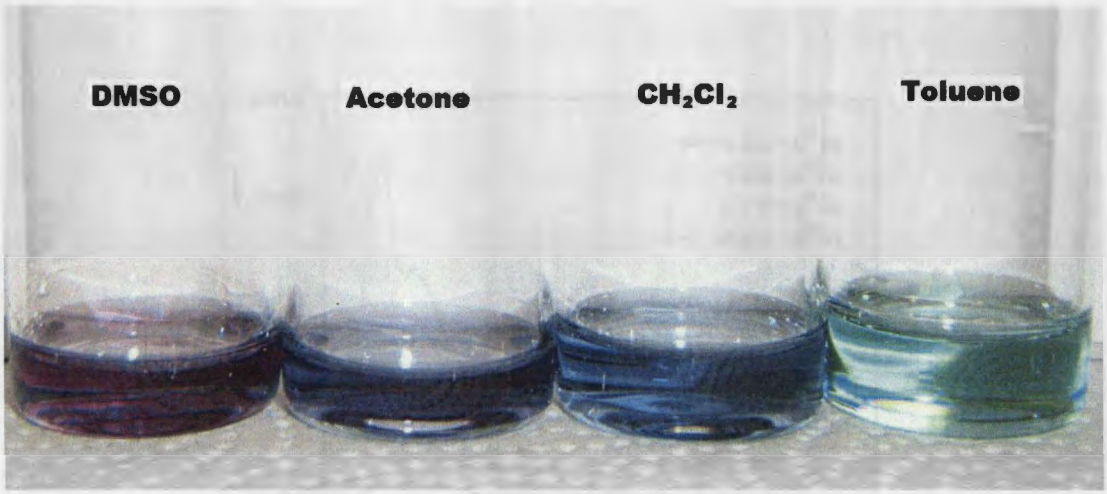

Figure 4.3. Negative solvatochromic effect of 6-phenyl-4-(7-benzothiazolyl-9,9-diethylfluoren-2-yl)-2,2'-bipyridine Pt(II) complexes (**4-1**) in different solvents.

fluorescence by the solution considering the significant absorption of the complex between 400 and 500 nm. The effect of the ground-state aggregation can be excluded because the UV-vis absorption study in this concentration region reveals that the solution of this complex obeys Lambert-Beer's law. However, the possibility of self-quenching could not be ruled out. Figure 4.5 displays the emission spectra of **4-1** (λ_{ex} = 374 nm) in different solvents at room temperature. Minor solvent effect was observed, which provides another piece of evidence to support that the observed emission arises from the acetylide ligand $^1\pi,\pi^*$ state.

4.4. Summary and Future Direction

In this project, introducing low-lying π^* orbital bidentate ligand bis(mesitylimino)acenaphthene is expected to shift the charge-transfer band to much lower energy. UV-vis spectrum shows a much red-shifted charge-transfer band at 599 nm in CH_2Cl_2. However, emission in the near-IR region was not observed, partially due to the

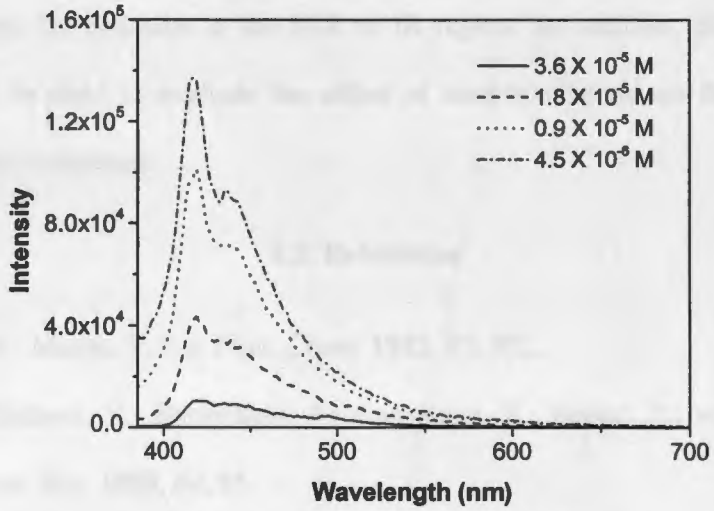

Figure 4.4. Concentration-dependent emission spectra for bis(mesitylimino)acenaphthene Pt(II) acetylide **4-1** (λ_{ex} = 374 nm) in CH_2Cl_2 at room temperature.

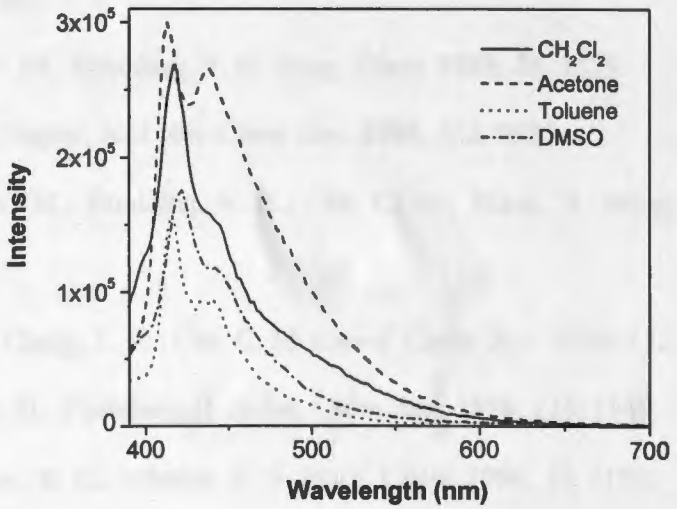

Figure 4.5. Emission spectra for bis(mesitylimino)acenaphthene Pt(II) acetylide **4-1** (λ_{ex} = 374 nm) in different solvents at room temperature (A_{abs} = 0.1 at 436 nm).

limitation of our spectrometer. In the future study, an appropriate spectrometer should be used to measure the emission in the NIR to IR region. In addition, different acetylide ligands should be used to evaluate the effect of acetylide ligand on the photophysical properties of the complexes.

4.5. References

1. Caspar, J. V.; Meyer, T. J. *J. Phys. Chem.* **1983**, *87*, 952.
2. Juris, A.; Balzani, V.; Barigelletti, F.; Campagna, S.; Belser, P.; von Zelewsky, A. *Coord. Chem. Rev.* **1988**, *84*, 85.
3. Caspar, J. V.; Kober, E. M.; Sullivan, B. P.; Meyer, T. J. *J. Am. Chem. Soc.* **1982**, *104*, 630.
4. Worl, L. A.; Duesing, R.; Chen, P.; Della Ciana, L.; Meyer, T. J. *J. Chem. Soc., Dalton Trans.* **1991**, 849.
5. Miskowski, V. M.; Houlding, V. H. *Inorg. Chem.* **1989**, *28*, 1529.
6. Kunkely, H.; Vogler, A. *J. Am. Chem. Soc.* **1990**, *112*, 5625.
7. Miskowski, V. M.; Houlding, V. H.; Che, C. M.; Wang, Y. *Inorg. Chem.* **1993**, *32*, 2518.
8. Chan, C. W.; Cheng, L. K.; Che, C. M. *Coord. Chem. Rev.* **1994**, *132*, 87.
9. Cummings, S. D.; Eisenberg, R. *J. Am. Chem. Soc.* **1996**, *118*, 1949.
10. Zhang, Y.; Ley, K. D.; Schanze, K. S. *Inorg. Chem.* **1996**, *35*, 7102.
11. Connick, W. B.; Gray, H. B. *J. Am. Chem. Soc.* **1997**, *119*, 11620.
12. Paw, W.; Cummings, S. D.; Mansour, M. A.; Connick, W. B.; Geiger, D. K.; Eisenberg, R. *Coord. Chem. Rev.* **1998**, *171*, 125.

13. Connick, W. B.; Geiger, D.; Eisenberg, R. *Inorg. Chem.* **1999**, *38*, 3264.

14. Connick, W. B. Miskowski, V. M.; Houlding, V. H.; Gray, H. B. *Inorg. Chem.* **2000**, *39*, 2585.

15. Hissler, M.; Connick, W. B.; Geiger, D. K.; McGarrah, J. E.; Lipa, D.; Lachiocotte, R. J.; Eisenberg, R. *Inorg. Chem.* **2000**, *39*, 447.

16. Hissler, M.; McGarrah, J. E.; Connick, W. B.; Geiger, D. K.; Cummings, S. D.; Eisenberg, R. *Coord. Chem. Rev.* **2000**, *208*, 115.

17. Adams, C. J.; James, S. L.; Liu, X. M.; Raithby, P. R.; Yellowlees, L. J. *J. Chem. Soc., Dalton Trans.* **2000**, 63.

18. Chan, S. C.; Chan, M. C. W.; Wang, Y.; Che, C. M.; Cheung, K. K.; Zhu, N. *Chem. Eur. J.* **2001**, 4180.

19. Whittle, C. E.; Weinstein, J. A.; George, M. W.; Schanze, K. S. *Inorg. Chem.* **2001**, *40*, 4053.

20. Geary, E. A. M.; Hirata, N.; Clifford, J.; Durrant, J. R.; Parsons, S.; Dawson, A.; Yellowlees, L. J.; Robertson, N. *Dalton Trans.* **2003**, 3757.

21. Geary, E. A. M.; Yellowlees, L. J.; Jack, L. A.; Oswald, I. D. H.; Parsons, S.; Hirata, N.; Durrant, J. R.; Robertson, N. *Inorg. Chem.* **2005**, *44*, 242.

22. Pritchett, T. M.; Sun, W.; Zhang, B.; Ferry, M. J.; Li, Y.; Haley, J. E.; Mackie, D. M.; Shensky III, W.; Mott, A. G. *Opt. Lett.* **2010**, *35*, 1305.

23. Zhang, B.; Li, Y.; Pritchett, T. M.; Sun, W. "Broad-band nonlinear absorbing platinum diimine complex: synthesis, photophysics and nonlinear absorption" (submitted to *J. Am. Chem. Soc.*)

24. Rogers, J. E.; Slagle, J. E.; Krein, D. M.; Burke, A. R.; Hall, B. C.; Fratini, A.; McLean, D. G.; Fleitz, P. A.; Cooper, T. M.; Drobizhev, M.; Makarov, N. S.; Rebane, A.; Kim, K. Y.; Farley, R.; Schanze, K. S. *Inorg. Chem.* **2007**, *46*, 6483.

25. Rachford, A. A.; Hua, F.; Adams, C. J.; Castellano, F. N. *Dalton Trans.* **2009**, 3950.

26. McGarrah, J. E.; Eisenberg, R. *Inorg. Chem.* **2003**, *42*, 4355.

27. Hua, F.; Kinayyigit, S.; Cable, J. R.; Castellano, F. N. *Inorg. Chem.* **2006**, *45*, 4304.

28. Castellano, F. N.; Pomestchenko, I. E.; Shikhova, E.; Hua, F.; Muro, M. L.; Rajapakse, N. *Coord. Chem. Rev.* **2006**, *250*, 1819.

29. Hua, F.; Kinayyigit, S.; Rachford, A. A.; Shikhova, E. A.; Goeb, S.; Cable, J. R.; Adams, C. J.; Kirschbaum, K.; Pinkerton, A. A.; Castellano, F. N. *Inorg. Chem.* **2007**, *46*, 8771.

30. Adams, C. J.; Fey, N.; Weinstein, J. A. *Inorg. Chem.* **2006**, *45*, 6105.